GENERAL
ENGINEERING
LABORATORY

BEARING ATTENUATION

by

J. W. Lund
B. Sternlicht

April 28, 1961

GENERAL ELECTRIC

GL-316B (4-59)

General Engineering Laboratory

BEARING ATTENUATION

by

J.W. Lund
B. Sternlicht

April 28, 1961

Technical Report

For: Bureau of Ships
Contract No. : NObs - 78930
Task Order No. : 3679, Sub Area F 131105

GENERAL ELECTRIC
SCHENECTADY, NEW YORK

OL-254A

TABLE OF CONTENTS

LIST OF FIGURES

LIST OF FIGURES (Continued)

ABSTRACT

The purpose of this report is to analyze the stiffness and damping properties of fluid film journal bearings and to determine the force transmitted to the bearing support. The results are presented in practical design charts and are given in dimensionless form to make them applicable to wide ranges of geometrically and dynamically similar units.

The analysis assumes that the rotor vibrations are of small amplitude. Thereby the non-linear oil film force is replaced by gradients, denoted spring and damping coefficients. The numerical values of these coefficients are obtained by computer calculations. Results are given for 3 bearing types: the plain cylindrical, the 4-axial groove and the elliptical bearing. Using these bearings to support a symmetrical two-bearing rotor the force transmitted to the bearing pedestals, due to a rotor imbalance, is calculated. Thus the bearings can be compared for a given rotor and for known operating conditions and the bearing with the optimum force attenuation can be selected.

INTRODUCTION

The hydrodynamic oil film force is obtained from Reynold's equation, assuming constant viscosity. The equation is approximated by a finite difference equation and solved on a computer. The resulting oil film force is a non-linear function of the eccentricity, the attitude angle and the corresponding velocity components. The non-linearity implies a complex relationship between the rotor and its bearings such that in an exact analysis the rotor and the bearing cannot be studied separately, but must be analyzed as a system. Even if an exact solution was available it would not be too useful for design purposes, firstly because of the vast number of bearing and rotor parameters, and secondly because it would be almost hopeless to tie the results in with the supporting structure. In the present analysis, therefore, the oil film force is linearized by replacing it with its gradients, mathematically expressed in the first order Taylor expansion. This is a justified approximation when it is assumed that the journal motion is small. A linear bearing force vastly simplifies the rotor analysis and makes it possible to assign an impedance to the bearing, a necessary presupposition for any overall investigation of the rotor and its supporting structure.

Three bearing types are studied: the plain cylindrical, the 4-axial groove and the elliptical bearing. The configurations are shown in figure 1, 2 and 3. The oil film force gradients are calculated on the computer as shown in table 1-4 and introducing the numerical values into the linearized expression for the oil film force (see eq. (6) and (7), page 4) yields the bearing spring and damping coefficients as shown in table 5.

Although the thus obtained data are completely sufficient for a rotor vibration calculation they are not in a too convenient form. The reason is that 8 coefficients are obtained whereas the normal rotor calculation is set up for only 4 coefficients, a spring and damping coefficient in two mutually perpendicular directions. No provision is made for taking into account the additional 4 cross-coupling coefficients. Therefore, it is a matter of practical importance to eliminate them. Unfortunately, they are unsymmetrical and do not vanish by the introduction of principal axis. Instead another method is employed making use of the fact that linear bearing forces result in harmonic rotor motion. Thus, it is possible to replace the original 8 coefficients with 4 equivalent coefficients that will give exactly the same rotor motion. It is clear that such a reduction depends on the rotor. A symmetrical, two-bearing rotor is selected since it represents the most commonly used rotor design. As a further simplification the rotor is given only one degree of freedom by concentrating the rotor mass at midspan. The simplified system is shown in figure 6.

The procedure is as follows: a force-balance in the vertical and the horizontal direction is set up for the rotor combining the rotor inertia, the unbalance force and the bearing force represented by the computed 8 spring and damping coefficients. This results in 4 equations in the unknown amplitudes set up in a matrix. By eliminating the 8 terms, representing the cross-coupling effect, the matrix is reduced to the same form as the matrix for a rotor with only 4 spring and damping coefficients and no cross-coupling coefficients. Therefore the remaining terms in the reduced matrix are the desired equivalent spring and damping coefficients. In addition, the matrix is solved for the rotor amplitudes, and combining the amplitude with the spring and damping coefficients gives the force transmitted by the bearing. All the results are given in dimensionless form as a function of a dimensionless parameter $\varkappa = \frac{\frac{1}{2}k}{\lambda\omega_c} \cdot \frac{\left(\frac{\omega}{\omega_c}\right)}{1-\left(\frac{\omega}{\omega_c}\right)^2}$. In plotting the results $\varkappa$ is replaced by the speed ratio $\left(\frac{\omega}{\omega_c}\right)'$, see eq. (29), page 14 . Curves are given for the dimensionless spring and damping coefficients, and the dimensionless transmitted force as shown in figures 12-43. The force attenuation, expressed as the ratio between the actual transmitted force and the force transmitted by a rotor in rigid bearings, is easily found from the graphs since the dimensionless rigid bearing transmitted force is also plotted.

THEORETICAL ANALYSIS

For an incompressible fluid Reynold's equation may be written:

$$(1)\quad \frac{\partial}{\partial \bar{x}}\left[\frac{\bar{h}^3}{\mu}\frac{\partial \bar{P}}{\partial \bar{x}}\right]+\frac{\partial}{\partial \bar{z}}\left[\frac{\bar{h}^3}{\mu}\frac{\partial \bar{P}}{\partial \bar{z}}\right] = 6R\omega\frac{\partial \bar{h}}{\partial \bar{x}} + 12\frac{de}{dt}\cos\theta + 12e\frac{d\alpha}{dt}\sin\theta$$

$$= 6R\omega\left(1-2\frac{\dot{\alpha}}{\omega}\right)\frac{\partial \bar{h}}{\partial \bar{x}} + 12\frac{de}{dt}\cos\theta$$

where $\bar{h} = C + e\cos\theta = C + e\cos\left(\frac{\bar{x}}{R}\right)$

Introducing: $\bar{h} = 2Ch \quad \bar{x} = 2Rx \quad \bar{z} = Lz \quad e = C\varepsilon$

$$\bar{P} = \mu N\left(1-2\frac{\dot{\alpha}}{\omega}\right)\left(\frac{R}{C}\right)^2 \quad \text{(constant } \mu \text{)}$$

Reynold's equation reduces to the following dimensionless equation:

$$(2)\quad \frac{\partial}{\partial x}\left[h^3\frac{\partial P}{\partial x}\right]+\left(\frac{D}{L}\right)^2\frac{\partial}{\partial z}\left[h^3\frac{\partial P}{\partial z}\right] = 6\pi\frac{\partial h}{\partial x} + 12\pi\frac{\frac{\dot{\varepsilon}}{\omega}}{\left(1-2\frac{\dot{\alpha}}{\omega}\right)}\cdot\cos\theta$$

The resulting oil film force is then:

$$(3)\quad \vec{F}_\alpha = \mu N\left(1-2\frac{\dot{\alpha}}{\omega}\right)\left(\frac{R}{C}\right)^2 DL\int_0^1\int_0^\pi P\cos(\theta+\alpha)\,dx\,dz = \lambda\omega\left(1-2\frac{\dot{\alpha}}{\omega}\right)\cdot f_\alpha\left(\frac{L}{D},\varepsilon,\alpha,\frac{\frac{\dot{\varepsilon}}{\omega}}{\left(1-2\frac{\dot{\alpha}}{\omega}\right)}\right)$$

where

$$(4)\quad \lambda = \frac{\mu RL}{\pi}\left(\frac{R}{C}\right)^2$$

For the subsequent analysis it is necessary to linearize the force with respect to displacement and velocity. The first order approximation of the Taylor expansion will be used:

$$d\vec{F}_\alpha = \lambda\omega\left(1-2\frac{\dot{\alpha}}{\omega}\right)\left[\frac{\partial f_\alpha}{\partial \varepsilon}d\varepsilon + \frac{\partial f_\alpha}{\varepsilon\partial\alpha}\varepsilon\,d\alpha + \frac{\partial f_\alpha}{\partial\left(\frac{\dot{\varepsilon}}{\omega}\right)}d\left(\frac{\dot{\varepsilon}}{\omega}\right) + \frac{\partial f_\alpha}{\partial\left(\frac{\dot{\alpha}}{\omega}\right)}d\left(\frac{\dot{\alpha}}{\omega}\right) - \frac{2f_\alpha}{\varepsilon\omega\left(1-2\frac{\dot{\alpha}}{\omega}\right)}\varepsilon\,d\dot{\alpha}\right]$$

Writing:

$$\frac{\partial f_\alpha}{\partial\left(\frac{\dot{\alpha}}{\omega}\right)} = \frac{\partial f_\alpha}{\partial\left(\frac{\dot{\varepsilon}}{\omega}/1-2\frac{\dot{\alpha}}{\omega}\right)}\cdot\frac{\partial\left(\frac{\dot{\varepsilon}}{\omega}/1-2\frac{\dot{\alpha}}{\omega}\right)}{\partial\left(\frac{\dot{\alpha}}{\omega}\right)} = \frac{\partial f_\alpha}{\partial\left(\frac{\dot{\varepsilon}}{\omega}/1-2\frac{\dot{\alpha}}{\omega}\right)}\cdot\frac{2\frac{\dot{\varepsilon}}{\omega}}{\left(1-2\frac{\dot{\alpha}}{\omega}\right)^2}$$

and taking as the reference for the Taylor expansion the steady state equilibrium position where

$$\dot{\varepsilon} = 0 \qquad \dot{\alpha} = 0$$

we get:

$$(5)\quad dF_x = \lambda\omega\left[\frac{\partial f_x}{\partial\varepsilon}\,d\varepsilon + \frac{\partial f_x}{\varepsilon\,\partial\alpha}\,\varepsilon\,d\alpha + \frac{\partial f_x}{\partial(\frac{\dot\varepsilon}{\omega})}\,d\left(\frac{\dot\varepsilon}{\omega}\right) - \frac{2f_x}{\varepsilon\omega}\,\varepsilon\,d\dot\alpha\right]$$

To change from polar to rectangular coordinates (see figure 4):

$$x = C\varepsilon\cos\alpha \qquad\qquad y = C\varepsilon\sin\alpha$$

$$d\varepsilon = \frac{1}{C}\left[\cos\alpha\,dx + \sin\alpha\,dy\right] \qquad \varepsilon\,d\alpha = \frac{1}{C}\left[-\sin\alpha\,dx + \cos\alpha\,dy\right]$$

Since the point ($C\varepsilon, \alpha$) is the steady state position, dx and dy represents the dynamic displacements and $d\dot x = (\dot{dx})$ and $d\dot y = (\dot{dy})$.

Thus we obtain:

$$(6)\quad dF_x = \frac{1}{C}\lambda\omega\left\{\left(\frac{\partial f_x}{\partial\varepsilon}\cos\alpha - \frac{\partial f_x}{\varepsilon\,\partial\alpha}\sin\alpha\right)dx + \left(\frac{\partial f_x}{\partial(\frac{\dot\varepsilon}{\omega})}\cos\alpha + \frac{2f_x}{\varepsilon}\sin\alpha\right)\frac{1}{\omega}\,d\dot x \right.$$
$$\left. + \left(\frac{\partial f_x}{\partial\varepsilon}\sin\alpha + \frac{\partial f_x}{\varepsilon\,\partial\alpha}\cos\alpha\right)dy + \left(\frac{\partial f_x}{\partial(\frac{\dot\varepsilon}{\omega})}\sin\alpha - \frac{2f_x}{\varepsilon}\cos\alpha\right)\frac{1}{\omega}\,d\dot y\right\}$$

or: $dF_x = -K_{xx}\,dx - C_{xx}\,d\dot x + K_{xy}\,dy + C_{xy}\,d\dot y$

$$(7)\quad dF_y = K_{yx}\,dx + C_{yx}\,d\dot x - K_{yy}\,dy - C_{yy}\,d\dot y$$

Three bearing configurations will be analyzed. For this purpose equation (6) is not in a convenient form and must be rewritten in terms of the force components normally used in bearing calculations.

Cylindrical Bearing

The force is given in terms of a radial component F_r, positive in the negative radial direction, and a tangential component F_t, positive in the positive α-direction, such that

$$F_x = -F_r\cos\alpha - F_t\sin\alpha \qquad\qquad F_y = -F_r\sin\alpha + F_t\cos\alpha$$

$$dF_x = -dF_r\cos\alpha + F_r\sin\alpha\,d\alpha - dF_t\sin\alpha - F_t\cos\alpha\,d\alpha$$

$$dF_y = -dF_r\sin\alpha - F_r\cos\alpha\,d\alpha + dF_t\cos\alpha - F_t\sin\alpha\,d\alpha$$

Expressing dF_r and dF_t by equation (6), the coefficients in equation (7) can be written:

$$K_{xx} = \frac{1}{c}\lambda\omega\left[\frac{\partial f_r}{\partial\varepsilon}\cos^2\alpha + \frac{f_r}{\varepsilon}\sin^2\alpha + \left(-\frac{f_t}{\varepsilon} + \frac{\partial f_t}{\partial\varepsilon}\right)\cos\alpha\sin\alpha\right]$$

$$\omega C_{xx} = \frac{1}{c}\lambda\omega\left[\frac{\partial f_r}{\partial(\dot\varepsilon/\omega)}\cos^2\alpha + \frac{2f_t}{\varepsilon}\sin^2\alpha + \left(\frac{2f_r}{\varepsilon} + \frac{\partial f_t}{\partial(\dot\varepsilon/\omega)}\right)\cos\alpha\sin\alpha\right]$$

$$K_{xy} = \frac{1}{c}\lambda\omega\left[-\frac{f_t}{\varepsilon}\cos^2\alpha - \frac{\partial f_t}{\partial\varepsilon}\sin^2\alpha + \left(\frac{f_r}{\varepsilon} - \frac{\partial f_r}{\partial\varepsilon}\right)\cos\alpha\sin\alpha\right]$$

(8)

$$\omega C_{xy} = \frac{1}{c}\lambda\omega\left[\frac{2f_r}{\varepsilon}\cos^2\alpha - \frac{\partial f_t}{\partial(\dot\varepsilon/\omega)}\sin^2\alpha + \left(\frac{2f_t}{\varepsilon} - \frac{\partial f_r}{\partial(\dot\varepsilon/\omega)}\right)\cos\alpha\sin\alpha\right]$$

$$K_{yx} = \frac{1}{c}\lambda\omega\left[\frac{\partial f_t}{\partial\varepsilon}\cos^2\alpha + \frac{f_t}{\varepsilon}\sin^2\alpha + \left(\frac{f_r}{\varepsilon} - \frac{\partial f_r}{\partial\varepsilon}\right)\cos\alpha\sin\alpha\right]$$

$$\omega C_{yx} = \frac{1}{c}\lambda\omega\left[\frac{\partial f_t}{\partial(\dot\varepsilon/\omega)}\cos^2\alpha - \frac{2f_r}{\varepsilon}\sin^2\alpha + \left(\frac{2f_t}{\varepsilon} - \frac{\partial f_r}{\partial(\dot\varepsilon/\omega)}\right)\cos\alpha\sin\alpha\right]$$

$$K_{yy} = \frac{1}{c}\lambda\omega\left[\frac{f_r}{\varepsilon}\cos^2\alpha + \frac{\partial f_r}{\partial\varepsilon}\sin^2\alpha - \left(-\frac{f_t}{\varepsilon} + \frac{\partial f_t}{\partial\varepsilon}\right)\cos\alpha\sin\alpha\right]$$

$$\omega C_{yy} = \frac{1}{c}\lambda\omega\left[\frac{2f_t}{\varepsilon}\cos^2\alpha + \frac{\partial f_r}{\partial(\dot\varepsilon/\omega)}\sin^2\alpha - \left(\frac{2f_r}{\varepsilon} + \frac{\partial f_t}{\partial(\dot\varepsilon/\omega)}\right)\cos\alpha\sin\alpha\right]$$

4-Axial Groove Bearing

The force is given in terms of a vertical component F_v, positive in the negative x-direction, and a horizontal component F_h, positive in the positive y-direction, such that

$$F_x = -F_v \qquad\qquad F_y = F_h$$

Using equation (6) directly the coefficients in eq. (7) become:

$$K_{xx} = \frac{1}{c}\lambda\omega\left[\frac{\partial f_v}{\partial\varepsilon}\cos\alpha - \frac{\partial f_v}{\varepsilon\partial\alpha}\sin\alpha\right]$$

(9) $$\omega C_{xx} = \frac{1}{c}\lambda\omega\left[\frac{\partial f_v}{\partial(\dot\varepsilon/\omega)}\cos\alpha + \frac{2f_h}{\varepsilon}\sin\alpha\right]$$

$$K_{xy} = \frac{1}{c}\lambda\omega\left[-\frac{\partial f_t}{\partial \varepsilon}\sin\alpha - \frac{\partial f_t}{\varepsilon\partial\alpha}\cos\alpha\right]$$

$$\omega C_{xy} = \frac{1}{c}\lambda\omega\left[-\frac{\partial f_t}{\partial(\dot{\varepsilon})}\sin\alpha + \frac{2f_t}{\varepsilon}\cos\alpha\right]$$

$$K_{yx} = \frac{1}{c}\lambda\omega\left[\frac{\partial f_r}{\partial \varepsilon}\cos\alpha - \frac{\partial f_t}{\varepsilon\partial\alpha}\sin\alpha\right]$$

$$\omega C_{yx} = \frac{1}{c}\lambda\omega\left[\frac{\partial f_r}{\partial(\dot{\varepsilon})}\cos\alpha + \frac{2f_r}{\varepsilon}\sin\alpha\right]$$

$$K_{yy} = \frac{1}{c}\lambda\omega\left[-\frac{\partial f_r}{\partial \varepsilon}\sin\alpha - \frac{\partial f_r}{\varepsilon\partial\alpha}\cos\alpha\right]$$

$$\omega C_{yy} = \frac{1}{c}\lambda\omega\left[-\frac{\partial f_r}{\partial(\dot{\varepsilon})}\sin\alpha + \frac{2f_r}{\varepsilon}\cos\alpha\right]$$

Elliptical Bearing

The elliptical bearing is made up of two partial arc bearings called the lower lobe, identified by subscript 1, and the upper lobe, identified by subscript 2. The radial bearing clearance is taken as the difference between the lobe radius and the journal radius. The origin of the x, y-coordinate system is located at the bearing center, midway between the lobe centers, with the x-axis vertical downwards.

From figure 5:

$$\varepsilon_1^2 = \varepsilon^2 + m^2 + 2\varepsilon m\cos\alpha \qquad \varepsilon_2^2 = \varepsilon^2 + m^2 - 2\varepsilon m\cos\alpha$$

$$\sin\alpha_1 = \frac{\varepsilon\sin\alpha}{\varepsilon_1} \qquad \sin\alpha_2 = \frac{\varepsilon\sin\alpha}{\varepsilon_2} \tag{10}$$

Furthermore

$$d\varepsilon_1 = \frac{1}{c}\left[\cos\alpha_1\, dx + \sin\alpha_1\, dy\right]$$

$$\varepsilon_1 d\alpha_1 = \frac{1}{c}\left[-\sin\alpha_1 dx + \cos\alpha_1\, dy\right] \tag{11}$$

$$d\varepsilon_2 = \frac{1}{c}\left[-\cos\alpha_2\, dx + \sin\alpha_2\, dy\right]$$

$$\varepsilon_2 d\alpha_2 = \frac{1}{c}\left[\sin\alpha_2\, dx + \cos\alpha_2\, dy\right]$$

The two lobes are calculated separately resulting in a vertical and a horizontal force component for each lobe. Then:

$$\text{(12)} \qquad F_x = -(F_{v1} - F_{v2}) = -F_v \qquad\qquad F_y = (F_{h1} - F_{h2}) = F_h$$

These equations are analogous to the 4-axial groove bearing. Therefore equations (9) are also applicable to the elliptical bearing. However, a difficulty is encountered in the calculation of the derivatives with respect to velocity because a pure radial velocity $\dot{\varepsilon}$ gives rise to both a radial and a tangential velocity component for the lobes. Thus $\frac{\partial f}{\partial(\frac{\dot{\varepsilon}}{\omega})} = -2f$ does not hold for the elliptical bearing as it did for the cylindrical and the 4-axial groove bearing, but it is still valid for each lobe taken by itself. Using eq. (5) and (7) together with eq. (12) we get:

$$-C_{xx}\, d\dot{x} + C_{xy}\, d\dot{y} = \lambda\omega\left[-\frac{\partial f_{v1}}{\partial(\frac{\dot{\varepsilon}}{\omega})}\frac{1}{\omega}\, d\dot{\varepsilon}_1 + \frac{\partial f_{v2}}{\partial(\frac{\dot{\varepsilon}}{\omega})}\frac{1}{\omega}\, d\dot{\varepsilon}_2 + \frac{2f_{v1}}{\varepsilon_1\omega}\,\varepsilon_1 d\alpha_1 - \frac{2f_{v2}}{\varepsilon_2\omega}\,\varepsilon_2 d\alpha_2\right]$$

$$C_{yx}\, d\dot{x} - C_{yy}\, d\dot{y} = \lambda\omega\left[\frac{\partial f_{h1}}{\partial(\frac{\dot{\varepsilon}}{\omega})}\frac{1}{\omega}\, d\dot{\varepsilon}_1 - \frac{\partial f_{h2}}{\partial(\frac{\dot{\varepsilon}}{\omega})}\frac{1}{\omega}\, d\dot{\varepsilon}_2 - \frac{2f_{h1}}{\varepsilon_1\omega}\,\varepsilon_1 d\alpha_1 + \frac{2f_{h2}}{\varepsilon_2\omega}\,\varepsilon_2 d\alpha_2\right]$$

Using equations (11) we get:

$$\omega C_{xx} = \frac{1}{c}\lambda\omega\left[\frac{\partial f_{v1}}{\partial(\frac{\dot{\varepsilon}}{\omega})}\cos\alpha_1 + \frac{\partial f_{v2}}{\partial(\frac{\dot{\varepsilon}}{\omega})}\cos\alpha_2 + \frac{2f_{v1}}{\varepsilon_1}\sin\alpha_1 + \frac{2f_{v2}}{\varepsilon_2}\sin\alpha_2\right]$$

$$\omega C_{xy} = \frac{1}{c}\lambda\omega\left[-\frac{\partial f_{v1}}{\partial(\frac{\dot{\varepsilon}}{\omega})}\sin\alpha_1 + \frac{\partial f_{v2}}{\partial(\frac{\dot{\varepsilon}}{\omega})}\sin\alpha_2 + \frac{2f_{v1}}{\varepsilon_1}\cos\alpha_1 - \frac{2f_{v2}}{\varepsilon_2}\cos\alpha_2\right]$$

$$\omega C_{yx} = \frac{1}{c}\lambda\omega\left[\frac{\partial f_{h1}}{\partial(\frac{\dot{\varepsilon}}{\omega})}\cos\alpha_1 + \frac{\partial f_{h2}}{\partial(\frac{\dot{\varepsilon}}{\omega})}\cos\alpha_2 + \frac{2f_{h1}}{\varepsilon_1}\sin\alpha_1 + \frac{2f_{h2}}{\varepsilon_2}\sin\alpha_2\right]$$

$$\omega C_{yy} = \frac{1}{c}\lambda\omega\left[-\frac{\partial f_{h1}}{\partial(\frac{e}{c})}\sin\alpha_1 + \frac{\partial f_{h2}}{\partial(\frac{e}{c})}\sin\alpha_2 + \frac{2f_{h1}}{\varepsilon_1}\cos\alpha_1 - \frac{2f_{h2}}{\varepsilon_2}\cos\alpha_2\right]$$

Thus we may use equations (9) by setting:

$$\frac{\partial f_v}{\partial \varepsilon} = \frac{\partial(f_{v1}-f_{v2})}{\partial \varepsilon} \qquad \frac{\partial f_h}{\partial \varepsilon} = \frac{\partial(f_{h1}-f_{h2})}{\partial \varepsilon}$$

$$\frac{\partial f_v}{\varepsilon\partial\alpha} = \frac{\partial(f_{v1}-f_{v2})}{\varepsilon\partial\alpha}$$

$$\frac{\partial f_h}{\varepsilon\partial\alpha} = \frac{\partial(f_{h1}-f_{h2})}{\varepsilon\partial\alpha}$$

(13) $$\frac{\partial f_v}{\partial(\frac{e}{c})} = \frac{\partial f_{v1}}{\partial(\frac{e}{c})}\cos(\alpha-\alpha_1) + \frac{\partial f_{v2}}{\partial(\frac{e}{c})}\cos(\alpha+\alpha_2) - \frac{2f_{v1}}{\varepsilon_1}\sin(\alpha-\alpha_1) + \frac{2f_{v2}}{\varepsilon_2}\sin(\alpha+\alpha_2)$$

$$\frac{2f_v}{\varepsilon} = \frac{\partial f_{v1}}{\partial(\frac{e}{c})}\sin(\alpha-\alpha_1) + \frac{\partial f_{v2}}{\partial(\frac{e}{c})}\sin(\alpha+\alpha_2) + \frac{2f_{v1}}{\varepsilon_1}\cos(\alpha-\alpha_1) - \frac{2f_{v2}}{\varepsilon_2}\cos(\alpha+\alpha_2)$$

$$\frac{\partial f_h}{\partial(\frac{e}{c})} = \frac{\partial f_{h1}}{\partial(\frac{e}{c})}\cos(\alpha-\alpha_1) + \frac{\partial f_{h2}}{\partial(\frac{e}{c})}\cos(\alpha+\alpha_2) - \frac{2f_{h1}}{\varepsilon_1}\sin(\alpha-\alpha_1) + \frac{2f_{h2}}{\varepsilon_2}\sin(\alpha+\alpha_2)$$

$$\frac{2f_h}{\varepsilon} = \frac{\partial f_{h1}}{\partial(\frac{e}{c})}\sin(\alpha-\alpha_1) + \frac{\partial f_{h2}}{\partial(\frac{e}{c})}\sin(\alpha+\alpha_2) + \frac{2f_{h1}}{\varepsilon_1}\cos(\alpha-\alpha_1) - \frac{2f_{h2}}{\varepsilon_2}\cos(\alpha+\alpha_2)$$

The above forces and derivatives are calculated by means of a computer as summarized in tables 1-3. The resulting spring and damping coefficients as calculated from equations (8), (9) and (13) are shown in table 4. These results can be used directly when calculating the vibrations of the rotor. However, the usual calculation procedure allows for only 4 coefficients, one spring and damping coefficient in the vertical and in horizontal direction. No provision is made for taking into account the 4 cross-coupling terms Kxy, Cxy, Kyx and Cyx. Therefore it becomes important to eliminate them to reduce the original 8 coefficients to 4 equivalent coefficients. Due to the non-symmetry of the cross-coupling terms they do not disappear by the introduction of principal axis. Instead, the 8 coefficients may be combined to 4 by coupling the bearing with the rotor in such a way that the resulting motion remains the same. This is the purpose of the following analysis.

The rotor is a simple, symmetrical, one-degree-of-freedom rotor. It is supported in two identical bearings and the rotor mass is considered concentrated at midspan, (see figure 6).

Let 0 be the steady state position of the journal center (i.e., at zero unbalance), A is the actual journal center, B is the shaft center at midspan and G is the center of gravity of the rotor. A force balance gives:

$$M\ddot{x}_b + k(x_b - x_a) = Me\omega^2\cos\omega t$$

$$k(x_b - x_a) = 2K_{xx}x_a + 2C_{xx}\dot{x}_a - 2K_{xy}y_a - 2C_{xy}\dot{y}_a$$

(14) $$M\ddot{y}_b + k(y_b - y_a) = Me\omega^2\sin\omega t$$

$$k(y_b - y_a) = -2K_{yx}x_a - 2C_{yx}\dot{x}_a + 2K_{yy}y_a + 2C_{yy}\dot{y}_a$$

The following parameters are introduced:

(15) $$\omega_c^2 = \frac{k}{M}$$

(16) $$\varkappa = \frac{1}{2}k\frac{\omega_c^2}{\omega_c^2 - \omega^2}$$

Furthermore the solution is taken in the form:

$$x_a = A\cos\omega t + B\sin\omega t$$

$$x_b = \frac{A\omega_c^2 + e\omega^2}{\omega_c^2 - \omega^2}\cos\omega t + \frac{B\omega_c^2}{\omega_c^2 - \omega^2}\sin\omega t$$

(17) $$y_a = E\cos\omega t + F\sin\omega t$$

$$y_b = \frac{E\omega_c^2}{\omega_c^2 - \omega^2}\cos\omega t + \frac{F\omega_c^2 + e\omega^2}{\omega_c^2 - \omega^2}\sin\omega t$$

Substituting eq. (15), (16) and (17) into eq. (14) yields:

(18)

$\frac{A}{\varkappa e}$	$\frac{B}{\varkappa e}$	$\frac{E}{\varkappa e}$	$\frac{F}{\varkappa e}$	
$(K_{xx}-\varkappa)$	ωC_{xx}	$-K_{xy}$	$-\omega C_{xy}$	1
$-\omega C_{xx}$	$(K_{xx}-\varkappa)$	ωC_{xy}	$-K_{xy}$	0
$-K_{yx}$	$-\omega C_{yx}$	$(K_{yy}-\varkappa)$	ωC_{yy}	0
ωC_{yx}	$-K_{yx}$	$-\omega C_{yy}$	$(K_{yy}-\varkappa)$	1

It is desired to reduce this matrix to the same form as a matrix for a rotor without cross-coupling terms. Such a rotor has only 4 spring and damping coefficients which are denoted K_x, B_x, K_y and B_y. The reduced matrix is then:

(19)

$\frac{A}{\varkappa e}$	$\frac{B}{\varkappa e}$	$\frac{E}{\varkappa e}$	$\frac{F}{\varkappa e}$	
$(K_x-\varkappa)$	ωB_x	0	0	1
$-\omega B_x$	$(K_x-\varkappa)$	0	0	0
0	0	$(K_y-\varkappa)$	ωB_y	0
0	0	$-\omega B_y$	$(K_y-\varkappa)$	1

After a substantial amount of algebra, eq. (18) is reduced to eq. (19) with the results:

$$
\begin{aligned}
K_x &= K_{xx} - \frac{1}{\psi_x}\left[\delta K_{xy} + \eta(\omega C_{xy})\right] \\
\omega B_x &= \omega C_{xx} + \frac{1}{\psi_x}\left[\eta K_{xy} - \delta(\omega C_{xy})\right] \\
K_y &= K_{yy} - \frac{1}{\psi_y}\left[\delta K_{yx} - \eta(\omega C_{yx})\right] \\
\omega B_y &= \omega C_{yy} - \frac{1}{\psi_y}\left[\eta K_{yx} + \delta(\omega C_{yx})\right]
\end{aligned}
\tag{20}
$$

where:

$$
\begin{aligned}
\psi_x &= (K_{yy} - \varkappa + \omega C_{xy})^2 + (K_{xy} - \omega C_{yy})^2 \\
\psi_y &= (K_{xx} - \varkappa - \omega C_{yx})^2 + (K_{yx} + \omega C_{xx})^2 \\
\delta &= (K_{xx} - \varkappa - \omega C_{yx})(K_{xy} - \omega C_{yy}) + (K_{yy} - \varkappa + \omega C_{xy})(K_{yx} + \omega C_{xx}) \\
\eta &= (K_{xx} - \varkappa - \omega C_{yx})(K_{yy} - \varkappa + \omega C_{xy}) - (K_{xy} - \omega C_{yy})(K_{yx} + \omega C_{xx})
\end{aligned}
\tag{21}
$$

Since eq. (19) are linear they may also be solved for the amplitudes:

$$
\begin{aligned}
\frac{A}{e} &= \frac{\varkappa(K_x - \varkappa)}{(K_x - \varkappa)^2 + (\omega B_x)^2} \\
\frac{B}{e} &= \frac{\varkappa(\omega B_x)}{(K_x - \varkappa)^2 + (\omega B_x)^2} \\
\frac{E}{e} &= \frac{-\varkappa(\omega B_y)}{(K_y - \varkappa)^2 + (\omega B_y)^2} \\
\frac{F}{e} &= \frac{\varkappa(K_y - \varkappa)}{(K_y - \varkappa)^2 + (\omega B_y)^2}
\end{aligned}
\tag{22}
$$

The x- and y-amplitudes are found by substituting eq. (22) into eq. (17):

(23)

$$\frac{x_a}{e} = \frac{\varkappa}{\sqrt{(K_x-\varkappa)^2+(\omega B_x)^2}} \cos(\omega t-\varphi_x)$$

$$\tan\varphi_x = \frac{\omega B_x}{(K_x-\varkappa)}$$

$$\frac{y_a}{e} = \frac{\varkappa}{\sqrt{(K_y-\varkappa)^2+(\omega B_y)^2}} \sin(\omega t-\varphi_y)$$

$$\tan\varphi_y = \frac{\omega B_y}{(K_y-\varkappa)}$$

x_b and y_b may be found similarly from eq. (17).

The force transmitted to the bearing pedestal is given by:

(24)

$$P_x = K_x \cdot x_a + B_x \cdot \dot{x}_a$$

$$P_y = K_y \cdot y_a + B_y \cdot \dot{y}_a$$

Substituting eq. (23) into eq. (24) yields:

(25)

$$\frac{P_x}{e} = \varkappa\sqrt{\frac{K_x^2+(\omega B_x)^2}{(K_x-\varkappa)^2+(\omega B_x)^2}} \cos(\omega t-\varphi_x+\gamma_x)$$

$$\tan\gamma_x = \frac{\omega B_x}{K_x}$$

$$\frac{P_y}{e} = \varkappa\sqrt{\frac{K_y^2+(\omega B_y)^2}{(K_y-\varkappa)^2+(\omega B_y)^2}} \sin(\omega t-\varphi_y+\gamma_y)$$

$$\tan\gamma_y = \frac{\omega B_y}{K_y}$$

In the calculation the above equations are made dimensionless by dividing through by $\varepsilon\lambda\omega_k\left(\frac{\omega}{\omega_k}\right)$ in order to make them general. As an assistance in plotting curves of the derived equations the following auxiliary expressions are set up:

For $\varkappa \rightarrow \infty$:

$$
\begin{aligned}
K_x &\rightarrow K_{xx} - \omega C_{xy} \\
\omega B_x &\rightarrow \omega C_{xx} + K_{xy} \\
K_y &\rightarrow K_{yy} + \omega C_{yx} \\
\omega B_y &\rightarrow \omega C_{yy} - K_{yx} \\
\tfrac{E}{e} &\rightarrow 1 \\
\tfrac{F}{e} &\rightarrow 1 \\
\tfrac{A}{e} &\rightarrow \sqrt{(K_{xx} - \omega C_{xy})^2 + (K_{xy} + \omega C_{xx})^2} \\
\tfrac{B}{e} &\rightarrow \sqrt{(K_{yy} + \omega C_{yx})^2 + (K_{yx} - \omega C_{yy})^2}
\end{aligned}
\tag{26}
$$

Instead of expressing the rotor amplitude in x and y-coordinates a better physical picture is obtained by finding the corresponding elliptical path of the journal center. Combining the first and the third of eq. (17) we get:

$$
\frac{a}{e} = \sqrt{\frac{1}{2}\left[\left(\frac{A}{e}\right)^2 + \left(\frac{B}{e}\right)^2 + \left(\frac{E}{e}\right)^2 + \left(\frac{F}{e}\right)^2\right] + \frac{1}{2}\sqrt{\left[\left(\frac{A}{e}\right)^2 + \left(\frac{B}{e}\right)^2 + \left(\frac{E}{e}\right)^2 + \left(\frac{F}{e}\right)^2\right]^2 - \left[\left(\frac{A}{e}\right)\left(\frac{F}{e}\right) - \left(\frac{B}{e}\right)\left(\frac{E}{e}\right)\right]^2}}
$$

$$
\frac{b}{e} = \sqrt{\frac{1}{2}\left[\left(\frac{A}{e}\right)^2 + \left(\frac{B}{e}\right)^2 + \left(\frac{E}{e}\right)^2 + \left(\frac{F}{e}\right)^2\right] - \frac{1}{2}\sqrt{\left[\left(\frac{A}{e}\right)^2 + \left(\frac{B}{e}\right)^2 + \left(\frac{E}{e}\right)^2 + \left(\frac{F}{e}\right)^2\right]^2 - \left[\left(\frac{A}{e}\right)\left(\frac{F}{e}\right) - \left(\frac{B}{e}\right)\left(\frac{E}{e}\right)\right]^2}}
\tag{27}
$$

$$
\tan 2\alpha = \frac{2\left[\left(\frac{A}{e}\right)\left(\frac{E}{e}\right) + \left(\frac{B}{e}\right)\left(\frac{F}{e}\right)\right]}{\left[\left(\frac{A}{e}\right)^2 + \left(\frac{B}{e}\right)^2 - \left(\frac{E}{e}\right)^2 - \left(\frac{F}{e}\right)^2\right]}
$$

Where a is the major axis of the ellipse, b is the minor axis and α is the angle between the x-axis and the major axis, see figure 7. $\left(\frac{A}{e}\right)$, $\left(\frac{B}{e}\right)$, $\left(\frac{E}{e}\right)$ and $\left(\frac{F}{e}\right)$ are given by eq. (22). Rotor resonance may be defined as the speed where the major axis is a maximum. This maximum is found by plotting the major axis as a function of $\varkappa$. The results are shown in figure 46-47. From these graphs the rotor critical speed can be found directly for a given rotor by a trial and error process.

Thus the results are obtained as a function of $\varkappa$, but to facilitate the interpretation of the results, $\varkappa$ is replaced by a speed parameter. From eq. (16) $\varkappa$ in dimensionless form is:

$$(28) \qquad \varkappa = \frac{\frac{1}{4}k}{\frac{\varepsilon}{2}\lambda\omega} \cdot \frac{\omega^2}{\omega_c^2 - \omega^2} = \frac{\frac{1}{4}k}{\frac{\varepsilon}{2}\lambda\omega_c} \cdot \frac{\left(\frac{\omega}{\omega_c}\right)}{1 - \left(\frac{\omega}{\omega_c}\right)^2}$$

Arbitratily setting $\frac{\frac{1}{4}k}{\frac{\varepsilon}{2}\lambda\omega_c} = 5$ (a rather stiff rotor) we get

$$\varkappa = 5 \cdot \frac{\left(\frac{\omega}{\omega_c}\right)'}{1 - \left(\frac{\omega}{\omega_c}\right)'^2}$$

or

$$(29) \qquad \left(\frac{\omega}{\omega_c}\right)' = \frac{5}{2\varkappa}\left[-1 + \sqrt{1 + \frac{4\varkappa^2}{25}}\right]$$

$\left(\frac{\omega}{\omega_c}\right)'$ is used instead of $\varkappa$ to present the dimensionless results as shown in figures 11-43. When a rotor with a dimensionless stiffness different from 5 is investigated, eq. (28) should be substituted into eq. (29) to find the value of $\left(\frac{\omega}{\omega_c}\right)'$ corresponding to the desired value of $\frac{\omega}{\omega_c}$. This relationship is shown for a wide range of dimensionless rotor stiffnesses in fig. 11.

The force attenuation may be expressed as the ratio between the actual transmitted force and the force transmitted with rigid bearings. The following relationship exists:

$$(30) \qquad \frac{P_m}{\frac{\varepsilon}{2}\lambda\omega_c\left(\frac{\omega}{\omega_c}\right)} = \frac{\frac{1}{4}k}{\frac{\varepsilon}{2}\lambda\omega_c} \cdot \frac{\left(\frac{\omega}{\omega_c}\right)}{1 - \left(\frac{\omega}{\omega_c}\right)^2} = \varkappa$$

SUMMARY OF RESULTS

Effective spring coefficient in vertical direction:

$$K_x = K_{xx} - \frac{1}{\psi_x}\left[\delta K_{xy} + \eta(\omega C_{xy})\right]$$

Effective damping coefficient in vertical direction:

$$\omega B_x = \omega C_{xx} + \frac{1}{\psi_x}\left[\eta K_{xy} - \delta(\omega C_{xy})\right]$$

Effective spring coefficient in horizontal direction:

$$K_y = K_{yy} - \frac{1}{\psi_y}\left[\delta K_{yx} - \eta(\omega C_{yx})\right]$$

Effective damping coefficient in horizontal direction:

$$\omega B_y = \omega C_{yy} - \frac{1}{\psi_y}\left[\eta K_{yx} + \delta(\omega C_{yx})\right]$$

where:

$$\psi_x = (K_{yy} - \varkappa + \omega C_{xy})^2 + (K_{xy} - \omega C_{yy})^2$$

$$\psi_y = (K_{xx} - \varkappa - \omega C_{yx})^2 + (K_{yx} + \omega C_{xx})^2$$

$$\delta = (K_{xx} - \varkappa - \omega C_{yx})(K_{xy} - \omega C_{yy}) + (K_{yy} - \varkappa + \omega C_{xy})(K_{yx} + \omega C_{xx})$$

$$\eta = (K_{xx} - \varkappa - \omega C_{yx})(K_{yy} - \varkappa + \omega C_{xy}) - (K_{xy} - \omega C_{yy})(K_{yx} + \omega C_{xx})$$

$$\varkappa = \frac{1}{2} k \frac{\omega^2}{\omega_c^2 - \omega^2}$$

K_{xx}, ωC_{xx}, K_{xy}, ωC_{xy}, K_{yx}, ωC_{yx}, K_{yy}, and ωC_{yy} are given in table 5.

Transmitted force in vertical direction

$$P_x = e \cdot \varkappa \cdot \sqrt{\frac{K_x^2 + (\omega B_x)^2}{(K_x - \varkappa)^2 + (\omega B_x)^2}} \cos(\omega t - \varphi_x + \gamma_x)$$

$$\tan \varphi_x = \frac{\omega B_x}{K_x - \varkappa} \qquad \tan \gamma_x = \frac{\omega B_x}{K_x}$$

Transmitted force in horizontal direction

$$P_y = e \cdot \varkappa \cdot \sqrt{\frac{K_y^2 + (\omega B_y)^2}{(K_y - \varkappa)^2 + (\omega B_y)^2}} \sin(\omega t - \varphi_y + \gamma_y)$$

$$\tan \varphi_y = \frac{\omega B_y}{K_y - \varkappa} \qquad \tan \gamma_y = \frac{\omega B_y}{K_y}$$

Amplitude of journal center in vertical direction

$$x_a = \frac{e \varkappa}{\sqrt{(K_x - \varkappa)^2 + (\omega B_x)^2}} \cos(\omega t - \varphi_x)$$

Amplitude of journal center in horizontal direction

$$y_a = \frac{e \varkappa}{\sqrt{(K_y - \varkappa)^2 + (\omega B_y)^2}} \sin(\omega t - \varphi_y)$$

Elliptical path of journal center

Major axis: $a = \sqrt{\frac{1}{2}[A^2 + B^2 + E^2 + F^2] + \frac{1}{2}\sqrt{[A^2 + B^2 + E^2 + F^2]^2 - [AF - BE]^2}}$

Minor axis: $b = \sqrt{\frac{1}{2}[A^2 + B^2 + E^2 + F^2] - \frac{1}{2}\sqrt{[A^2 + B^2 + E^2 + F^2]^2 - [AF - BE]^2}}$

Angle between vertical and major axis: $\alpha = \frac{1}{2} \tan^{-1}\left[\frac{2(AE + BF)}{(A^2 + B^2 - E^2 - F^2)}\right]$

where:

e is rotor mass eccentricity, i.e., $e = \dfrac{\text{Unbalance (lbs-in)}}{\text{Rotor Weight (lbs)}}$

$$A = \frac{e\varkappa(K_x-\varkappa)}{(K_x-\varkappa)^2+(\omega B_x)^2}$$

$$B = \frac{e\varkappa(\omega B_x)}{(K_x-\varkappa)^2+(\omega B_x)^2}$$

$$E = \frac{-e\varkappa(\omega B_y)}{(K_y-\varkappa)^2+(\omega B_y)^2}$$

$$F = \frac{e\varkappa(K_y-\varkappa)}{(K_y-\varkappa)^2+(\omega B_y)^2}$$

DESIGN INFORMATION

This section has been prepared to assist the designer. The method is directly applicable and does not assume familiarity with the underlying analysis. Thus, the designer should be able to extract any desired information without further reference.

In selecting the bearing on the basis of minimum transmitted force, the designer is faced with the problem of how to choose bearing type, unit bearing load, $\frac{L}{D}$ -ratio, clearance and oil viscosity. To answer these questions, the procedure below can be employed.

It is assumed that the rotor is given such that the following quantities are known:

1) The rotor critical speed, ω_c $^{rad}/sec.$, for rigid rotor supports (i.e., the classical critical speed calculation).

2) The bearing reaction F lbs.

3) The rotor stiffness k $^{lbs}/in.$ Since the results are valid only for a two bearing rotor and for rotor speeds below the second critical speed, the rotor stiffness is calculated from $k = M \cdot \omega_c^2$ where M $\frac{lbs \cdot sec^2}{in}$ is the vibratory mass of the rotor. M is somewhat smaller than the actual rotor mass and may be estimated by methods as shown in "Vibration Problems in Engineering", by Timoshenko, Chapter 1, Article 4.

4) The journal radius R, in.

For later use, we shall define the bearing parameter λ as:

$$\lambda = \frac{\mu R L}{\pi}\left(\frac{R}{C}\right)^2 \qquad \text{lbs} \cdot \text{sec}$$

(μ : viscosity, $\frac{lbs \cdot sec}{in^2}$ - P: bearing radius, in - L: effective bearing length, in - C: radial bearing clearance, in.)

In addition we shall define:

the dimensionless bearing reaction: $\frac{F}{\lambda\omega_c}$

the dimensionless rotor stiffness : $\frac{\frac{1}{2}k}{\varepsilon\lambda\omega_c}$

the dimensionless speed ratio : $\frac{\omega}{\omega_c}$

(ω: operating rotor speed, $^{rad}/sec$)

Once these three parameters are known the transmitted force can be found directly. Thus, the problem is to choose the bearing dimensions in such a way that the value of the above parameters minimize the transmitted force.

Selection of bearing type and of $\frac{L}{D}$ - ratio

The selection will be done on a basis of comparison. For this purpose it is necessary first to estimate a bearing clearance C and an oil viscosity μ. Since the journal radius R is known it is then possible to compute λ for $\frac{L}{D} = \frac{1}{2}$ and $\frac{L}{D} = 1$. In addition $\frac{F}{\lambda\omega_c}$ and $\frac{\frac{1}{2}k}{\varepsilon\lambda\omega_c}$ are obtained. For a given operating speed ω $^{rad}/sec$ the transmitted force can be found as follows:

a) calculate the speed ratio $\frac{\omega}{\omega_c}$.

b) calculate $\frac{F}{\lambda\omega_c} \Big/ \frac{\omega}{\omega_c}$ and enter figure 8-10 to get the corresponding value of eccentricity ratio ε.

c) enter figure 11 with $\frac{\omega}{\omega_c}$ to find the equivalent speed ratio $\left(\frac{\omega}{\omega_c}\right)'$.

d) enter figure 28-43 with $\left(\frac{\omega}{\omega_c}\right)'$ and the corresponding value of ε to find the dimensionless transmitted force $\frac{P}{\frac{e}{c}\lambda\omega_c\frac{\omega}{\omega_c}}$ for all desired bearing types and $\frac{L}{D}$ - ratio. If the curves are spaced too far for linear interpolation it is necessary to make a cross-plot. Multiply the result by $\frac{e}{c}\lambda\omega_c\frac{\omega}{\omega_c}$ (e : distance between shaft center and center of gravity of rotor mass, inches. e may be calculated from the equation: e = $^{\text{rotor unbalance, lbs}\cdot\text{in}}/_{\text{rotor weight, lbs.}}$) to obtain the transmitted force P lbs.

This procedure can be repeated for a number of operating speeds to cover the entire operating speed range. By plotting the curves of transmitted force versus rotor speed, the effect of bearing type and of $\frac{L}{D}$ -ratio is readily seen and a selection on the basis of minimum transmitted force can be made. An example of the results obtained by the outlined method is given in figures 44-45.

<u>Selection of bearing clearance</u>

In principle, the selection of clearance is done by the same procedure as above. Thus the goal is to obtain curves of transmitted force versus rotor speed for various values of the bearing clearance and from that select the actual clearance value on the basis of minimum transmitted force.

As before, the rotor is assumed known. In addition, an oil viscosity must be chosen. Since the journal radius R is given, it is then possible to compute λ and consequently $\frac{F}{\lambda\omega_c}$ and $\frac{\frac{\ell}{C}k}{\frac{\ell}{C}\lambda\omega_c}$ for $\frac{L}{D}=\frac{1}{2}$ and $\frac{L}{D}=1$ and for various values of the clearance C.

As it would be time consuming to cover the complete speed range, it should be sufficient to base the comparison on rather few points. This is most easily done in the following way:

a) enter figure 8-10 with $\varepsilon = .2$, $.5$ and $.7$ (except for the elliptical bearing with ellipticity $m = .5$ where the values are $\varepsilon = .15$, $.3$ and $.5$) to find $\frac{F}{\lambda\omega_c\frac{\omega}{\omega_c}}$.

b) divide the result into $\frac{F}{\lambda\omega_c}$ to get $\frac{\omega}{\omega_c}$ and enter figure 11 with $\frac{\omega}{\omega_c}$ to obtain the equivalent speed ratio $\left(\frac{\omega}{\omega_c}\right)'$.

c) enter figures 28-43 with the values of $\left(\frac{\omega}{\omega_c}\right)'$ to the intersection with the corresponding ε-curve. Read off the value of $\frac{P}{\frac{\ell}{C}\lambda\omega_c\frac{\omega}{\omega_c}}$ and multiply by $\frac{\ell}{C}\lambda\omega_c\frac{\omega}{\omega_c}$ to find the actual transmitted force P lbs.

Thus, for each clearance value and for each bearing type and $\frac{L}{D}$ -ratio, three points are readily obtained on the curve of transmitted force versus rotor speed. A fourth point is P=0 for $\frac{\omega}{\omega_c}=0$.

Although four points are not sufficient to define the graph of P versus speed with any high degree of accuracy, it may at least be enough to serve as a basis for comparison and a subsequent selection of bearing clearance.

The effect of oil viscosity is treated in the same way.

DYNAMIC OPERATION

Attenuation of structure borne noise through bearings is only one dynamic characteristic of bearings. There are several other examples of dynamic operations, e.g.:

a.) Transient conditions during starting or shutting down.

b.) Orbiting of the journal under a constant vibrating load.

c.) Motions of the journal center under oscillating loads.

The locus of the journal may be in a closed path of fixed amplitude or it may increase. In the latter case the system may be unstable causing the journal to rub the bearing. Fig. 50 shows several cases of dynamic behavior.

The previous section which deals with the analysis of structure borne noise through bearings indicates that for most effective noise attenuation the journal should operate at low eccentricity ratio. On the other hand it has also been shown (Ref. 1) that rotors operating at low eccentricity ratio are susceptible to instability at relatively low speed. In fact it has been proved theoretically and experimentally (Ref. 2) that the threshold of instability for vertical rotor in plain cylindrical journal bearings is zero speed. These two conditions are, therefore, somewhat incompatible. Since the system must be stable it is, therefore, necessary to optimize noise attenuation without sacrificing stability.

To make the report more complete a section dealing with Stability and Balancing is also discussed briefly in this report. Several definitions are given so as to clarify the usage of some of the terms used.

DYNAMIC OPERATION

Under this condition, the journal center moves relative to the bearing center and the local fluid film pressures vary with time. (Ref. 3)

Instability

This is a dynamic condition in which the journal center moves away from the bearing center, until breakdown of the film occurs and there is physical contact between the journal and the bearing. Another condition that may be defined as unstable is that in which the journal center whirls along a random locus.

Threshold of Instability

Corresponds to frequency at which instability is initiated.

Resonant Whip

This is a resonant vibration of a journal in a fluid-film bearing which, for low eccentricity ratio, sets in at approximately twice the actual first system critical and persists at higher speeds with frequency of vibration approximately equal to the first system critical regardless of running speed. The motion of the shaft center is in the same direction as shaft rotation. Resonant whip is a self-supported vibration, as is half-frequency whirl. In the case of resonant whip, the vibration is supported by the fluid film action, while the frequency is controlled by the system critical speed.

Critical Speed

Critical speed is the rotating speed of a system which corresponds to resonance frequency of the system. The system's critical speeds include rigid body as well as bending or torsional critical speeds. (In this text when we refer to first critical we mean bending body critical.)

Synchronous Whirl

This is a whirling orbital motion of the journal at a frequency equal to the rotational frequency. The motion of the journal is in the same direction as the direction of the rotating member.

An example of the synchronous whirl is the case of unbalanced rotating load. (In the case of vertical rotor in plain cylindrical journal bearings, the whirling locus is a circle; in the case of horizontal machine with plain cylindrical journal bearings the whirling locus is an ellipse. See Fig. 50.)

STABILITY

Using the coordinate system of Fig. 51 the dynamic equations may be represented by

$$\begin{aligned} &\lambda\left(-\frac{\omega f_r \xi}{\epsilon_o C} - \frac{2 f_t \dot{\xi}}{\epsilon_o C} + \frac{\omega\,\partial f_t}{\partial\epsilon}\frac{\eta}{C} + \frac{\partial f_t}{\partial\epsilon'}\frac{\dot{\eta}}{C}\right) = \frac{M}{2}(\ddot{x} + \ddot{\xi}) = -\frac{kx}{2} \\ &\lambda\left(-\frac{\omega f_t \xi}{\epsilon_o C} + \frac{2 f_r \dot{\xi}}{\epsilon_o C} - \frac{\omega\,\partial f_r}{\partial\epsilon}\frac{\eta}{C} - \frac{\partial f_r}{\partial\epsilon'}\frac{\dot{\eta}}{C}\right) = \frac{M}{2}(\ddot{y} + \ddot{\eta}) = -\frac{ky}{2} \end{aligned} \tag{31}$$

Here the functions f_r, f_t and their derivatives with respect to ϵ, ϵ' are all evaluated at the equilibrium eccentricity ratio ϵ_o, and for $\epsilon' = 0$.

$$\lambda = \frac{\mu L R}{\pi}\left(\frac{R}{C}\right)^2 \text{, M is rotor mass,} \qquad d\epsilon = \frac{\eta}{C}\ , \qquad d\alpha = \frac{\xi}{\epsilon_o C}$$

$$d\epsilon' = \frac{d\dot{\epsilon}}{\omega} = \frac{\dot{\eta}}{C\omega}\ , \quad d\dot{\alpha} = \frac{\dot{\xi}}{\epsilon_o C}$$

The differential Eqs. (31) are linear in the variables ξ, η; x, y, and their solutions contain time as an exponential. These may be expressed in dimensionless form as

$$e^{\nu\tau} \quad \text{where } \tau = \omega_o t \qquad \omega_o = \sqrt{\frac{k}{M}} \tag{32}$$

Here ω_o is the critical speed of the simply supported shaft-rotor system whose mass is M and whose stiffness is k.

From the right-hand pair of Eqs.(31), there results

$$x = -\frac{M\,(\nu\omega_o)^2}{k + M\,(\nu\omega_o)^2}\,\xi \qquad y = -\frac{M\,(\nu\omega_o)^2}{k + M\,(\nu\omega_o)^2}\,\eta \tag{33}$$

Equation (31) now leads to the determinantal equation

$$\begin{vmatrix} \left(\omega f_r + 2\nu\omega_o f_t + \dfrac{kM\epsilon_o C\,(\nu\omega_o)^2}{2\lambda\left[k + M\,(\nu\omega_o)^2\right]}\right) & \left(\omega \dfrac{\partial f_t}{\partial \epsilon} + \nu\omega_o \dfrac{\partial f_t}{\partial \epsilon'}\right) \\ \left(-\omega f_t + 2\nu\omega_o f_r\right) & \left(\omega \dfrac{\partial f_r}{\partial \epsilon} + \nu\omega_o \dfrac{\partial f_r}{\partial \epsilon'} + \dfrac{kmC\,(\nu\omega_o)^2}{2\lambda\left[k + M\,(\nu\omega_o)^2\right]}\right) \end{vmatrix} = 0 \tag{34}$$

If we now introduce the dimensionless ratio

$$s = \frac{\omega}{\omega_o} \tag{35}$$

where ω is the angular speed at the threshold of instability, we get

$$f(\nu) = \omega_o^{\,2} \begin{vmatrix} \left(sf_r + 2\nu f_t + \dfrac{A\epsilon_o \nu^2}{1 + \nu^2}\right) & \left(s\dfrac{\partial f_t}{\partial \epsilon} + \nu \dfrac{\partial f_t}{\partial \epsilon'}\right) \\ \left(-sf_t + 2\nu f_r\right) & \left(\dfrac{A\nu^2}{1 + \nu^2} + s\dfrac{\partial f_r}{\partial \epsilon} + \nu \dfrac{\partial f_r}{\partial \epsilon'}\right) \end{vmatrix} = 0 \tag{36}$$

where

$$A = \frac{kC^3\pi}{2\mu LR^3\omega_o} \tag{37}$$

By writing

$$\zeta = \frac{A\nu^2}{1 + \nu^2} \tag{38}$$

Eq. (36) becomes

$$\omega_o^2 \begin{vmatrix} \left(sf_r + 2\nu f_t + \epsilon_o\zeta\right) & \left(s\dfrac{\partial f_t}{\partial \epsilon} + \nu\dfrac{\partial f_t}{\partial \epsilon'}\right) \\ \left(-sf_t + 2\nu f_r\right) & \left(s\dfrac{\partial f_r}{\partial \epsilon} + \nu\dfrac{\partial f_r}{\partial \epsilon'} + \zeta\right) \end{vmatrix} = 0 \qquad (39)$$

ω_o is not, in general, equal to zero, so that the factor ω_o^2 can be divided out of Eq. (39).

It was assumed in the derivation of Eq. (34) that the solutions of the equations of motion were of the form $e^{\nu\tau}$, where ν is a complex number. If the system is dynamically stable, the real part of the complex number ν is negative. Conversely, if the system is dynamically unstable, the real part of ν is positive. Thus, at the threshold of instability, ν will be a pure imaginary number.

We now solve Eq. (39) for the condition where ν is wholly imaginary in order to obtain the value of ω at the onset of instability.

Considering first the imaginary part of Eq. (39), we have

$$\nu \begin{vmatrix} 2f_t & s\dfrac{\partial f_t}{\partial \epsilon} \\ 2f_r & \left(s\dfrac{\partial f_r}{\partial \epsilon} + \zeta\right) \end{vmatrix} + \nu \begin{vmatrix} \left(sf_r + \epsilon\zeta\right) & \dfrac{\partial f_t}{\partial \epsilon'} \\ -sf_t & \dfrac{\partial f_r}{\partial \epsilon'} \end{vmatrix} = 0$$

Since $\nu \neq 0$,

$$\zeta\left(2f_t + \epsilon\frac{\partial f_r}{\partial \epsilon'}\right) + s\left(f_r\frac{\partial f_r}{\partial \epsilon'} + f_t\frac{\partial f_t}{\partial \epsilon'}\right) + 2s\left(f_t\frac{\partial f_r}{\partial \epsilon} - f_r\frac{\partial f_t}{\partial \epsilon}\right) = 0$$

If $s = 0$, we obtain a trivial solution; for $s \neq 0$, we have

$$\frac{\zeta}{s} = \frac{-2(f_t\,\partial f_r/\partial\epsilon - f_r\,\partial f_t/\partial\epsilon) - (f_r\,\partial f_r/\partial\epsilon' + f_t\,\partial f_t/\partial\epsilon')}{2f_t + \epsilon\,\partial f_r/\partial\epsilon'} \qquad (40)$$

Next considering the real part of Eq. (39), we have

$$\begin{vmatrix} \left(sf_r + \epsilon\zeta\right) & s\dfrac{\partial f_t}{\partial \epsilon} \\ -sf_t & \left(s\dfrac{\partial f_r}{\partial \epsilon} + \zeta\right) \end{vmatrix} + 2\nu^2 \begin{vmatrix} f_t & \dfrac{\partial f_t}{\partial \epsilon'} \\ f_r & \dfrac{\partial f_r}{\partial \epsilon'} \end{vmatrix} = 0$$

Therefore

$$s^2\left(f_r\frac{\partial f_r}{\partial \epsilon} + f_t\frac{\partial f_t}{\partial \epsilon}\right) + s\zeta\left(f_r + \epsilon\frac{\partial f_r}{\partial \epsilon}\right) + \epsilon\zeta^2 + 2\nu^2\left(f_t\frac{\partial f_r}{\partial \epsilon'} - f_r\frac{\partial f_t}{\partial \epsilon'}\right) = 0$$

Again, for $s \neq 0$, we have

$$\left(\frac{\nu}{s}\right)^2 = \frac{-\epsilon(\zeta/s)^2 - (f_r + \epsilon\,\partial f_r/\partial\epsilon)(\zeta/s) - (f_r\,\partial f_r/\partial\epsilon + f_t\,\partial f_t/\partial\epsilon)}{2\left[f_t\,\partial f_r/\partial\epsilon' - f_r\,\partial f_t/\partial\epsilon'\right]} \qquad (41)$$

From Eq. (38) we have

$$\zeta\nu^2 - A\nu^2 + \zeta = 0$$

Once again, for $s \neq 0$, we can write

$$s^2\frac{\zeta}{s}\left(\frac{\nu}{s}\right)^2 - s\,A\left(\frac{\nu}{s}\right)^2 + \frac{\zeta}{s} = 0$$

or

$$s = \frac{A\,(\nu/s)^2 \pm \sqrt{\left[A\,(\nu/s)^2\right]^2 - 4\,(\zeta/s)^2(\nu/s)^2}}{2\,(\zeta/s)\,(\nu/s)^2} \qquad (42)$$

The speed ω at which instability starts to occur is now defined, since $\omega = s\omega_o$.

The above defined speed at which instability sets in is, in general, different from the critical speed of the shaft-rotor-bearing system. For a symmetrical, two-bearing system the critical speed may be calculated as follows:

a. Shaft stiffness $= k$

b. Lubricant film stiffness $= \dfrac{dF}{de} = \dfrac{\mu L\omega R(R/C)^2}{C}\,\dfrac{df}{de}$

$$= \frac{sk}{2A}\,\frac{df}{d\epsilon}$$

The critical speed of the system is then

$$\omega_{CR}^{2} = \frac{1}{M\left(\frac{1}{k} + \frac{1}{2} \cdot \frac{2A}{ks} \Big/ \frac{df}{d\epsilon}\right)} = \frac{k/M}{1 + \frac{A}{s} \Big/ \frac{df}{d\epsilon}}$$

or

$$\left(\frac{\omega_{CR}}{\omega_o}\right)_r = \left(\frac{df_r/d\epsilon}{df_r/d\epsilon + A/s}\right)^{1/2} \qquad (43)$$

where subscript r refers to radial stiffness.

The dimensionless number A [defined in Eq. (37)], is a function of bearing geometry, shaft stiffness, and fluid viscosity. Calculations for the threshold of instability in which A was varied from 0.1 to 100 for $0.1 \leq \epsilon \leq 0.8$ and L/D = 0.5 and 1 were performed. The values of f_r, f_t, $\partial f_r/\partial\epsilon$, $\partial f_t/\partial\epsilon$, $\partial f_r/\partial\epsilon'$ and $\partial f_t/\partial\epsilon'$ were obtained from the solution of the dimensionless Reynolds equation. By introducing these values into Eqs. (37), (40), (42), and (43), we obtain the results of Table 6. The results indicate that, while for low eccentricity ratios instability sets in at approximately twice the critical speed, this number increases with an increase in eccentricity ratio. Thus, the onset of instability for eccentricity ratios of 0.8 is about four times the critical speed. This conclusion agrees with observations which show that stability increases with an increase in eccentricity ratio and also that instability may occur even at high eccentricity ratios.

The number $(1/i)(\nu/s)$ shown in Table 6 (where $i = \sqrt{-1}$) represents the ratio of the frequency of the oscillation of the shaft center to the running frequency of the shaft, calculated at the onset of instability. Note that this ratio is always below 0.5 and is independent of the magnitude of A.

BALANCING

A rotor is said to be balanced perfectly when it rotates in free space about one of its principal axes of inertia, which would be an axis of symmetry if such exists, with no wobble. If circular journals are now constructed concentric with this axis, by definition, these journals would also rotate with no wobble and may be enclosed in bearing housings with no rotating forces.

From this it follows that journals which are not concentric with a principal axis of inertia tend to wobble and for a rotor to revolve about an axis defined by such journals it must be driven by a set of applied forces which rotate with the rotor If the center of gravity of the rotor is not on the line of bearing center there must be a net force which furnishes the centripetal acceleration of the center of gravity. This force is equal to the mass of the rotor times the centripetal acceleration of the C.G. The C.G. may be moved to the axis of bearing center by suitable weight or weights. Such correction is commonly called static balancing.

Once the C.G. is moved to the line of bearing centers a rotating couple must be applied to keep the rotor rotating about an axis at an angle to that of a principal axis of inertia. This couple may be exerted by the centrifugal action of two equal and opposite weights in any two arbitrary planes. This correction plus that of the C.G. correction is known as dynamic balance and may only be determined on a rotating rotor-bearing system.

The most fundamental, but not unusual, description of unbalance appears to be that of the deviation of the line of bearing centers from the principal axis of inertia. It is important to note that the specifications of unbalance depends on the location of the line of bearing centers. The two simplest descriptions of unbalance would appearto be the displacement of the C.G. and the angle of the inertia axis from the bearing axis or the displacement of the geometric centers of the journals from the bearing axis. (Refer to Fig. 51)

Under dynamical conditions either $\dot{e}$ or α or both may not be constant. The conditions of dynamical equilibrium gives rise to the following equations.

$$F_r = -m \left\{ \delta \left[\omega^2 \cos (\beta - \alpha) + \dot{\omega} \sin (\beta - \alpha) \right] + \ddot{e} - e(\dot{\alpha})^2 \right\} + W \cos \alpha \quad (44a)$$

$$F_t = m \left\{ \delta \left[\omega^2 \sin (\beta - \alpha) - \dot{\omega} \cos (\beta - \alpha) \right] + e\ddot{\alpha} + 2 \dot{e} \alpha \right\} + W \sin \alpha \quad (44b)$$

where

$\dot{\omega}$ = is the angular acceleration of the rotor (generally very small)

δ = is distance between rotor geometric center and mass center

These are equations of motion with e and α as the two degrees of freedom. Once the fluid film forces are known it is possible to solve these equations.

The fluid film forces are to be found by integrating the pressure over the projected journal surfaces normal and parallel to the plane of maximum film thickness respectively.

$$F_r = - \int_{-L/2}^{L/2} dz \int_{o}^{2\pi} d\theta \; R \; p \cos \theta \quad (45a)$$

$$F_t = \int_{-L/2}^{L/2} dz \int_{o}^{2\pi} d\theta \; R \; p \sin 0 \quad (45b)$$

The fluid film pressure satisfies the generalized Reynolds equation

$$\frac{\partial}{\partial \theta} \left[(1 + \epsilon \cos \theta)^3 \frac{\partial p}{\partial \theta} \right] + R^2 \frac{\partial}{\partial z} \left[(1 + \epsilon \cos \theta)^3 \frac{\partial p}{\partial z} \right]$$

$$= 6\mu \left(\frac{R}{C} \right)^2 \left[-c(\omega - 2\dot{\alpha}) \sin \theta + 2 \dot{c} \cos \theta \right] \quad (46)$$

Thus it can be shown that the radial and tangential forces are a function of

$$F_r = -\frac{\mu L R}{\pi}\left(\frac{R}{C}\right)^2 (\omega - 2\dot{\alpha})\ f_r\ (\epsilon, \frac{\dot{\epsilon}}{(\omega - 2\dot{\alpha})}, L/D) \tag{57a}$$

$$F_t = \frac{\mu L R}{\pi}\left(\frac{R}{C}\right)^2 (\omega - 2\dot{\alpha})\ f_t\ (\epsilon, \frac{\dot{\epsilon}}{(\omega - 2\dot{\alpha})}, L/D) \tag{57b}$$

Thus for a specified bearing geometry and speed of rotation once ϵ, $\dot{\epsilon}$ and $\dot{\alpha}$ are measured the fluid film forces can be readily calculated. They may be constant per cycle $\dot{\epsilon} = 0$ (e.g., vertical rotor in plain cylindrical journal bearings) or they may vary from point to point along the journal locus this case corresponds to the horizontal rotor with gravity and unbalance load. Once these forces are established the magnitude and phase angle of the unbalance force can be calculated from the dynamic equations (54a,b). This permits balancing of the rotor without a trial and error procedure.

The measurements of displacement (ϵ) and velocity ($\dot{\epsilon}, \dot{\alpha}$) of journal center can be obtained by use of two capacitive or inductive probes located at 90° to each other within the bearing bore. They would then measure the motion of the journal center with respect to the bearing center as a function of time. These capacitive or inductive probes can also serve as monitoring devices to determine bearing performance in service. Thus they serve a dual function of providing the necessary measurements for balancing and monitoring bearing performance. Figs. 48 and 49 show the locus of the shaft center that such pickups would see.

Without the use of such instrumentation within the bearing there is still another method which may be employed for balancing. The analysis presented in this report indicates that there is a relation between the driving force and the transmitted force. The difference being the attenuation.

Since the attenuation has been theoretically calculated by measurement of force transmitted it is possible to calculate the driving force and the phase angle. Once this is done it is possible to balance the rotor without resorting to trial and error procedure.

This analysis indicates that by either measurements of journal locus or transmitted force it is possible to determine the magnitude and phase angle of the unbalance. Corrections can then be incorporated to balance the system.

To illustrate this point, theoretical and experimental analysis have been carried out on synchronous whirl (e.g., whirl produced at running speed, unbalance load) with circular orbit about the bearing center (e.g., vertical rotor). (Ref. 4) The comparison between the measured unbalance force and phase angle and calculated values appear to be very good, similar comparisons will be carried out on horizontal rotor.

CONCLUSIONS

1. Attenuation of structure borne noise should be done as close to the source of noise as possible. Fluid film bearings provide the source of attenuation. Close

2. The report provides means for calculating noise attenuation of rotors supported by bearings of three geometries. The results are presented in dimensionless form so as to be applicable to a large range of geometrically similar configurations. The report also provides means for calculating system critical speeds and the static load carrying capacity.

3. The report shows that fluid film bearings can provide considerable amount of viscous damping which absorb the vibrational energy and in this way attenuate the force transmitted to the structure. Bearing geometry plays a major role on the level of attenuation as exemplified by the differences of the three bearings studied, see figures 44-45.

4. Since the fluid film is an elastic media, accurate predictions of the system critical speeds must include the elasticity and the damping of the journal bearings, see figures 46-47.

5. Indications are that for maximum attenuation one should operate at low eccentricity ratio, low stiffness and high damping. However, this implies low critical speed and tendency for resonant whip. Therefore, one must optimize the design to ensure stability and at the same time get maximum attenuation.

6. The dynamic response of a rotor can be measured by capacitor or inductive pick-ups. These can serve also as monitory devices for controlling bearing performance. Obtaining the dynamic response and knowing the bearing characteristics, it is possible to determine the magnitude and phase angle of the unbalance load thus eliminating trial and error in balancing. in RTE's?

RECOMMENDATIONS

1. Other geometries such as pivoted shoes and elastically supported members in which stiffness and damping can be controlled and varied should be investigated. These studies should be both theoretical and experimental for these geometries offer considerable potential in noise attenuation and at the same time have a tendency of being stable.

2. Further studies should be continued to determine rotor dynamics around the second bending critical and higher.

3. Computational techniques should be set up which would include, without transformations, the bearing cross-coupling coefficients.

4. The application of capacitive or inductive pick-ups as permanent measuring devices in bearings should be investigated. Such measurements provide means for continually checking rotor balance and for monitoring bearing performance.

ACKNOWLEDGEMENT

This paper is based on the work performed under Contract Number NObs-78930, Task Order Number 3679, Sub Area F131105 sponsored by the Bureau of Ships.

The authors are indebted to Miss Ann Doughty, David Taylor Model Basin for her assistance in performing the computer calculations and to Mr. Roland Racko who made most of the figures.

REFERENCES

1.) "Dynamic Stability Aspects of Compressible and Incompressible Cylindrical Journal Bearings" by B. Sternlicht, H. Poritsky and E. Arwas, Proceedings from the First Intern. Gas Bearing Symposium, 1959.

2.) "Investigation of Translatory Fluid Whirl in Vertical Machines" by B. Sternlicht, Doctorial Thesis, Columbia University, 1953.

3.) "Elastic and Damping Properties of Cylindrical Journal Bearings" by B. Sternlicht, A.S.M.E. Basic Engineering, June 1959.

4.) "Synchronous Whirl in Plain Journal Bearings" by B. Sternlicht and R.C. Elwell, ONR Report, Contract No. NONR 2844(00), January 30, 1961.

TABLE 1

PLAIN CYLINDRICAL BEARING
Computer Results

$\frac{L}{D}$	ε	$\left(\frac{\dot{\varepsilon}}{\omega}\right)$	f_v	α	f_r	f_t
	.2	0	.4653	75.772	.11436	.45102
	.2	.03			.28010	.48125
	.2	-.03			-.02311	.41915
	.22	0			.14035	.50170
	.18	0			.09149	.40187
	.5	0	1.862	54.763	1.0744	1.5210
	.5	.03			1.4528	1.6485
	.5	-.03			.7538	1.3971
$\frac{1}{2}$	.52	0			1.2172	1.6367
	.48	0			.9508	1.4192
	.7	0	5.160	40.432	3.9274	3.3462
	.7	.03			5.1132	3.6797
	.7	-.03			3.0057	3.0218
	.715	0			4.3861	3.5934
	.685	0			3.5368	3.1349
	.2	0	1.504	76.836	.34257	1.4647
	.2	.03			.86908	1.5517
	.2	-.03			-.10182	1.3768
	.22	0			.41810	1.6240
	.18	0			.27556	1.3089
	.5	0	5.299	57.502	2.8470	4.4693
	.5	.03			3.9082	4.7825
1	.5	-.03			1.9853	4.1527
	.52	0			3.1858	4.7621
	.48	0			2.5455	4.2090
	.7	0	12.34	43.280	8.9832	8.4594
	.7	.03			11.455	9.1654
	.7	-.03			6.805	7.7610
	.715	0			9.8687	8.9177
	.685	0			8.1932	8.0365

TABLE 2

4-AXIAL GROOVE BEARING
Computer Results

$\frac{L}{D}$	ε	α	$\frac{\dot{\varepsilon}}{\omega}$	f_v	f_h
	.2	80.000	0	.2711	.007144
	.2	81.647	0	.26946	.000218
	.2	81.696	0	.26941	0
	.2	81.696	.03	.29197	-.042655
	.2	81.696	-.03	.25277	.022276
	.22	81.696	0	.29980	-.004059
	.18	81.696	0	.23986	.003245
	.5	61.000	0	1.1700	-.004287
	.5	60.413	0	1.1789	-.000642
	.5	60.315	0	1.1805	0
	.5	60.315	.03	1.2164	-.010655
	.5	60.315	-.03	1.1482	.005458
	.52	60.315	0	1.2847	-.019631
$\frac{1}{2}$	.48	60.315	0	1.0848	.016799
	.7	36.000	0	4.3096	-.041049
	.7	35.181	0	4.3135	-.002017
	.7	35.139	0	4.3137	0
	.7	35.139	.03	4.4712	.010973
	.7	35.139	-.03	4.1559	-.010862
	.715	35.139	0	4.7899	-.073303
	.685	35.139	0	3.8962	.059837
	.2	80.000	0	.52918	.023913
	.2	83.881	0	.51908	-.002508
	.2	83.531	0	.52004	0
	.2	83.531	.03	.55702	-.074742
	.2	83.531	-.03	.49585	.038249
	.22	83.531	0	.57700	-.005625
	.18	83.531	0	.46426	.004520
	.5	61.000	0	2.2295	.039473
	.5	64.123	0	2.1370	.003321
	.5	64.431	0	2.1279	0
	.5	64.431	.03	2.1846	-.022831
	.5	64.431	-.03	2.0730	.018699
	.52	64.431	0	2.2948	-.030393
1	.48	64.431	0	1.9714	.026434
	.7	36.000	0	7.7047	-.006564
	.7	35.918	0	7.7060	-.000638
	.7	35.909	0	7.7061	0
	.7	35.909	.03	7.9922	.001840
	.7	35.909	-.03	7.4203	-.001750
	.715	35.909	0	8.4906	-.12758
	.685	35.909	0	7.0118	.10588

TABLE 3

ELLIPTICAL BEARING

Computer Results

	ϵ	α	f_v	f_h	ϵ_1	ϕ_1	$(\dot{\epsilon}_1)$	f_{v1}	f_{h1}	ϵ_2	ϕ_2	$(\dot{\epsilon}_2)$	f_{v2}	f_{h2}
	.2	103.797	.51882	.00002	.28045	43.833	0	.61757	.12873	.35546	33.122	0	.09874	.12871
	.2	100	.56567	.03009	.29178	42.457	0	.64848	.14102	.34622	34.674	0	.08281	.11093
	.2	105	.50359	-.00944	.27680	44.261	0	.60762	.12512	.35830	32.627	0	.10403	.13456
	.2	103.797			.28045	43.833	.03	.79123	.06618	.35546	33.122	.03	.19696	.22105
	.2	103.797			.28045	43.833	-.03	.47744	.16161	.35546	33.122	-.03	.04035	.06220
	.22	103.797	.57692	-.01623	.29098	47.245	0	.67017	.10981	.37031	35.236	0	.09326	.12604
	.18	103.797	.46239	.01538	.27099	40.170	0	.56563	.14603	.34112	30.827	0	.10323	.13065
	.5	55.861	4.3933	-.00220	.67291	37.953	0	4.3933	-.00220	.41497	85.771	0	0	0
	.5	54	4.5213	.05936	.67783	36.640	0	4.5213	.05936	.40688	83.811	0	0	0
$\frac{L}{D} = \frac{1}{2}$	.5	57	4.3114	-.03537	.66982	38.759	0	4.3114	-.03537	.41993	86.958	0	0	0
	.5	55.861			.67291	37.953	.03	5.3265	-.35063	.41497	85.771	.03	0	0
m = .25	.5	55.861			.67291	37.953	-.03	3.5767	.24689	.41497	85.771	-.03	0	0
	.52	55.861	4.9324	-.12343	.69196	38.461	0	4.9324	-.12343	.43242	84.453	0	0	0
	.48	55.861	3.9271	.09314	.65390	37.414	0	3.9271	.09314	.39776	87.216	0	0	0
	.7	24.931	55.096	-.24058	.93268	18.443	0	55.262	-.00608	.48489	37.484	0	.16607	.23450
	.7	23	56.591	1.3452	.93524	17.005	0	56.895	1.6153	.47992	34.744	0	.20402	.27002
	.7	29	49.981	-2.4458	.92662	21.484	0	50.093	-2.2712	.49637	43.133	0	.11239	.17497
	.7	24.931			.93268	18.443	.03	78.739	-4.3878	.48489	37.484	.03	.30661	.38396
	.7	24.931			.93268	18.443	-.03	37.607	2.5599	.48489	37.484	-.03	.07941	.12701
	.71	24.931	68.015	-1.5541	.94261	18.512	0	68.197	-1.2984	.49465	37.231	0	.18257	.25573
	.69	24.931	45.601	.61758	.92274	18.373	0	45.752	-.8332	.47513	37.745	0	.15167	.21566
	.15	89.728	.90262	.00002	.52270	16.676	0	1.6100	.66137	.52133	16.722	0	.70742	.66135
	.15	88	.96191	.03285	.52701	16.926	0	1.6459	.67508	.51698	16.856	0	.68394	.64223
	.15	91	.85855	-.02429	.51950	16.780	0	1.5837	.65151	.52452	16.615	0	.72537	.67580
	.15	89.728			.52270	16.676	.03	2.0538	.68905	.52133	16.722	.03	1.0166	.85694
	.15	89.728			.52270	16.676	-.03	1.2394	.61299	.52133	16.722	-.03	.46709	.48771
	.17	89.728	1.0342	-.00490	.52887	18.750	0	1.7035	.64976	.52735	18.806	0	.66925	.65466
	.13	89.728	.77582	.00535	.51722	14.557	0	1.5187	.67130	.51603	14.591	0	.74285	.66595
	.3	84.491	2.4814	.00067	.60729	29.454	0	2.8966	.52047	.55785	32.364	0	.41515	.51979
$\frac{L}{D} = \frac{1}{2}$	.3	80	2.8740	.15687	.62618	28.153	0	3.2077	.58384	.53657	33.410	0	.33363	.42698
	.3	85	2.4382	-.01778	.60510	29.597	0	2.8636	.51359	.56023	32.240	0	.42546	.53136
m = .50	.3	84.491			.60729	29.454	.03	3.5861	.39014	.55785	32.364	.03	.66512	.75307
	.3	84.491			.60729	29.454	-.03	2.3463	.57677	.55785	32.364	-.03	.22776	.32351
	.32	84.491	2.7378	-.04439	.61897	30.971	0	3.1320	.46528	.56717	34.167	0	.39426	.50968
	.28	84.491	2.2696	.03571	.59605	27.878	0	2.7007	.56154	.54911	30.501	0	.43117	.52583
	.5	20.678	298.93	-.15595	.98376	10.339	0	298.93	-.15595	.17947	79.667	0	0	0
	.5	20	290.39	5.5707	.98481	10.000	0	290.39	5.5707	.17365	80.000	0	0	0
	.5	25	239.49	-8.4445	.97630	12.500	0	239.49	-8.4445	.21644	77.500	0	0	0
	.5	20.678			.98376	10.339	.03	700.79	-56.134	.17947	79.667	.03	.00056	.00137
	.5	20.678			.98376	10.339	-.03	145.05	14.503	.17947	79.667	-.03	0	0
	.51	20.678	775.40	-59.809	.99360	10.442	0	775.40	-59.809	.18153	82.776	0	0	0
	.49	20.678	182.28	6.9082	.97393	10.233	0	182.28	6.9082	.17798	76.496	0	0	0
	.2	105.652	1.4664	-.00048	.27481	44.491	0	1.6448	.21708	.35983	32.358	0	.17845	.21755
	.2	105	1.4862	.00993	.27680	44.261	0	1.6581	.22110	.35830	32.627	0	.17197	.21117
	.2	110	1.3309	-.06822	.26134	45.983	0	1.5541	.19212	.36973	30.551	0	.22319	.26034
	.2	105.652			.27481	44.491	.03	2.1236	.05678	.35983	32.358	.03	.39306	.40089
	.2	105.652			.27481	44.491	-.03	1.2333	.31543	.35983	32.358	-.03	.06671	.09808
	.22	105.652	1.6282	-.04982	.28500	48.015	0	1.7953	.16166	.37494	34.403	0	.16709	.21147
	.18	105.652	1.3012	.03769	.26574	40.710	0	1.4977	.26527	.34523	30.137	0	.19654	.22758
	.5	54.288	10.010	-.00007	.67707	36.842	0	10.010	-.00007	.40813	84.113	0	0	0
	.5	51	10.301	.29239	.68544	34.534	0	10.301	.29239	.39392	80.553	0	0	0
$\frac{L}{D} = 1$	.5	57	9.7394	-.23160	.66982	38.759	0	9.7394	-.23160	.41993	86.958	0	0	0
	.5	54.288			.67707	36.842	.03	12.159	-.73831	.40813	84.113	.03	0	0
m = .25	.5	54.288			.67707	36.842	-.03	8.1820	.50890	.40813	84.113	-.03	0	0
	.52	54.288	11.101	-.23287	.69618	37.336	0	11.101	-.23287	.42560	82.773	0	0	0
	.48	54.288	9.0474	.18671	.65802	36.320	0	9.0474	.18671	.39091	85.571	0	0	0
	.7	25.628	80.156	.00028	.93170	18.964	0	80.401	.33508	.48676	38.464	0	.24576	.33480
	.7	25	81.039	.58077	.93258	18.495	0	81.305	.93516	.48507	37.581	0	.26580	.35439
	.7	27.5	76.911	-1.4131	.92895	20.362	0	77.103	-1.1332	.49198	41.070	0	.19230	.27996
	.7	25.628			.93170	18.964	.03	109.66	-4.7174	.48676	38.464	.03	.49286	.58856
	.7	25.628			.93170	18.964	-.03	53.209	4.7403	.48676	38.464	-.03	.10437	.16437
	.71	25.628	96.227	-1.8917	.94164	19.034	0	96.497	-1.5264	.49651	38.207	0	.27005	.36528
	.69	25.628	68.075	1.2639	.92177	18.891	0	68.299	1.5704	.47701	38.731	0	.22330	.30652

TABLE 3
(Continued)

ELLIPTICAL BEARING
Computer Results

	ϵ	α	f_x	f_y	ϵ_L	α_L	$(\frac{\delta}{\delta})$	f_{xL}	f_{yL}	ϵ_R	α_R	$(\frac{\delta}{\delta})$	f_{xR}	f_{yR}
	.15	94.263	2.0616	.00001	.51122	17.014	0	3.5147	1.2483	.53259	16.312	0	1.4531	1.2483
	.15	93	2.1490	.04401	.51444	16.930	0	3.5673	1.2661	.52948	16.434	0	1.4183	1.2221
	.15	95	2.0101	-.02575	.50934	17.060	0	3.4840	1.2381	.53439	16.238	0	1.4739	1.2638
	.15	94.263			.51122	17.014	.03	4.5497	1.2912	.53259	16.312	.03	2.1909	1.6634
	.15	94.263			.51122	17.014	-.03	2.6536	1.1529	.53259	16.312	-.03	.91724	.89050
	.17	94.263	2.3271	-.02857	.51601	19.180	0	3.7276	1.2161	.53994	18.299	0	1.4004	1.2447
	.13	94.263	1.7678	.01590	.50719	14.810	0	3.3031	1.2773	.52589	14.271	0	1.5353	1.2614
	.3	87.235	5.5986	-.00009	.59538	30.218	0	6.3631	.90295	.57055	31.682	0	.76481	.99304
$\frac{L}{D} = 1$	.3	84	6.1060	.20133	.60939	29.314	0	6.7522	.98053	.55556	32.483	0	.64621	.77920
	.3	90	5.1412	-.17954	.58310	30.964	0	6.0241	.84342	.58310	30.964	0	.86294	1.02296
m = .50	.3	87.235			.59538	30.218	.03	7.8472	.60341	.57055	31.682	.03	1.2947	1.3640
	.3	87.235			.59538	30.218	-.03	5.0667	1.0708	.57055	31.682	-.03	.42279	.55739
	.32	87.235	6.0708	-.10044	.60650	31.803	0	6.8003	.78855	.58049	33.409	0	.72940	.88899
	.28	87.235	5.1252	.07084	.58473	28.574	0	5.9506	1.0032	.56115	29.893	0	.82538	.93231
	.5	21.256	361.66	-.61222	.98285	10.628	0	361.66	-.61222	.18443	79.367	0	0	0
	.5	20	349.96	9.8135	.98481	10.000	0	349.96	9.8135	.17365	80.000	0	0	0
	.5	25	294.90	-6.5638	.97630	12.500	0	294.90	-6.5638	.21644	77.500	0	0	0
	.5	21.256			.98285	10.628	.03	759.62	-54.350	.18443	79.367	.03	.00067	.00161
	.5	21.256			.98285	10.628	-.03	165.36	19.725	.18443	79.367	-.03	0	0
	.51	21.256	904.50	-73.916	.99268	10.735	0	904.50	-73.916	.18654	82.388	0	0	0
	.49	21.256	227.18	9.3925	.97302	10.519	0	227.18	9.3925	.18285	76.287	0	0	0

TABLE 4

Computed on basis of Tables 1, 2, and 3

Bearing Type	$\frac{L}{D}$	m	ε	α	$\frac{\partial f_t}{\partial \varepsilon}$	$\frac{\partial f_t}{\varepsilon \partial \alpha}$	$\frac{\partial f_t}{\partial (L/D)}$	$\frac{2f_t}{\varepsilon}$	$\frac{\partial f_r}{\partial \varepsilon}$	$\frac{\partial f_r}{\varepsilon \partial \alpha}$	$\frac{\partial f_r}{\partial (L/D)}$	$\frac{2f_r}{\varepsilon}$
Plain Cylindrical Bearing	$\frac{1}{2}$		.2	75.772	2.719	0	2.245	4.791	-.571	-2.396	-4.644	0
			.5	54.763	8.235	0	10.14	7.449	-2.304	-3.725	-7.098	0
			.7	40.432	31.46	0	33.85	14.74	-6.726	-7.371	-14.43	0
	1		.2	76.836	6.483	0	6.524	15.04	-1.676	-7.521	-15.09	0
			.5	57.502	20.26	0	26.07	21.20	-6.073	-19.60	-21.39	0
			.7	43.280	60.79	0	72.47	32.26	-16.91	-17.63	-35.09	0
4-Axial Groove Bearing	$\frac{1}{2}$		.2	81.695	1.499	-.270	.653	2.694	-.183	-1.286	-.108	0
			.5	60.315	4.998	-1.753	1.137	4.722	-.911	-.723	-.269	0
			.7	35.139	29.79	-.399	5.255	12.33	-4.438	-3.901	.364	0
	1		.2	83.531	2.819	-.781	1.020	5.200	-.254	-2.044	-1.883	0
			.5	64.431	8.085	-3.382	1.860	8.512	-1.421	-1.267	-.692	0
			.7	35.939	49.29	-1.240	9.532	22.02	-7.782	-5.916	.060	0
Elliptical Bearing	$\frac{1}{2}$	.25	.2	103.799	2.863	-3.606	-2.722	8.921	-.7902	-2.256	-3.030	1.419
			.5	55.789	25.13	-8.085	23.73	21.39	-5.414	-3.531	-9.471	-3.061
			.7	24.609	1121	-75.17	670.1	198.2	-108.6	-62.32	-112.2	-9.234
		.50	.15	89.729	6.460	-13.18	-1.928	24.33	-.2563	-7.281	-1.361	8.570
			.3	84.510	11.70	-16.28	2.056	29.57	-2.003	-6.896	-4.758	5.662
			.5	20.656	29660	794.2	9057	1961	-3336	-818.5	-1158	-211.2
	1	.25	.2	105.622	8.175	-8.709	-6.706	23.15	-2.138	-4.571	-6.406	1.261
			.5	54.287	51.35	-11.41	54.37	48.68	-10.49	-10.04	-19.83	-6.233
			.7	25.628	1408	-121.8	918.2	286.9	-157.8	-72.17	-152.3	-11.82
		.50	.15	94.263	13.98	-26.61	-8.788	55.65	-1.112	-13.33	-4.391	17.03
			.3	87.234	23.64	-31.49	2.613	64.52	-4.282	-12.26	-10.51	8.412
			.5	21.155	33870	52.03	9598	2553	-4165	-717.9	-1214	-227.7

Bearing Type	$\frac{L}{D}$	m	ε	$\frac{\partial f}{\partial \varepsilon}$	$\frac{\partial f}{\partial (L/D)}$	$\frac{2f}{\varepsilon}$	$\frac{\partial f}{\partial \varepsilon}$	$\frac{\partial f}{\partial (L/D)}$	$\frac{2f}{\varepsilon}$
Plain Cylindrical Bearing	$\frac{1}{2}$		.2	1.222	5.054	1.144	2.496	1.035	4.653
			.5	6.662	11.65	4.298	5.438	4.190	6.094
			.7	29.31	35.13	11.22	15.28	10.96	9.561
	1		.2	3.564	16.18	3.426	7.878	2.916	14.65
			.5	16.01	32.05	11.39	13.83	10.50	17.88
			.7	55.85	77.50	25.67	29.37	23.41	24.17

Bearing Type	$\frac{L}{D}$	m	ε	$\frac{\partial f_{xx}}{\partial (L/D)}$	$\frac{\partial f_{xy}}{\partial (L/D)}$	$\frac{2f_{xx}}{\varepsilon}$	$\frac{2f_{xy}}{\varepsilon_x}$	$\frac{\partial f_{y}}{\partial (L/D)}$	$\frac{\partial f_{yx}}{\partial (L/D)}$	$\frac{2f_{y}}{\varepsilon_x}$	$\frac{2f_{yy}}{\varepsilon_x}$
Elliptical Bearing	$\frac{1}{2}$	.25	.2	5.230	2.610	4.424	.5556	-1.591	2.647	.9180	.7242
			.5	29.15	0	13.06	0	-9.954	0	0	0
			.7	685.5	3.787	118.5	.6850	-115.8	4.283	.5412	1.043
		.50	.15	13.57	9.158	6.161	2.714	1.267	6.154	2.531	2.537
			.3	20.65	7.289	9.539	1.488	-3.111	7.159	1.714	1.864
			.5	9252	.0094	303.9	0	-1177	.0228	0	0
	1	.25	.2	14.84	5.439	11.97	.9918	-4.371	5.047	1.560	1.209
			.5	66.28	0	29.57	0	-20.79	0	0	0
			.7	940.9	6.475	172.6	1.010	-157.6	7.070	.7193	1.376
		.50	.15	31.60	21.23	13.75	5.457	2.395	12.88	4.883	4.683
			.3	46.34	14.53	21.38	2.650	-7.789	13.44	3.033	3.165
			.5	9904	.01117	7359	0	-1235	.0269	0	0

Note:

For the elliptical bearing $\frac{\partial f}{\partial (L/D)}$, $\frac{2f}{\varepsilon}$, $\frac{\partial f}{\partial (L/D)}$ and $\frac{2f}{\varepsilon}$ are not computed directly but calculated from eq. (13), page 8

TABLE 5

Computed from Table 4 and Equation (9), page 5-6

Bearing Type	$\frac{L}{D}$	m	ε	$\frac{K_{xx}}{\epsilon\lambda\omega}$	$\frac{\omega C_{xx}}{\epsilon\lambda\omega}$	$\frac{K_{xy}}{\epsilon\lambda\omega}$	$\frac{\omega C_{xy}}{\epsilon\lambda\omega}$	$\frac{K_{yx}}{\epsilon\lambda\omega}$	$\frac{\omega C_{yx}}{\epsilon\lambda\omega}$	$\frac{K_{yy}}{\epsilon\lambda\omega}$	$\frac{\omega C_{yy}}{\epsilon\lambda\omega}$
Plain Cylindrical Bearing	$\frac{1}{2}$		.2	.651	5.20	-2.64	-.999	2.18	-1.11	1.14	4.51
			.5	4.78	11.94	-6.77	-3.99	1.71	-4.10	4.03	5.80
			.7	23.95	35.32	-20.40	-10.73	-.339	-10.99	9.97	9.36
	1		.2	1.93	16.13	-8.26	-2.93	6.94	-3.44	3.34	14.70
			.5	10.89	31.88	-17.09	-10.60	5.68	-11.49	10.82	18.04
			.7	44.26	76.93	-41.68	-24.02	-.233	-26.28	24.42	24.74
4-Axial Groove Bearing	$\frac{1}{2}$		.2	.484	2.76	-1.44	-.257	1.25	-.156	.366	1.07
			.5	4.00	4.67	-3.47	1.35	.177	-.133	1.15	.233
			.7	24.59	11.39	-16.83	7.05	-1.38	.298	5.74	-.209
	1		.2	1.09	5.28	-2.71	-.428	2.00	-.212	.482	1.87
			.5	6.54	8.48	-5.83	2.00	.530	-.299	1.83	.624
			.7	40.65	20.63	-27.90	12.24	-2.83	.048	9.36	-.035
Elliptical Bearing	$\frac{1}{2}$	.25	.2	2.819	9.313	-3.640	.5157	2.379	2.101	.2293	2.604
			.5	20.82	31.03	-16.24	-7.598	-.1239	-7.856	6.462	6.111
			.7	1050	691.8	-398.5	-98.85	-72.78	-105.9	101.9	38.33
		.50	.15	13.21	24.32	-6.398	2.043	7.280	8.563	.2907	1.402
			.3	17.32	29.63	-10.09	.7824	6.673	5.181	2.654	5.278
			.5	27470	9166	-11210	-1360	-2833	-1158	1943	210.9
	1	.25	.2	6.186	24.10	-10.22	.2242	4.991	2.939	.8763	5.830
			.5	39.24	70.78	-35.03	-16.08	2.029	-16.64	14.38	12.46
			.7	1322	951.6	-499.2	-139.3	-111.1	-142.4	133.3	55.22
		.50	.15	25.50	56.15	-15.92	4.627	13.38	17.31	.1181	3.113
			.3	32.59	64.57	-22.09	.5038	12.04	7.895	4.869	10.90
			.5	31570	9871	-12270	-1086	-3625	-1214	2173	225.8

TABLE 6

THRESHOLD OF INSTABILITY FOR SYMMETRICAL ROTOR

SUPPORTED BY PLAIN JOURNAL BEARINGS

L/D	ϵ	A	ζ/s	$(\nu/\lambda)^2$	$\frac{1}{i}\ \frac{\nu}{s}$	s	$\frac{(\omega_{CR})_r}{\omega_o}$	$\frac{\omega}{(\omega_{CR})_r}$
1/2	0.2	0.1	- 0.9429	-0.1411	0.3756	2.6096	0.9852	2.6488
	0.5	0.1	- 3.1968	-0.1252	0.3538	2.8104	0.9974	2.8177
	0.8	0.1	-13.4452	-0.05543	0.2354	4.2438	0.9998	4.2446
1/2	0.2	100.0	- 0.9429	-0.1411	0.3756	0.06678	0.02910	2.2948
	0.5	100.0	- 3.1968	-0.1252	0.3538	0.2533	0.1315	1.9262
	0.8	100.0	-13.4452	-0.05543	0.2354	1.9267	0.7751	2.4857
1	0.2	0.1	- 2.6761	-0.1377	0.37	2.6763	0.9948	2.6903
	0.3	0.1	- 4.324	-0.1338	0.37	2.7224	0.9971	2.7303
	0.7	0.1	-18.484	-0.0846	0.29	3.4179	0.9998	3.4186
	0.8	0.1	-29.2005	-0.04898	0.22	4.5169	0.9999	4.5173
1	0.2	100.0	- 2.6761	-0.1377	0.37	0.1951	0.0834	2.3420
	0.3	100.0	- 4.324	-0.1338	0.37	0.3198	0.1390	2.300
	0.7	100.0	-18.483	-0.0846	0.29	1.6553	0.7000	2.3647
	0.8	100.0	-29.2005	-0.04898	0.22	3.1199	0.8998	3.4675

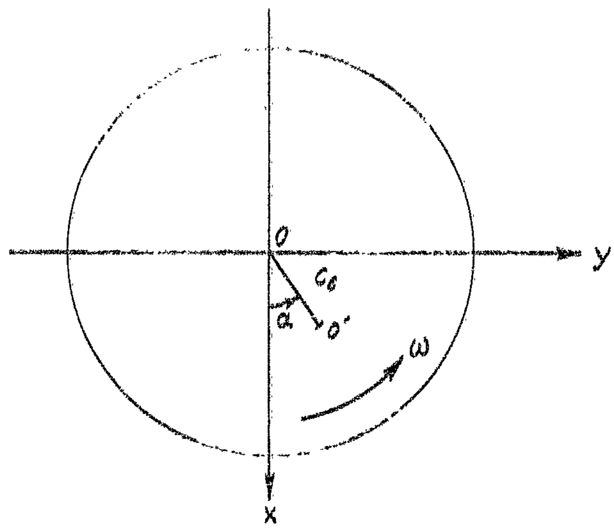

Figure 1   Plain Cylindrical Bearing

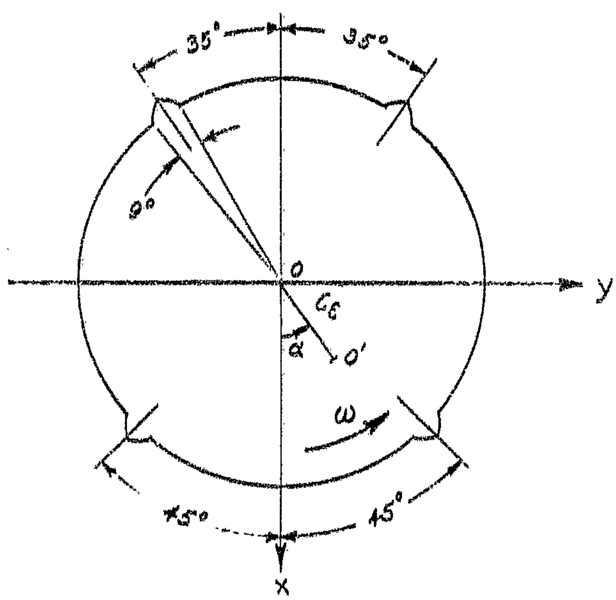

Figure 2   4-Axial Groove Bearing

O' - Steady-state position at journal center

A - Actual journal center

B - Shaft center at midspan

G - Center of gravity of rotor

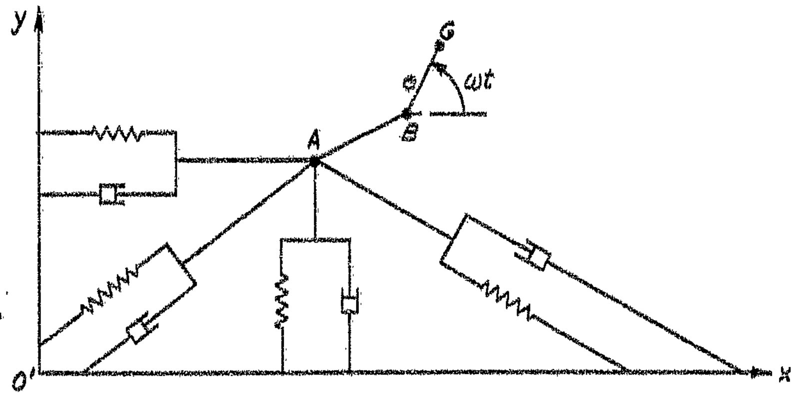

Figure 6 Rotor - Bearing System

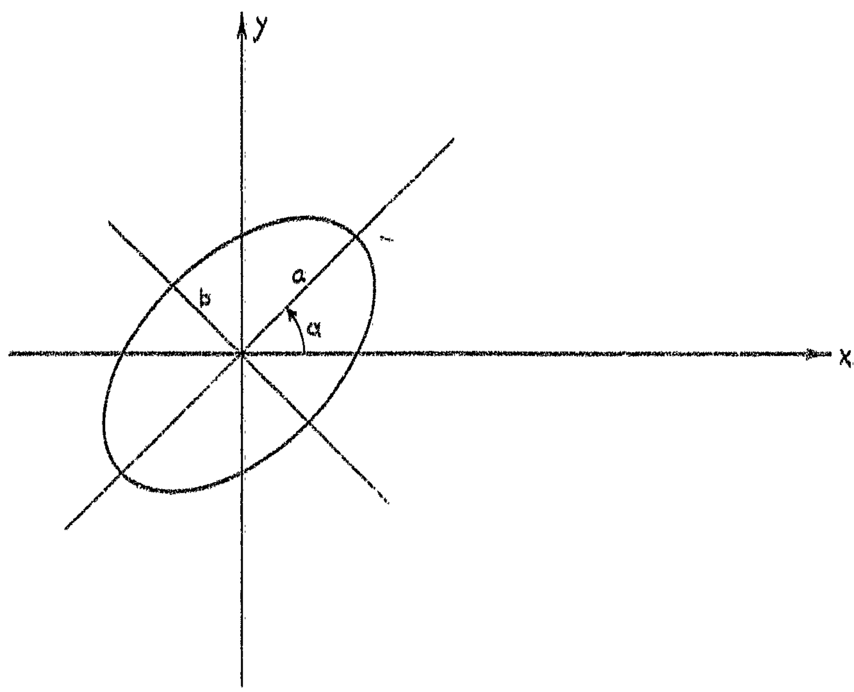

Figure 7 Journal Center Path

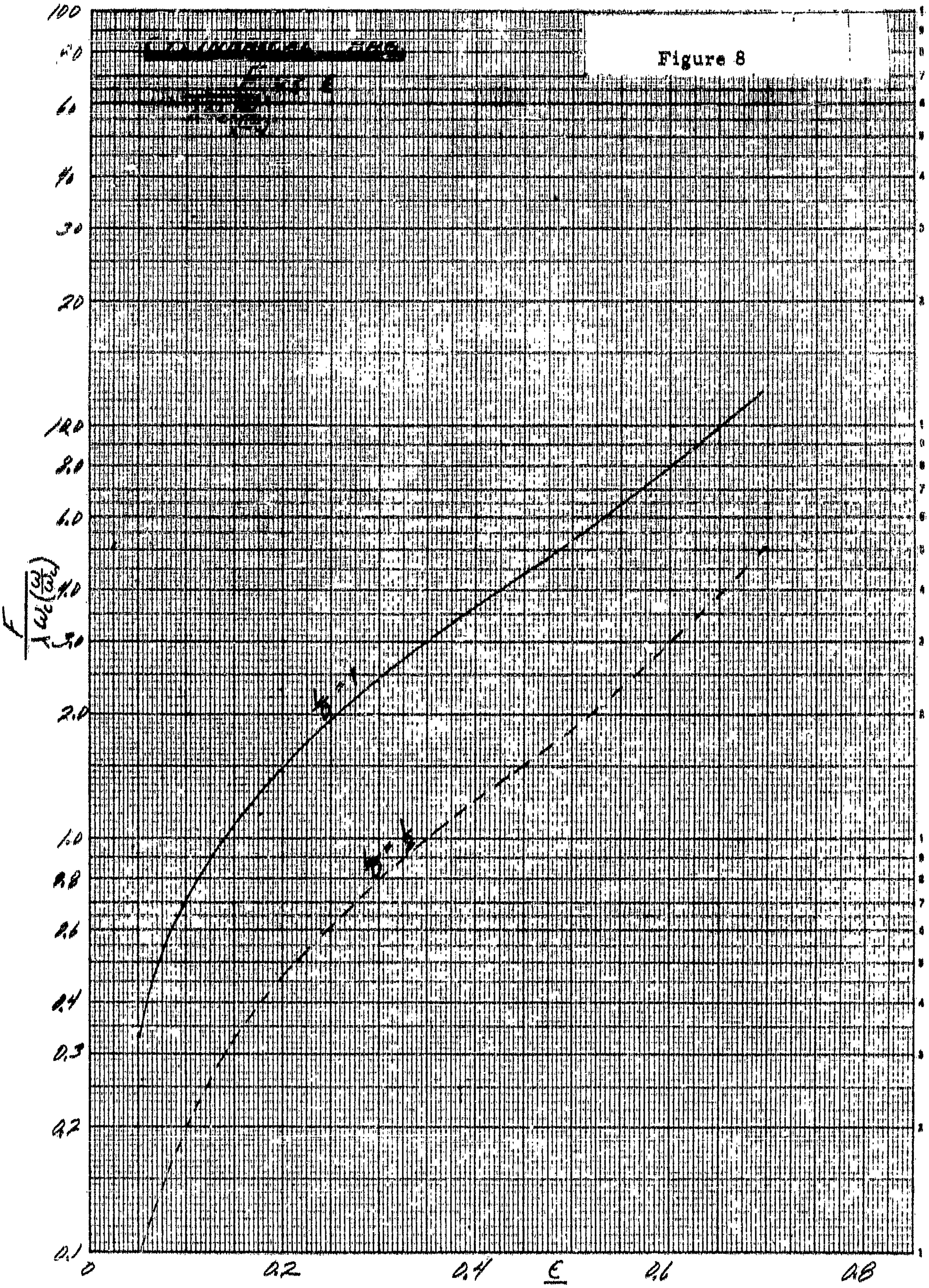
100
80
60
40
30
20
10.0
8.0
6.0
4.0
3.0
2.0
1.0
0.8
0.6
0.4
0.3
0.2
0.1
0
0.2
0.4
ε
0.6
0.8

Figure 8

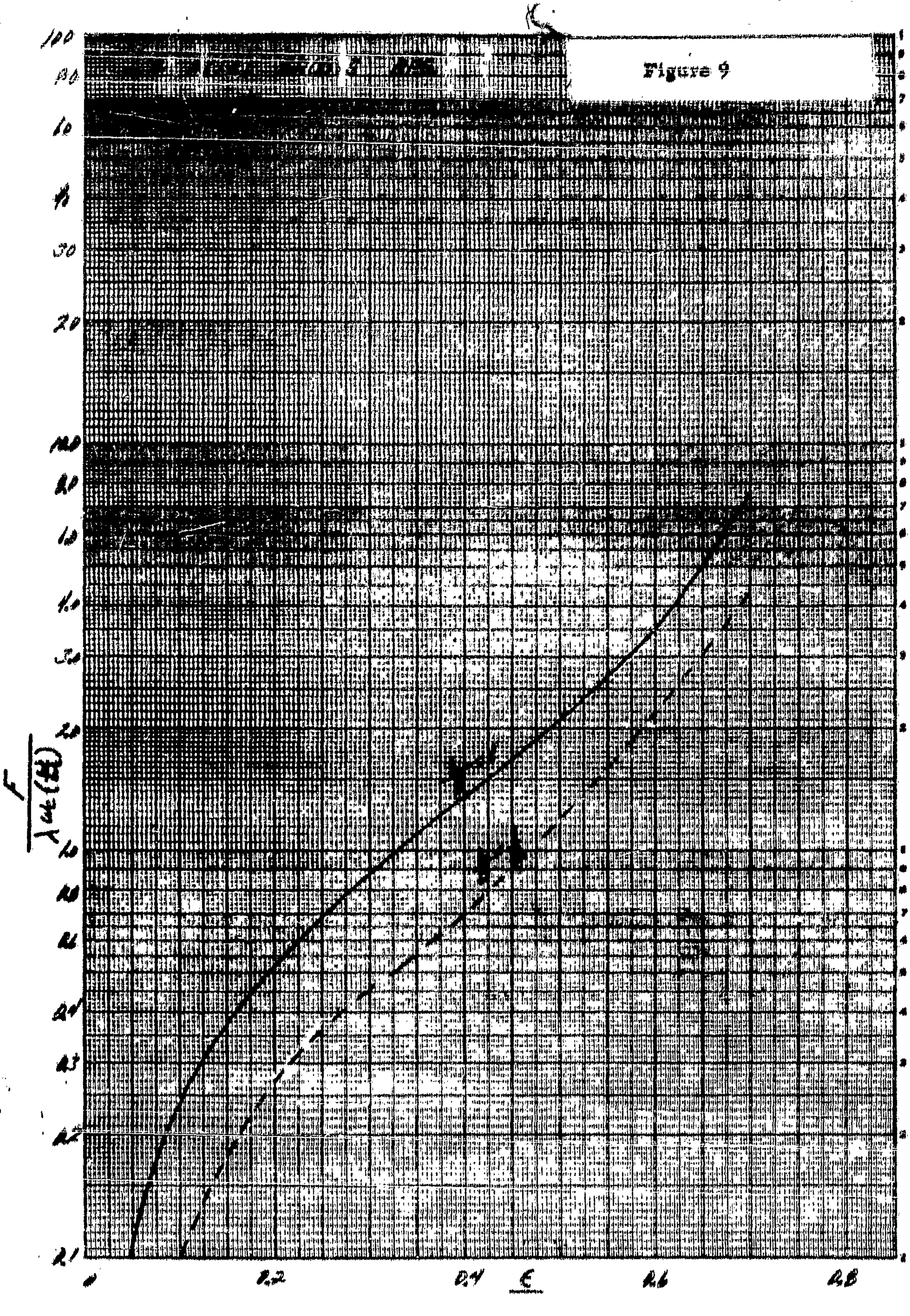
Figure 9

Figure 10

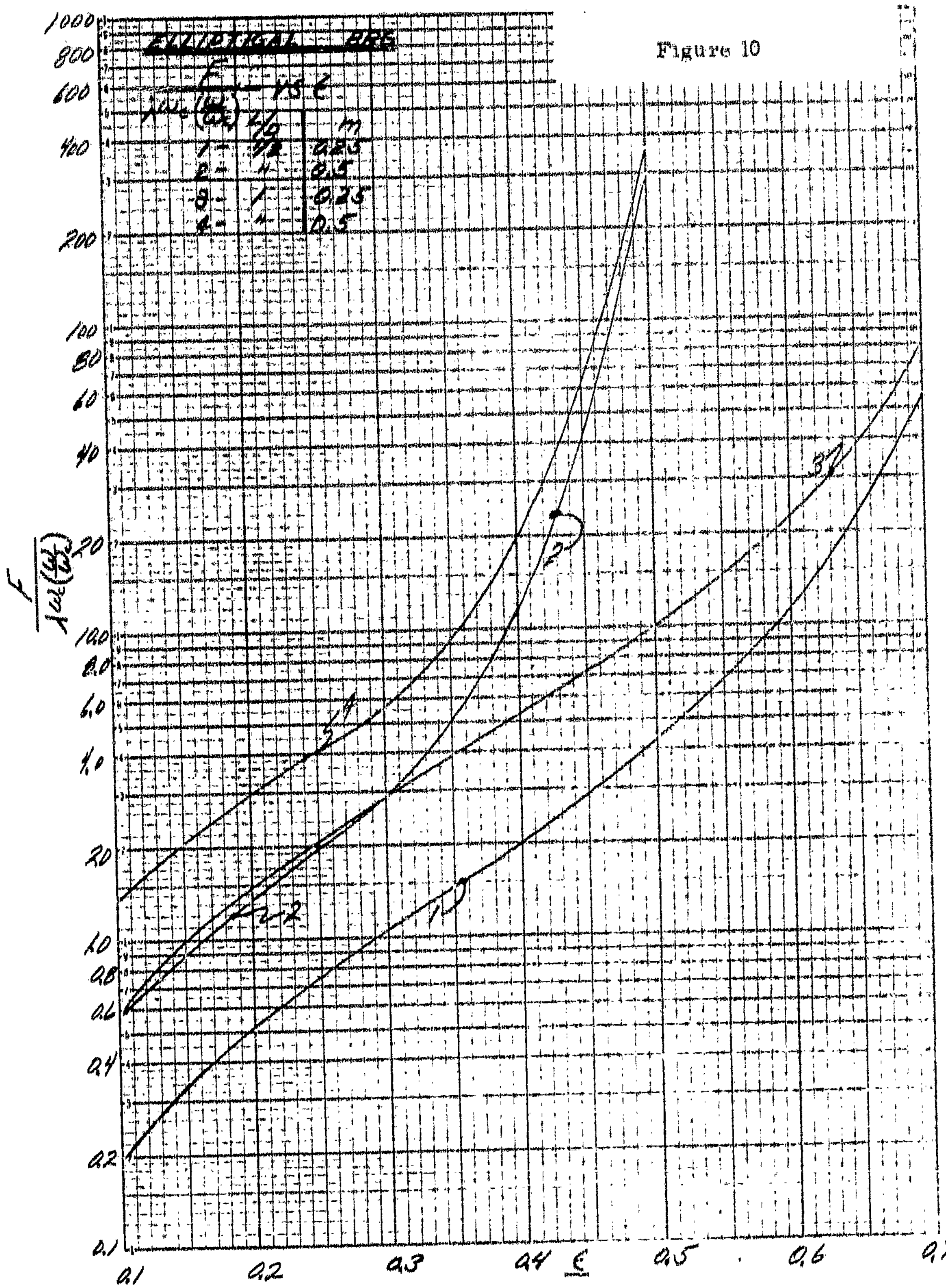

ELLIPTICAL BRG
F/λω vs ε
1 - 1/2 - 0.25
2 - 4 - 0.5
3 - 1 - 0.25
4 - 4 - 0.5
1000
800
600
400
200
100
80
60
40
20
10.0
8.0
6.0
4.0
2.0
1.0
0.8
0.6
0.4
0.2
0.1
0.1
0.2
0.3
0.4
ε
0.5
0.6
0.7

Figure 11

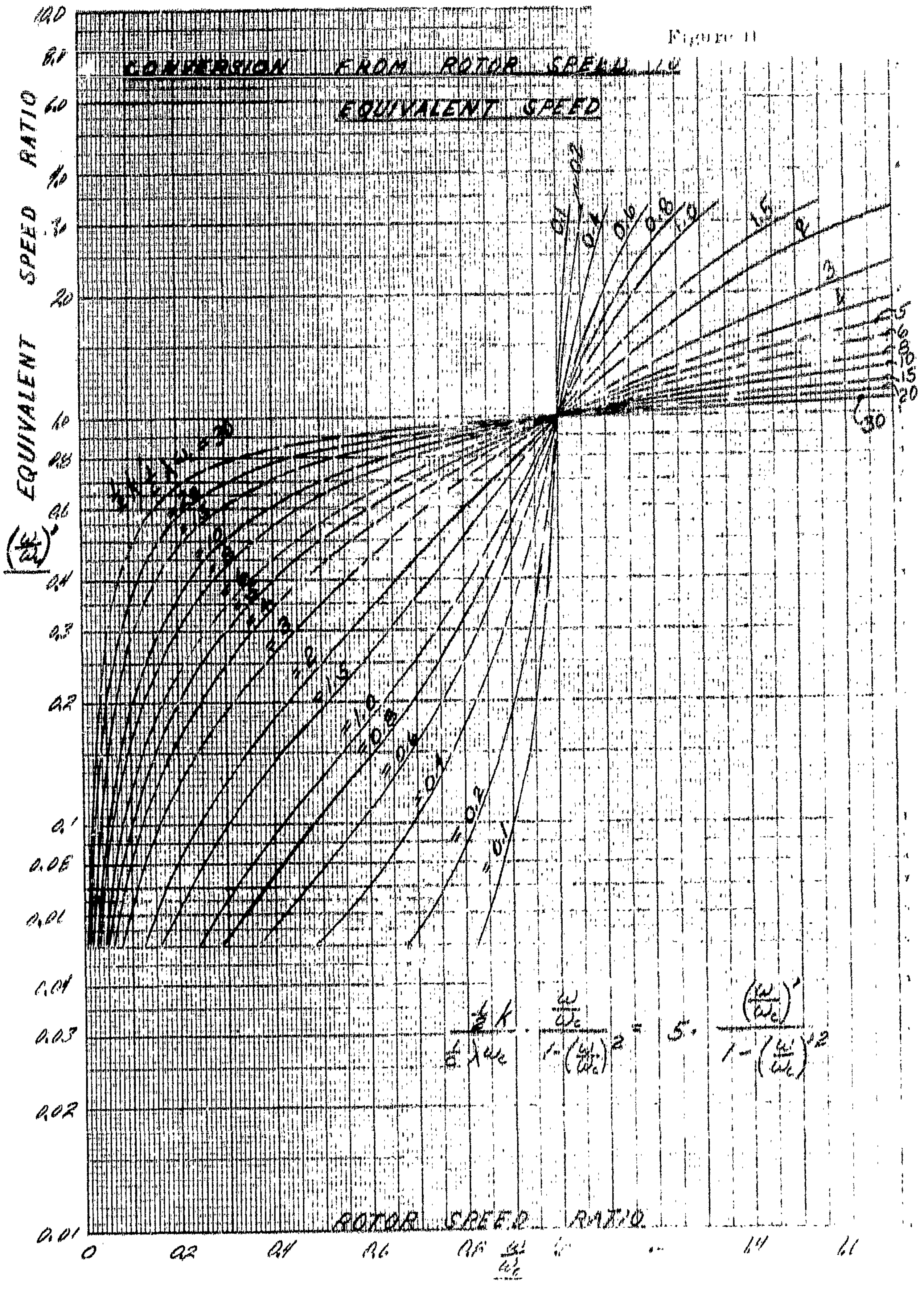
CONVERSION FROM ROTOR SPEED TO
EQUIVALENT SPEED
EQUIVALENT SPEED RATIO
ROTOR SPEED RATIO
0
0.2
0.4
0.6
0.8
0.01
0.02
0.03
0.04
0.1
0.2
0.3
0.4
0.6
0.8
1.0
20

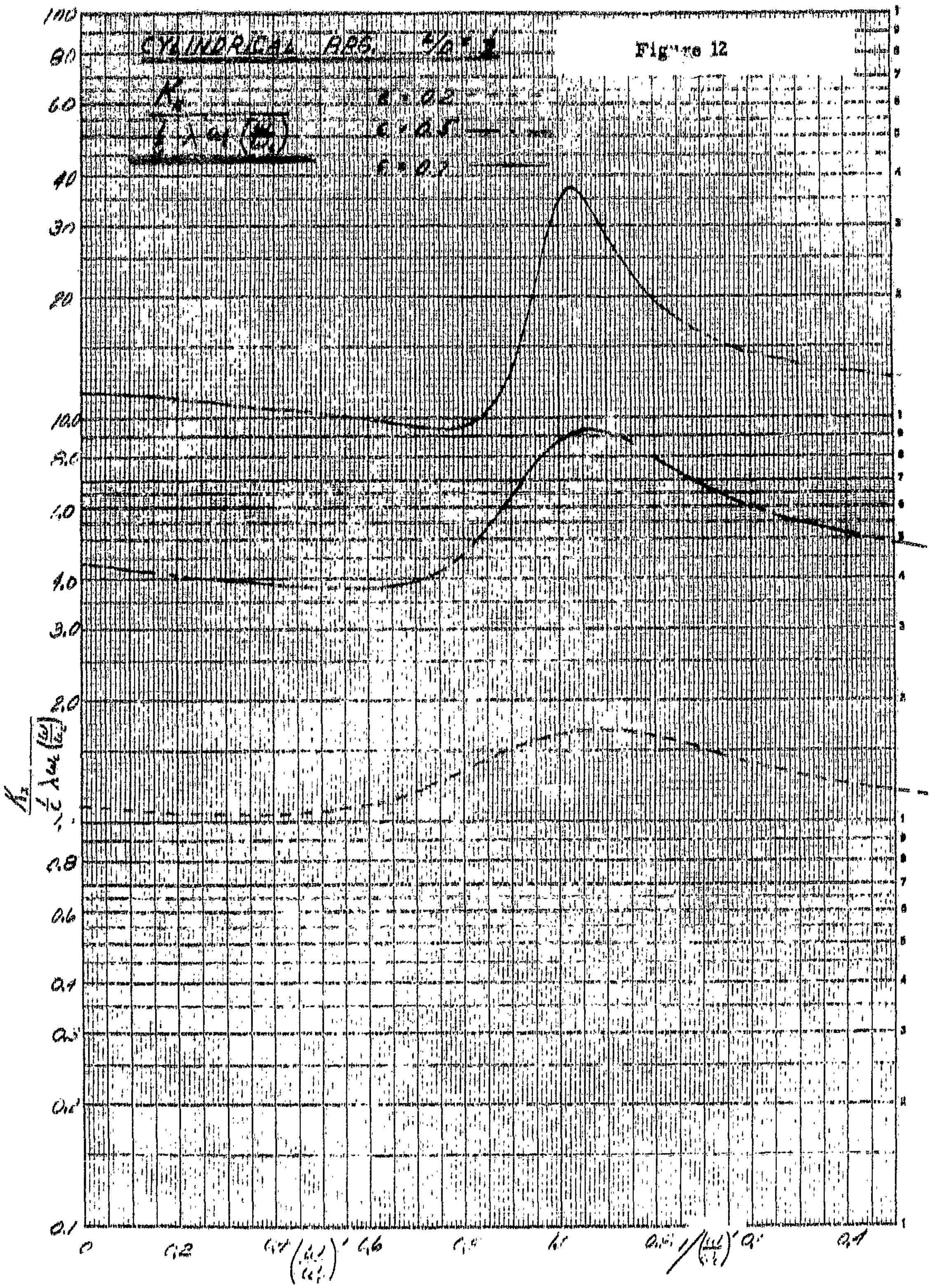
CYLINDRICAL ARRS.
Figure 12
ε = 0.2
ε = 0.5
ε = 0.7
100
80
60
40
30
20
10.0
8.0
6.0
4.0
3.0
2.0
0.8
0.6
0.4
0.1
0
0.2
0.6
1.0

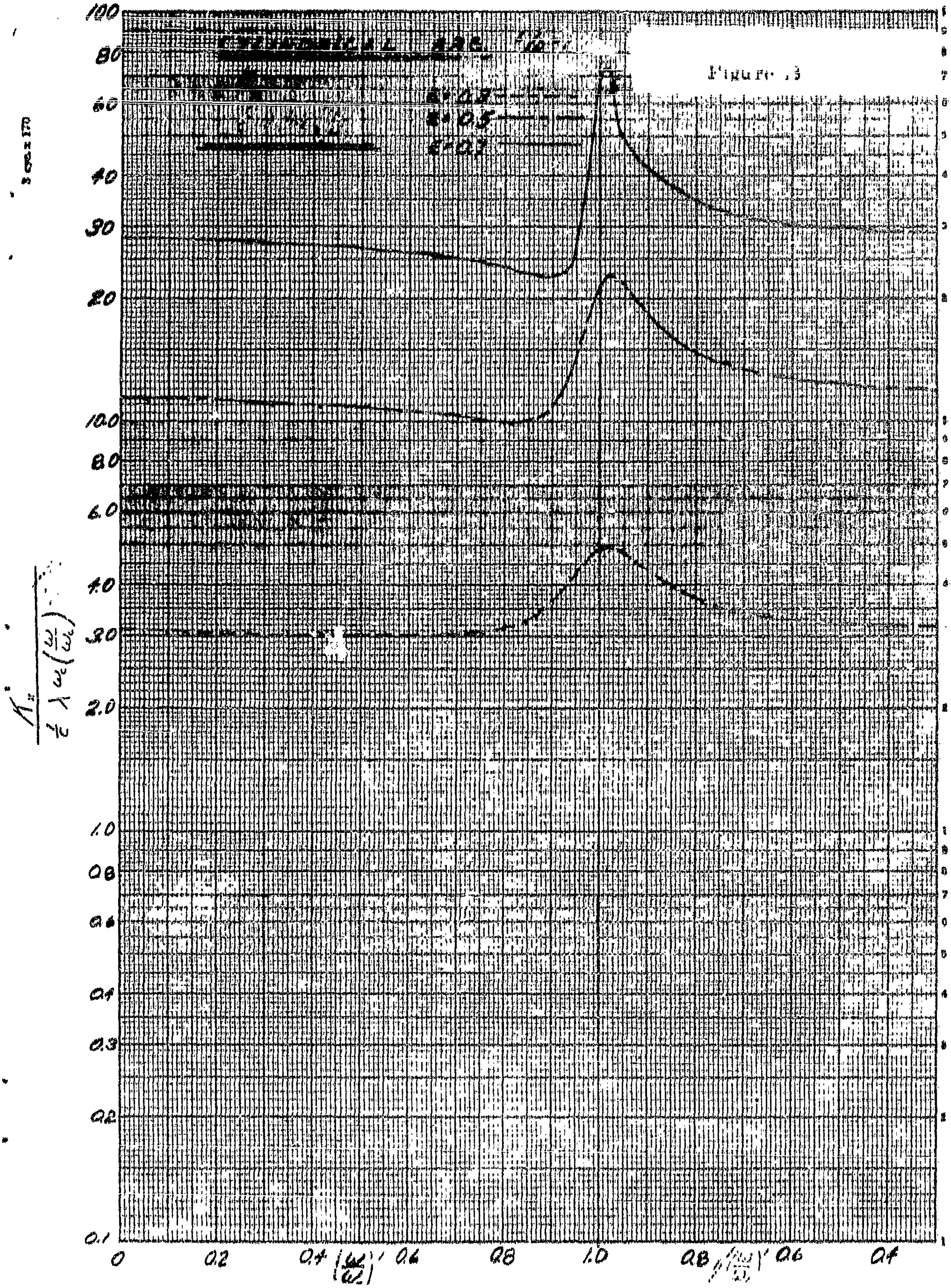
CYLINDRICAL ARC
ε=0.7
ε=0.5
ε=0.3
100
80
60
40
30
20
10.0
8.0
6.0
4.0
3.0
2.0
1.0
0.8
0.6
0.4
0.3
0.2
0.1
0
0.2
0.4
0.6
0.8
1.0
0.8
0.6
0.4

Figure 13

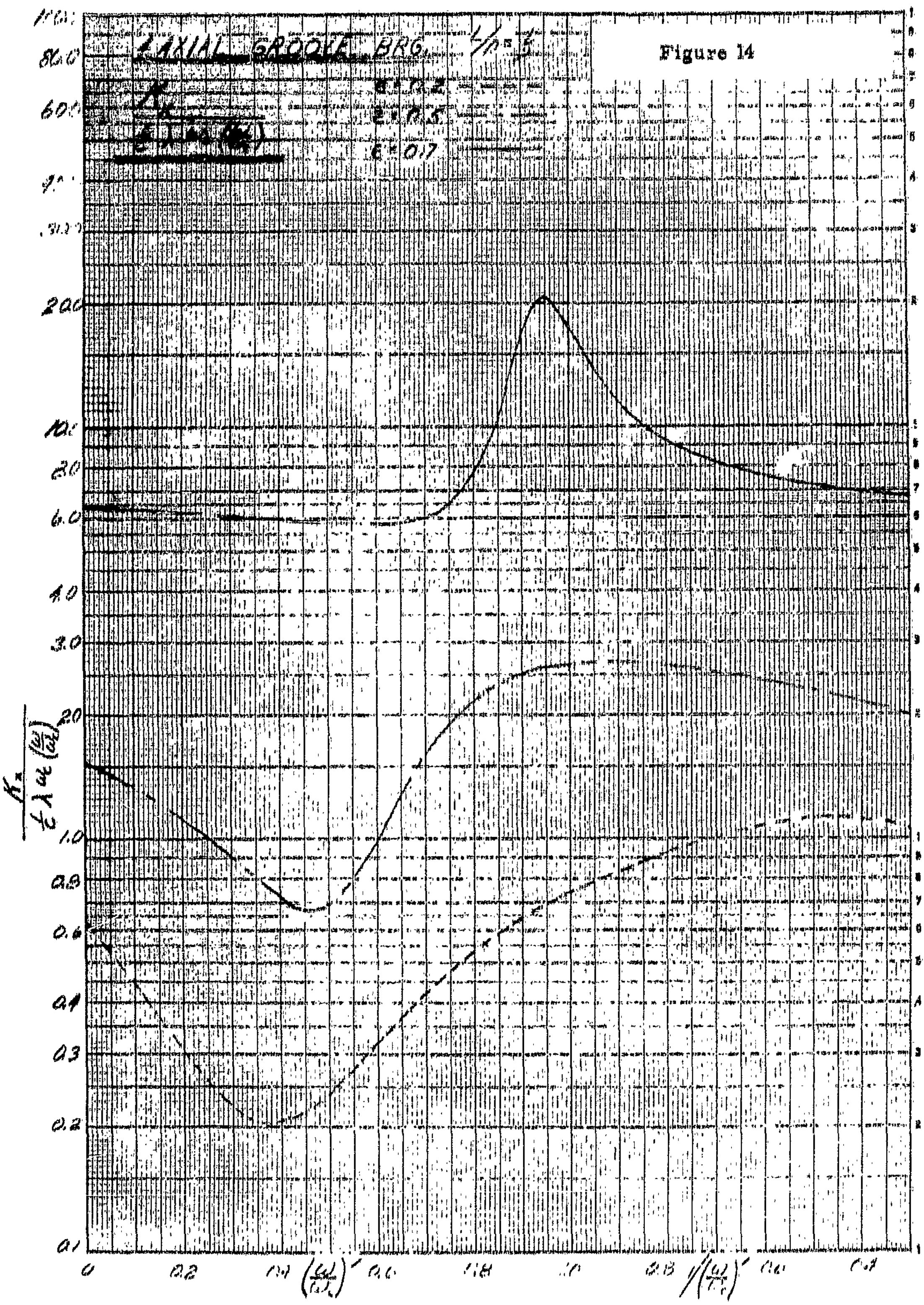
AXIAL GROOVE BRG.
Figure 14
0.2
0.4
0.6
0.8
1.0
2.0
3.0
4.0
6.0
8.0
10.0
20.0

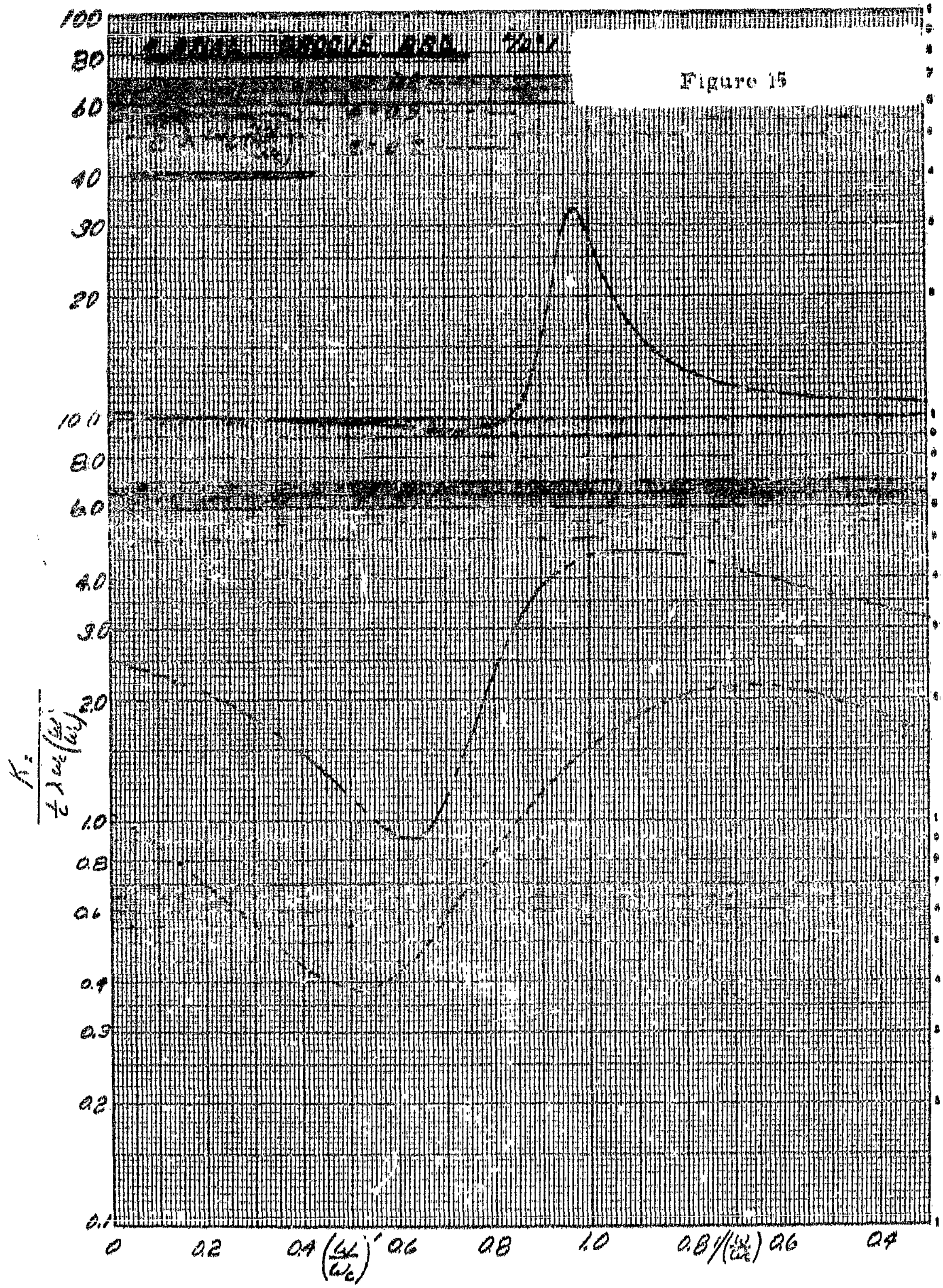
100
80
60
40
30
20
10.0
8.0
6.0
4.0
3.0
2.0
1.0
0.8
0.6
0.4
0.3
0.2
0.1
0
0.2
0.4
0.6
0.8
1.0
0.8
0.6
0.4

Figure 15

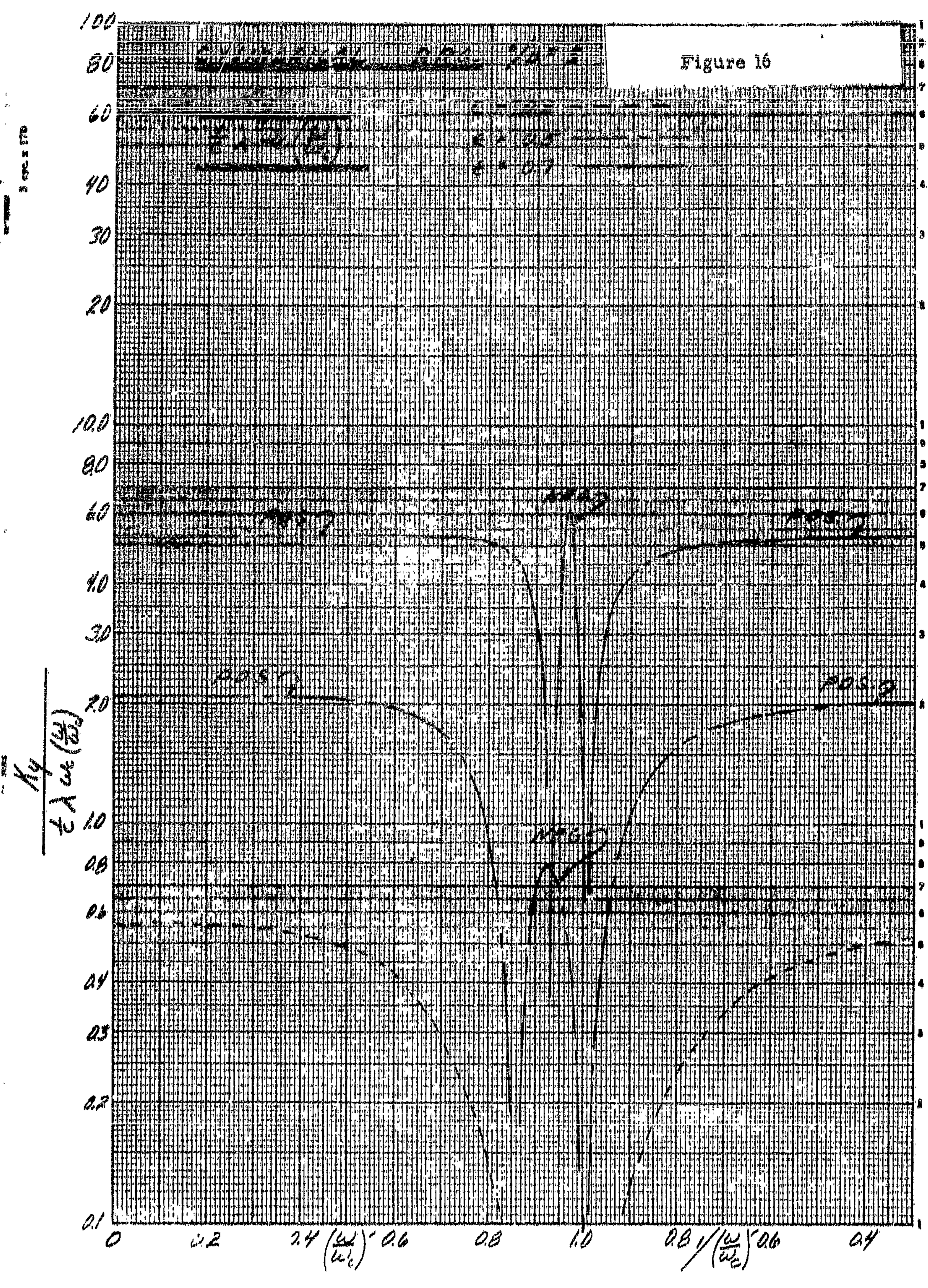
Figure 16
POS 1
NEG 2
POS 2
NEG
$\frac{K_y}{\tau \lambda \omega_c (\omega/\omega_c)}$
0
0.2
0.4 (ω/ω_c) 0.6
0.8
1.0
0.8 $1/(\omega/\omega_c)$ 0.6
0.4
0.1
0.2
0.3
0.4
0.6
0.8
1.0
2.0
3.0
4.0
6.0
8.0
10.0
20
30
40
60
80
100

Figure 17

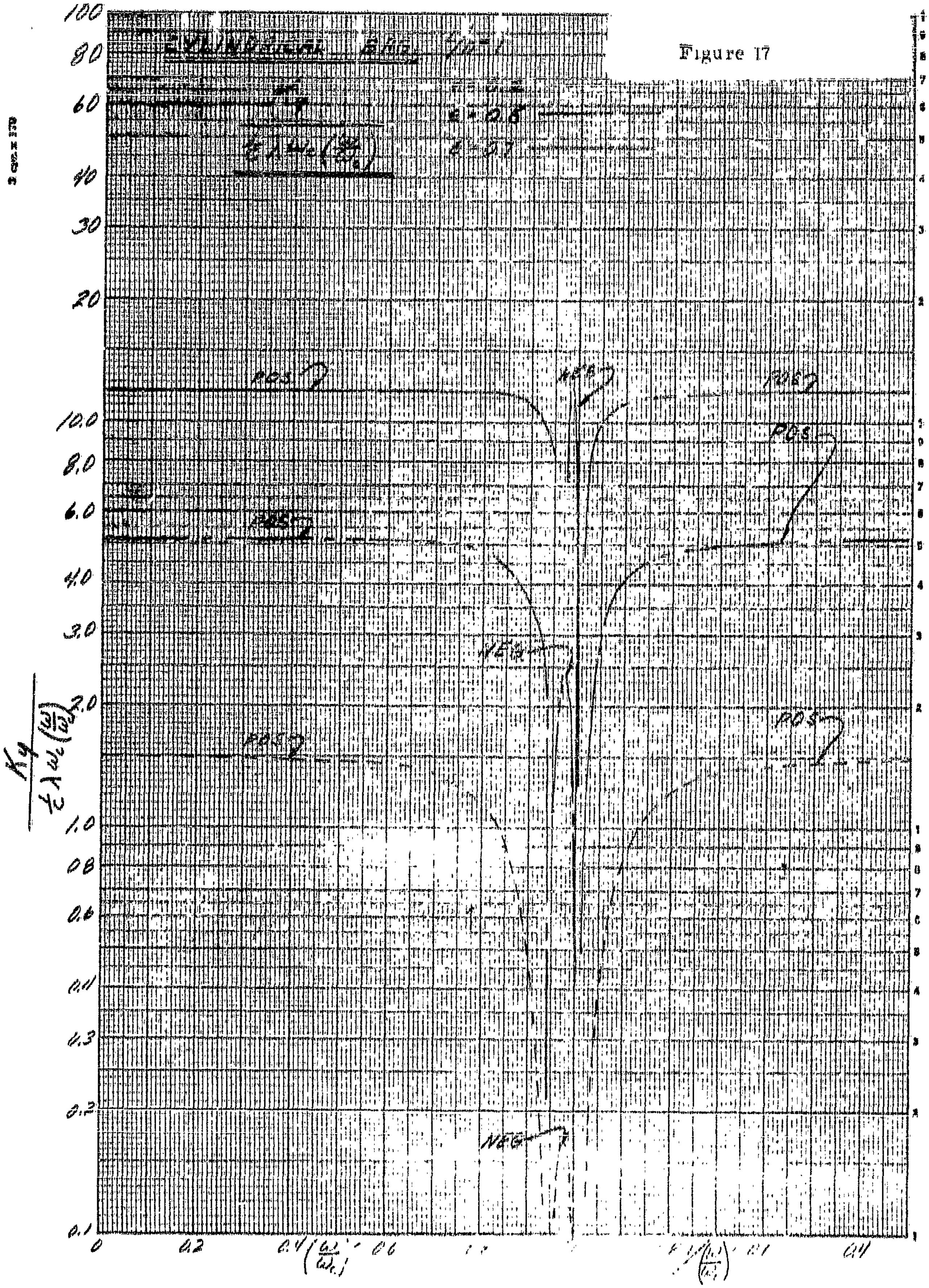
POS
NEG
POS
POS
POS
NEG
POS
POS
NEG
100
80
60
40
30
20
10.0
8.0
6.0
4.0
3.0
2.0
1.0
0.8
0.6
0.3
0.2
0.1
0
0.2
0.6

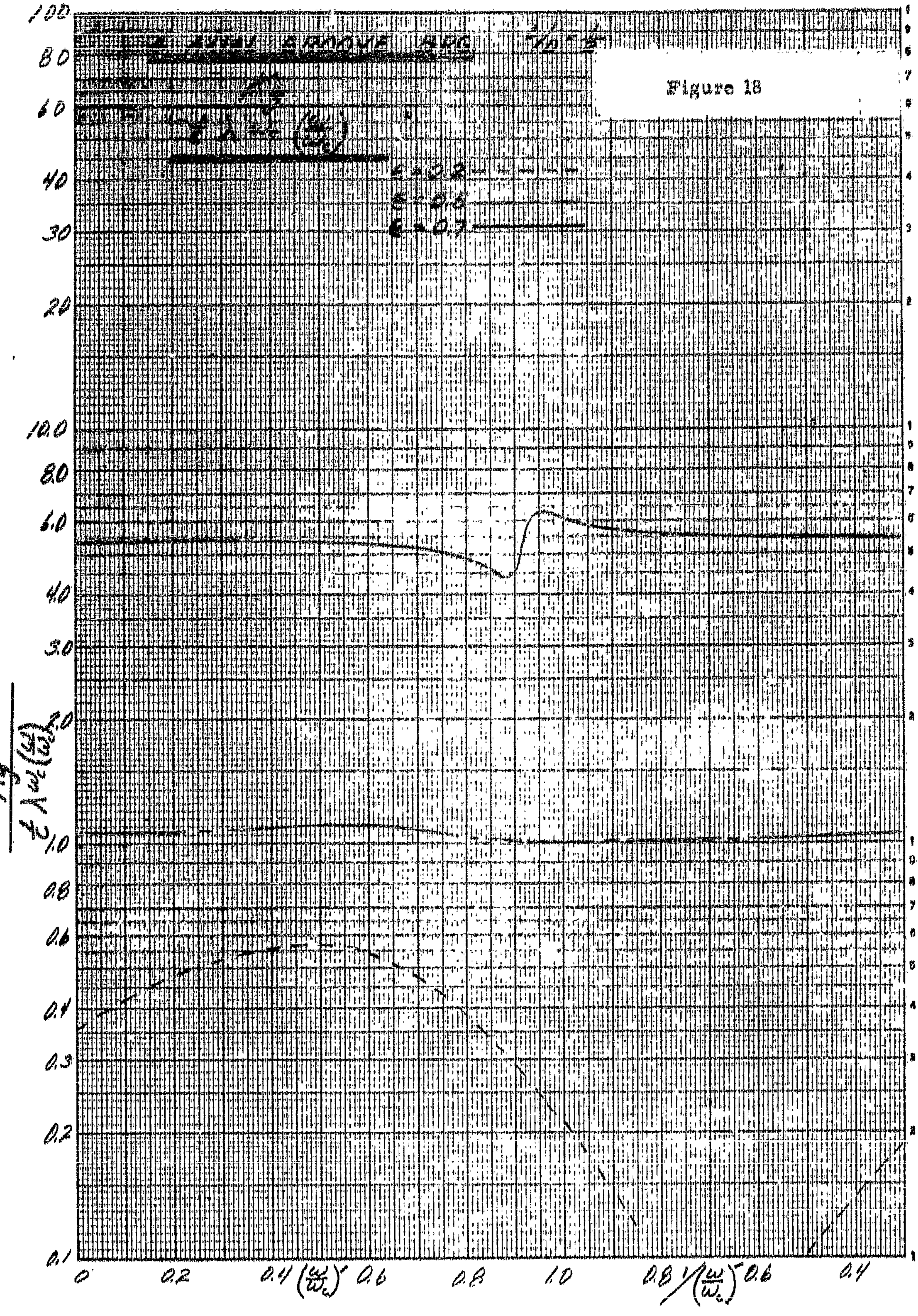
100
80
60
40
30
20
10.0
8.0
6.0
4.0
3.0
2.0
1.0
0.8
0.6
0.4
0.3
0.2
0.1
0
0.2
0.4
0.6
0.8
1.0
0.8
0.6
0.4

Figure 18

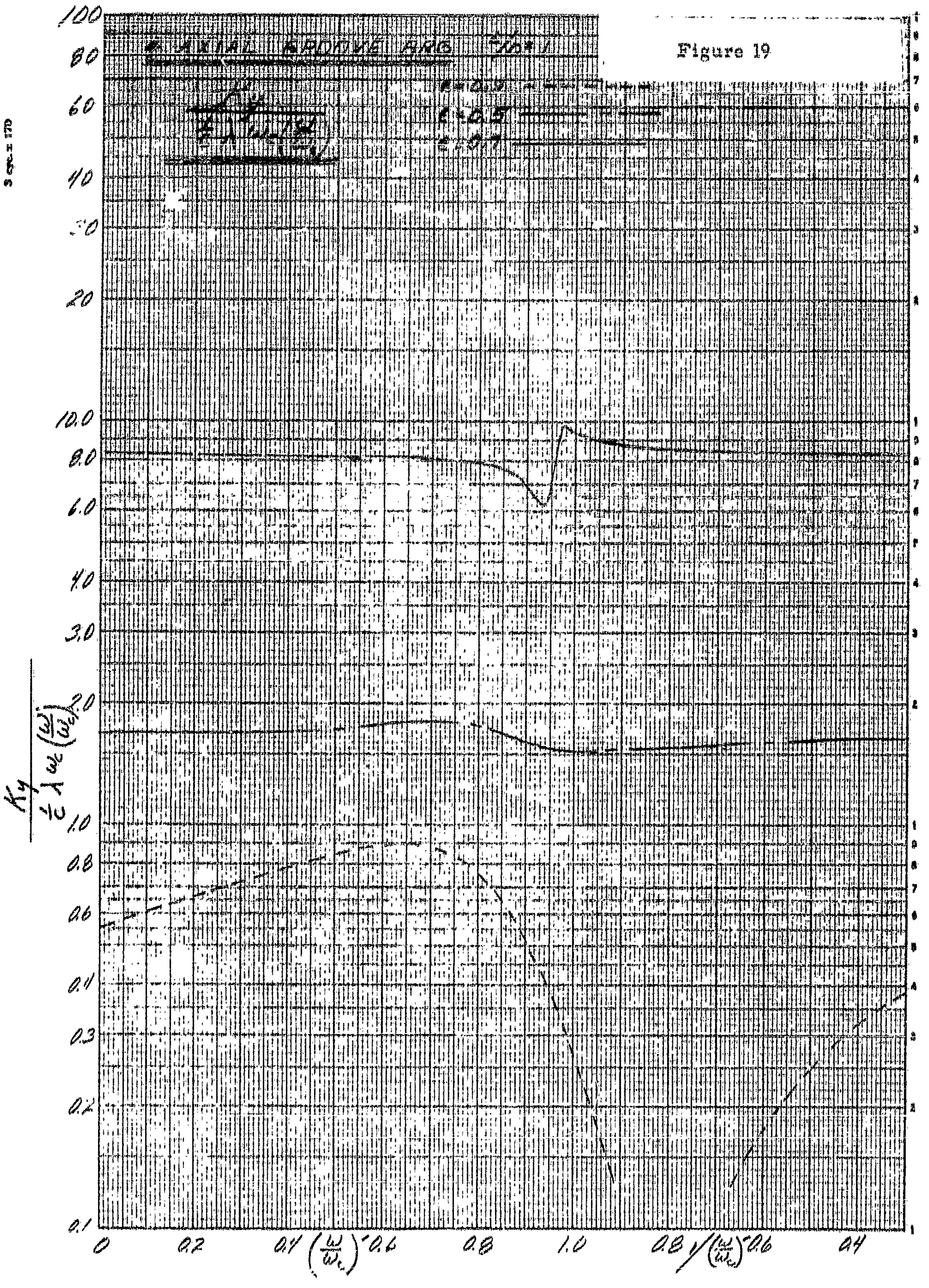
AXIAL GROOVE BRG
ε = 0.5
100
80
60
40
20
10.0
8.0
6.0
4.0
3.0
2.0
1.0
0.8
0.6
0.3
0.2
0.1
0
0.2
0.4
0.6
0.8
1.0
0.8
0.6
0.4

Figure 19

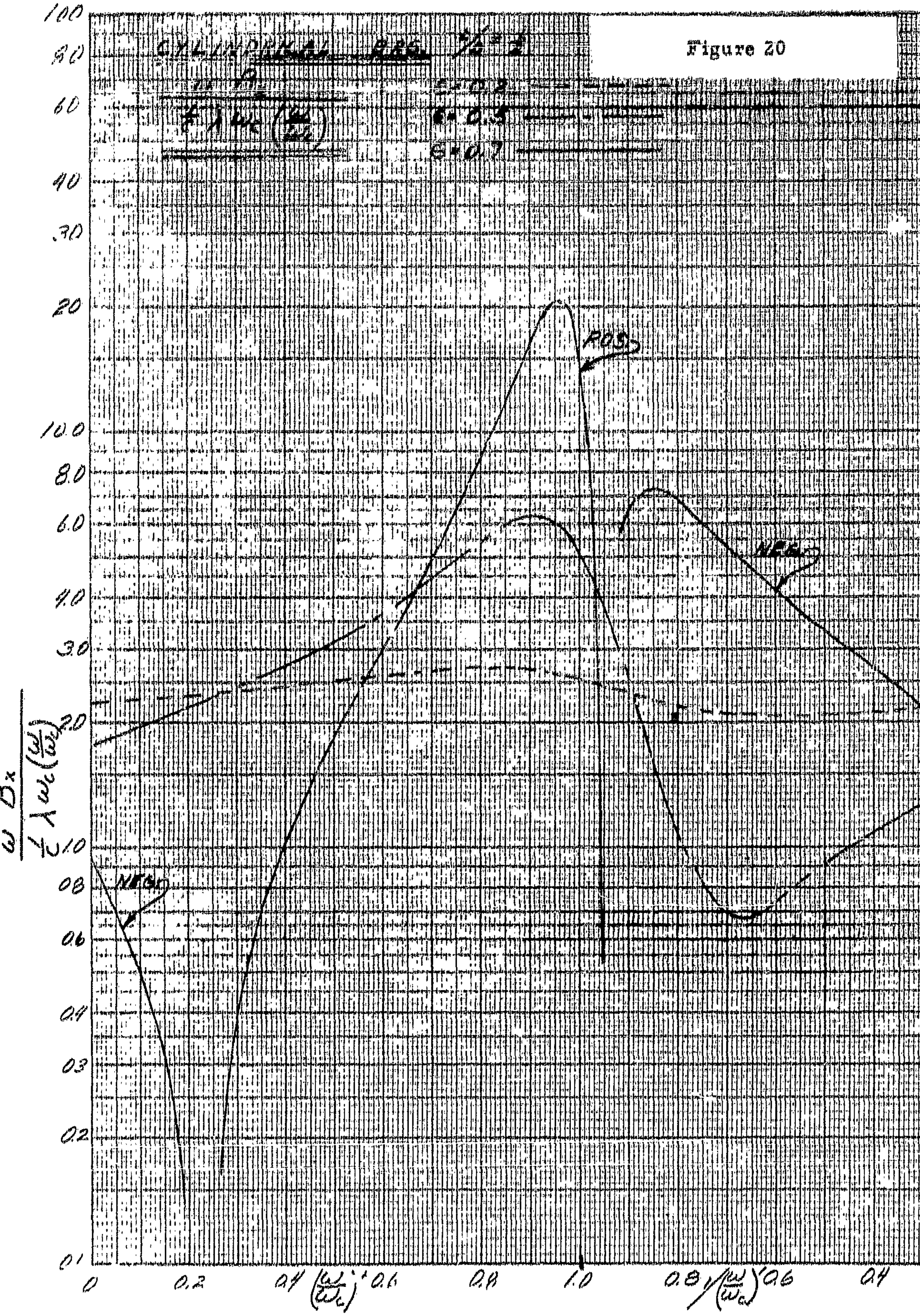

CYLINDRICAL RES.
Figure 20
δ=0.2
δ=0.5
δ=0.7
POS
NEG
NEG
100
80
60
40
30
20
10.0
8.0
6.0
4.0
3.0
2.0
1.0
0.8
0.6
0.4
0.3
0.2
0.1
0
0.2
0.4
0.6
0.8
1.0
0.8
0.6
0.4
$\frac{\omega B_x}{\frac{1}{c}\lambda\omega_c\left(\frac{\omega}{\omega_c}\right)}$
$\left(\frac{\omega}{\omega_c}\right)$
$1/\left(\frac{\omega}{\omega_c}\right)$

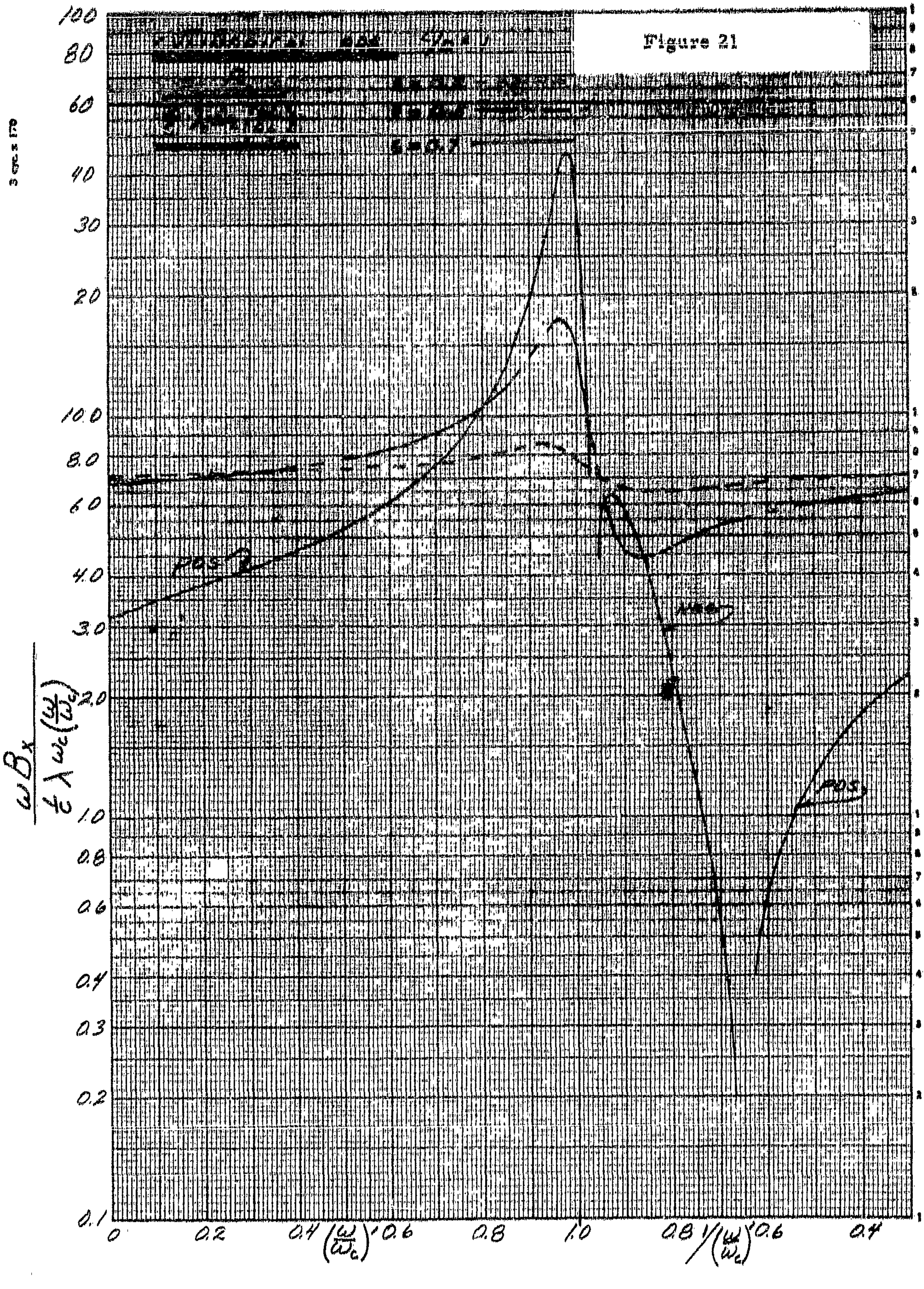
100
80
60
40
30
20
10.0
8.0
6.0
4.0
3.0
2.0
1.0
0.8
0.6
0.4
0.3
0.2
0.1
$\frac{\omega B_x}{\frac{\ell}{c}\lambda\omega_c\left(\frac{\omega}{\omega_c}\right)}$
POS
NEG
POS
0
0.2
0.4 $\left(\frac{\omega}{\omega_c}\right)$ 0.6
0.8
1.0
0.8 $1/\left(\frac{\omega}{\omega_c}\right)$ 0.6
0.4

Figure 21

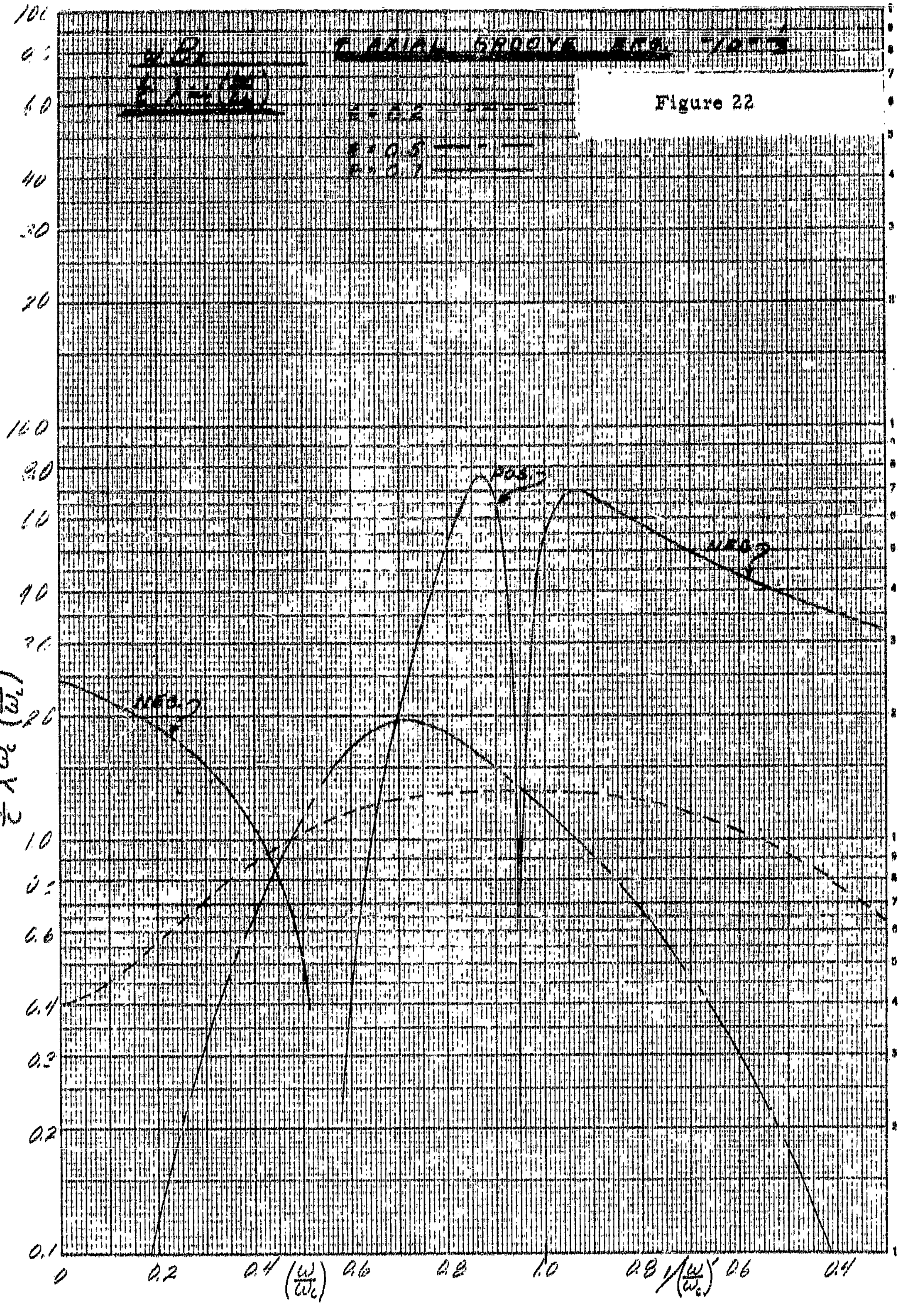
Figure 22
NEG.
POS.
NEG.
$\frac{\omega B_x}{\frac{1}{c}\lambda\omega_c\left(\frac{\omega}{\omega_c}\right)}$
$\left(\frac{\omega}{\omega_c}\right)$
$1/\left(\frac{\omega}{\omega_c}\right)$
0
0.2
0.4
0.6
0.8
1.0
0.8
0.6
0.4
0.1
0.2
0.3
0.4
0.6
1.0
2.0
10.0

Figure 23

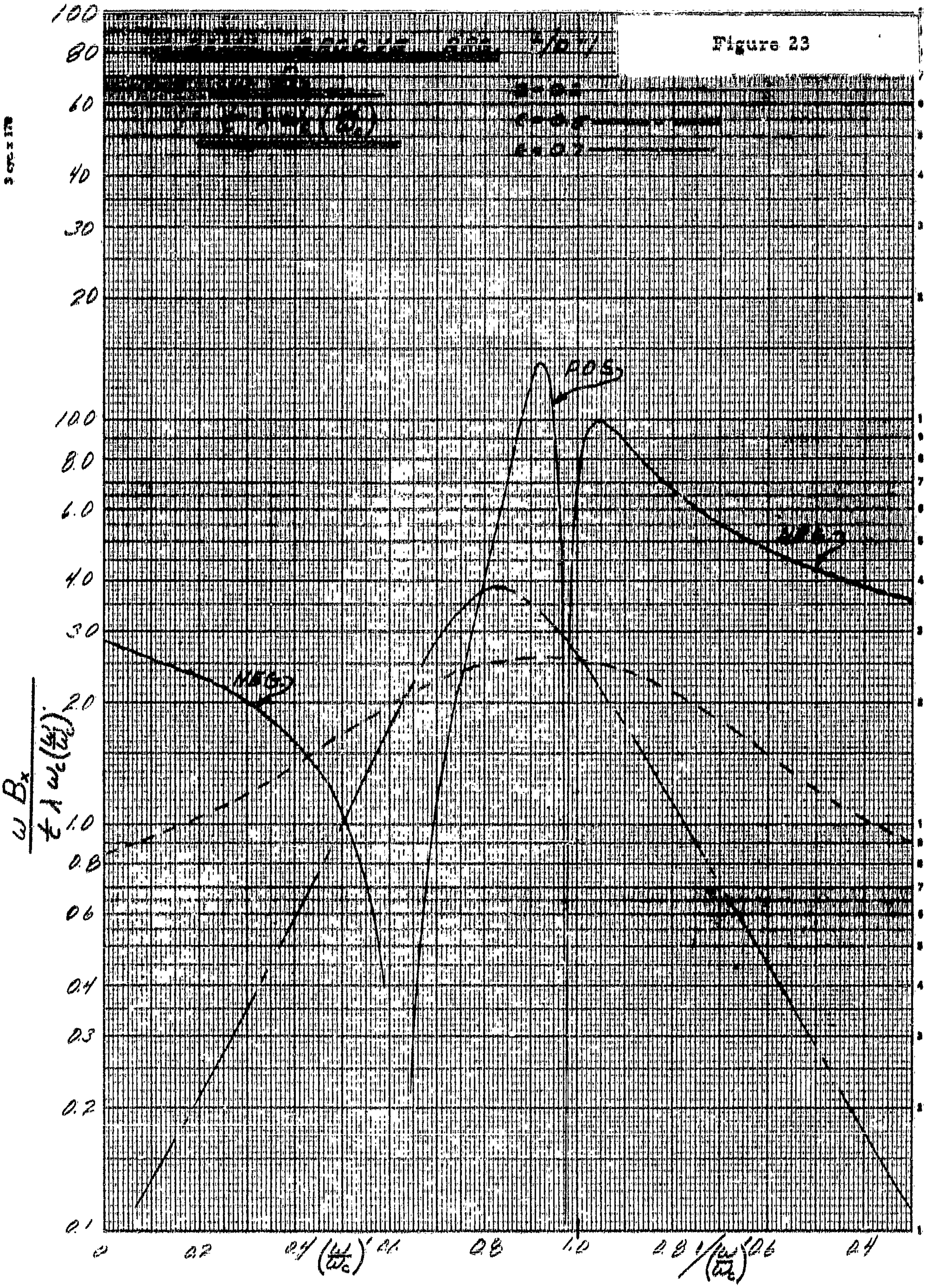

NEG
POS
$\frac{\omega B_x}{\epsilon \lambda \omega_c \left(\frac{\omega}{\omega_c}\right)}$
$\left(\frac{\omega}{\omega_c}\right)$
$1/\left(\frac{\omega}{\omega_c}\right)$

Figure 24

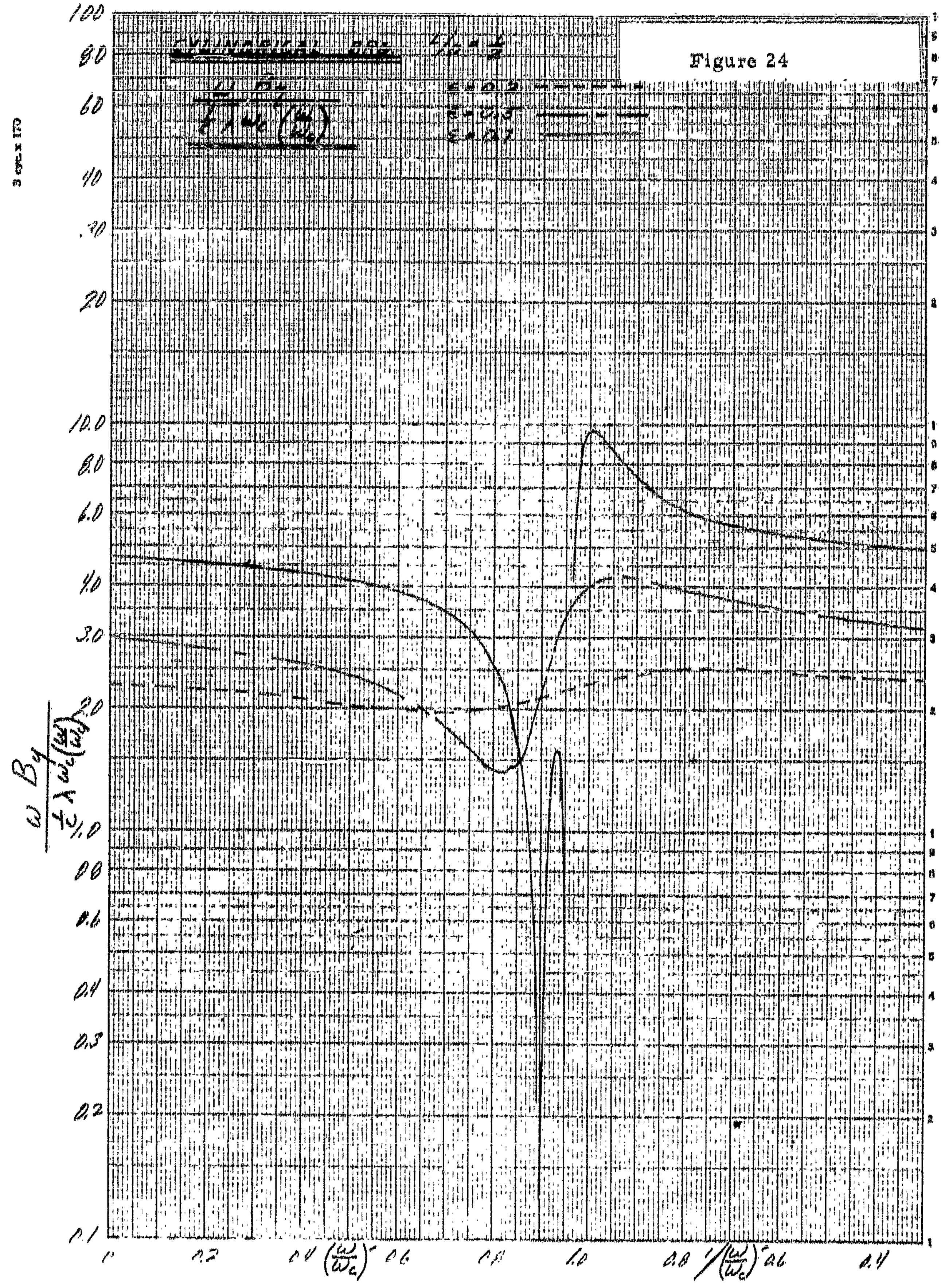

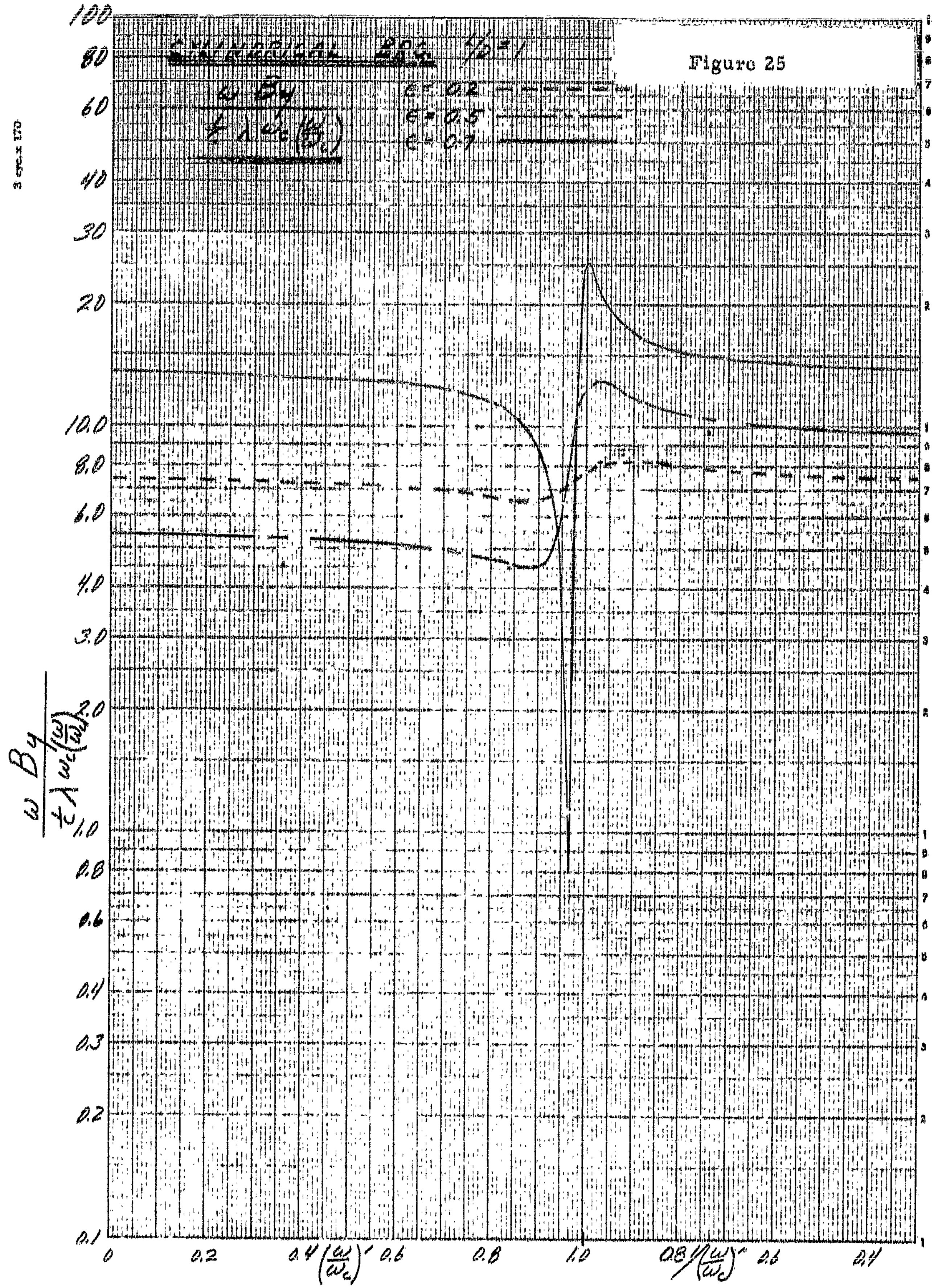
c = 0.2
c = 0.5
c = 0.7
100
80
60
40
30
20
10.0
8.0
6.0
4.0
3.0
2.0
1.0
0.8
0.6
0.4
0.3
0.2
0.1
0
0.2
0.6
0.8
1.0

Figure 25

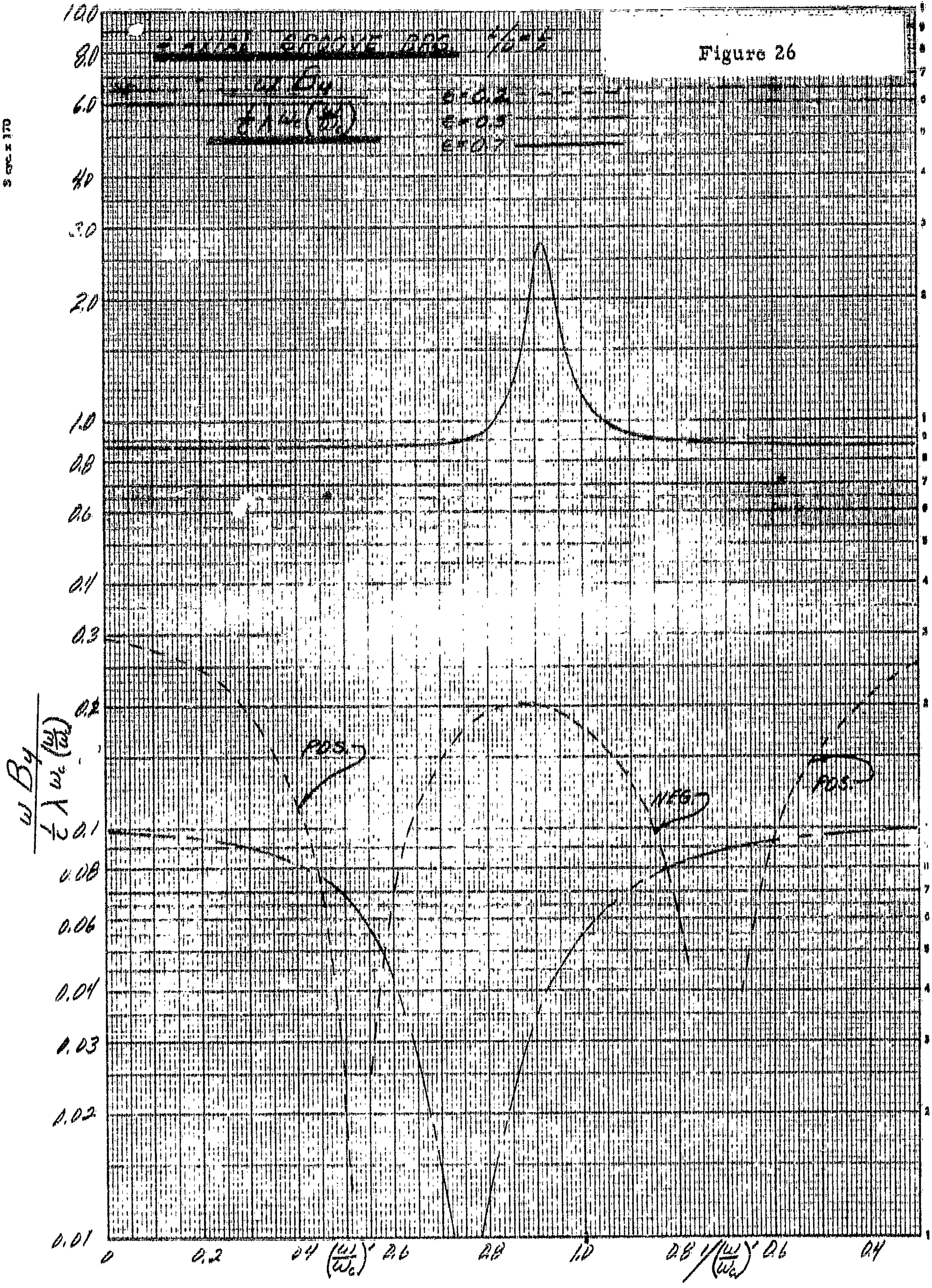

ε=0.2
ε=0.5
ε=0.7
POS.
NEG.
POS.
10.0
8.0
6.0
4.0
3.0
2.0
1.0
0.8
0.6
0.4
0.3
0.2
0.1
0.08
0.06
0.04
0.03
0.02
0.01
0
0.2
0.4
0.6
0.8
1.0
0.8
0.6
0.4

Figure 26

Figure 27

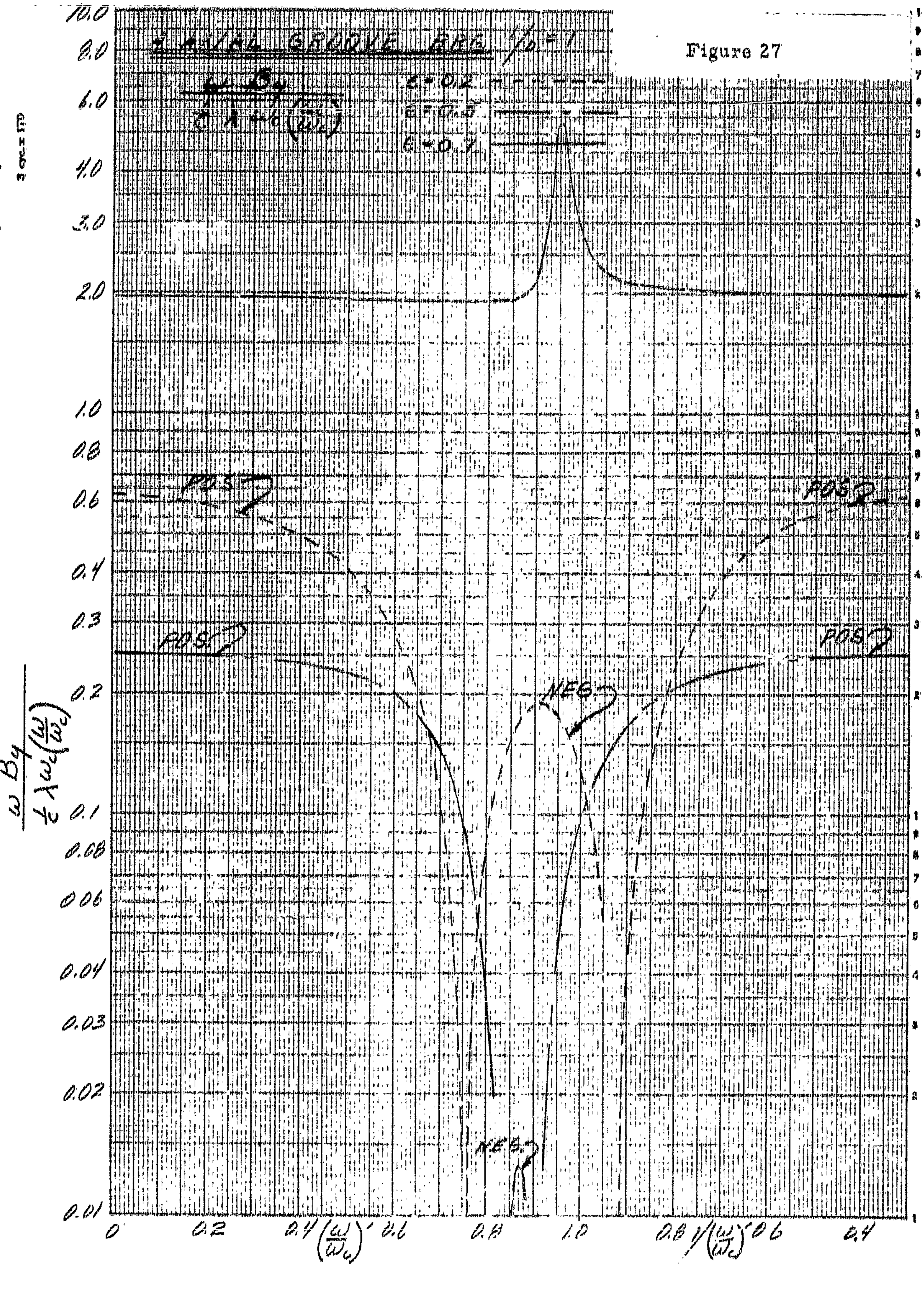

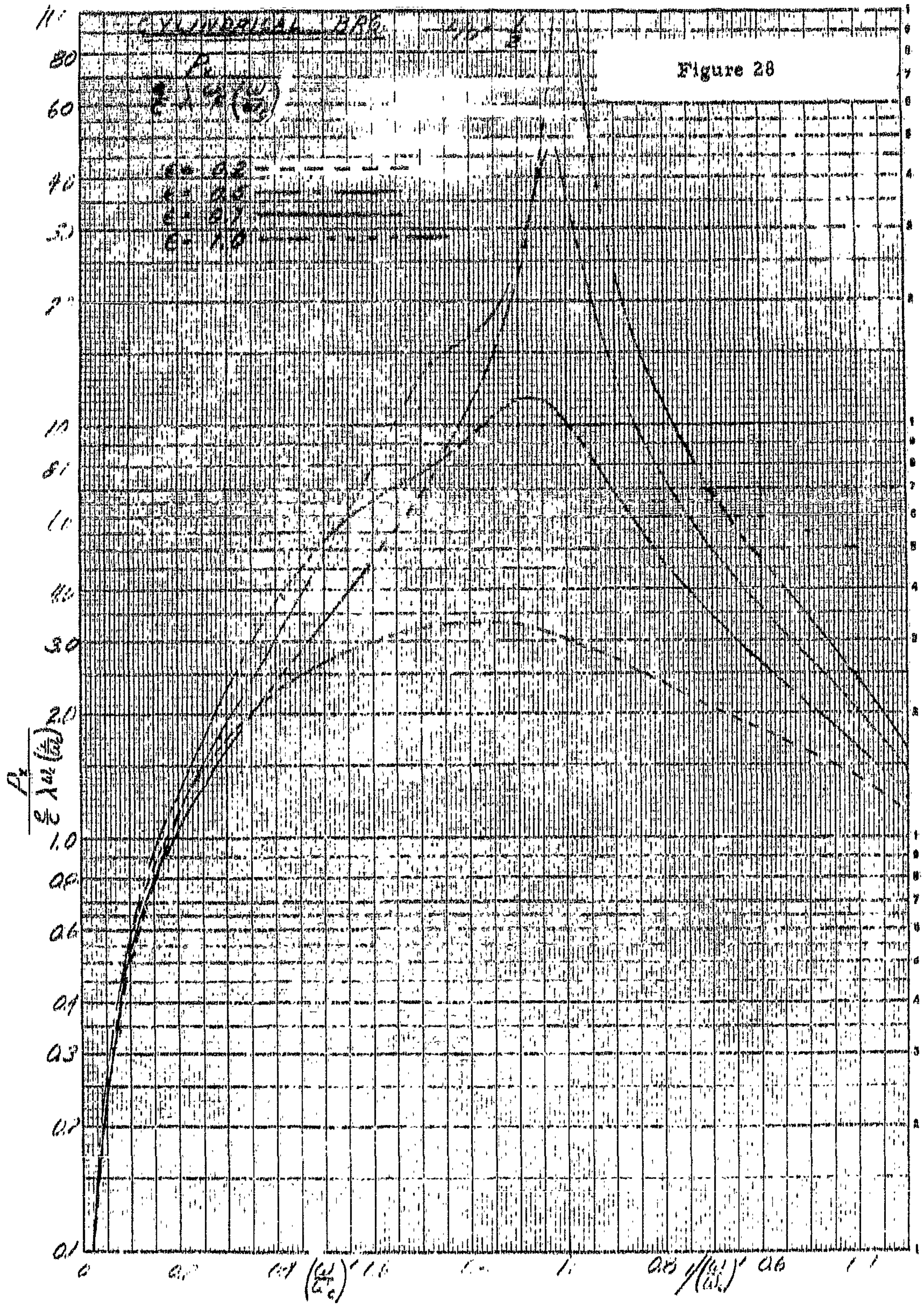

Figure 28

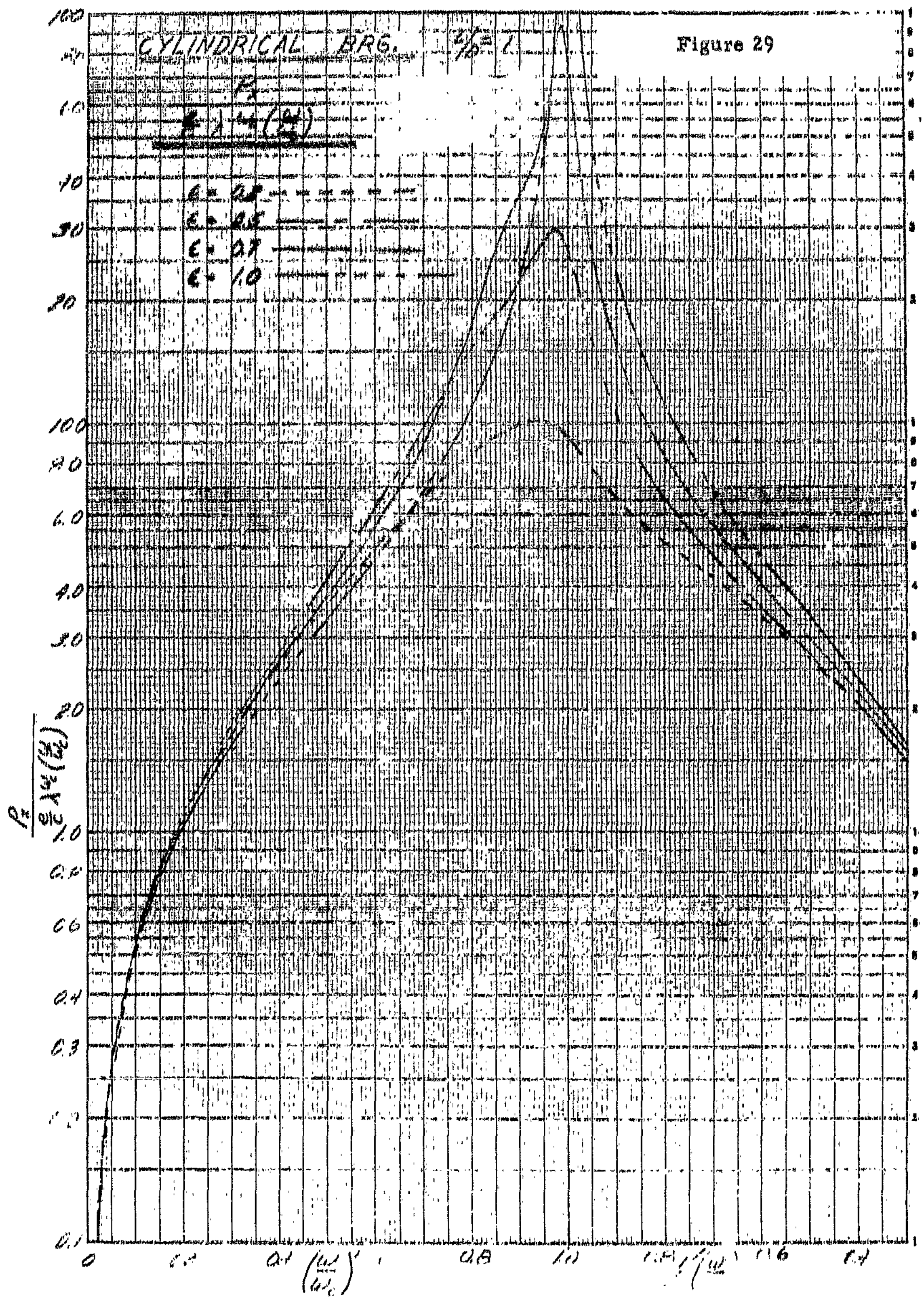
CYLINDRICAL BRG.
Figure 29

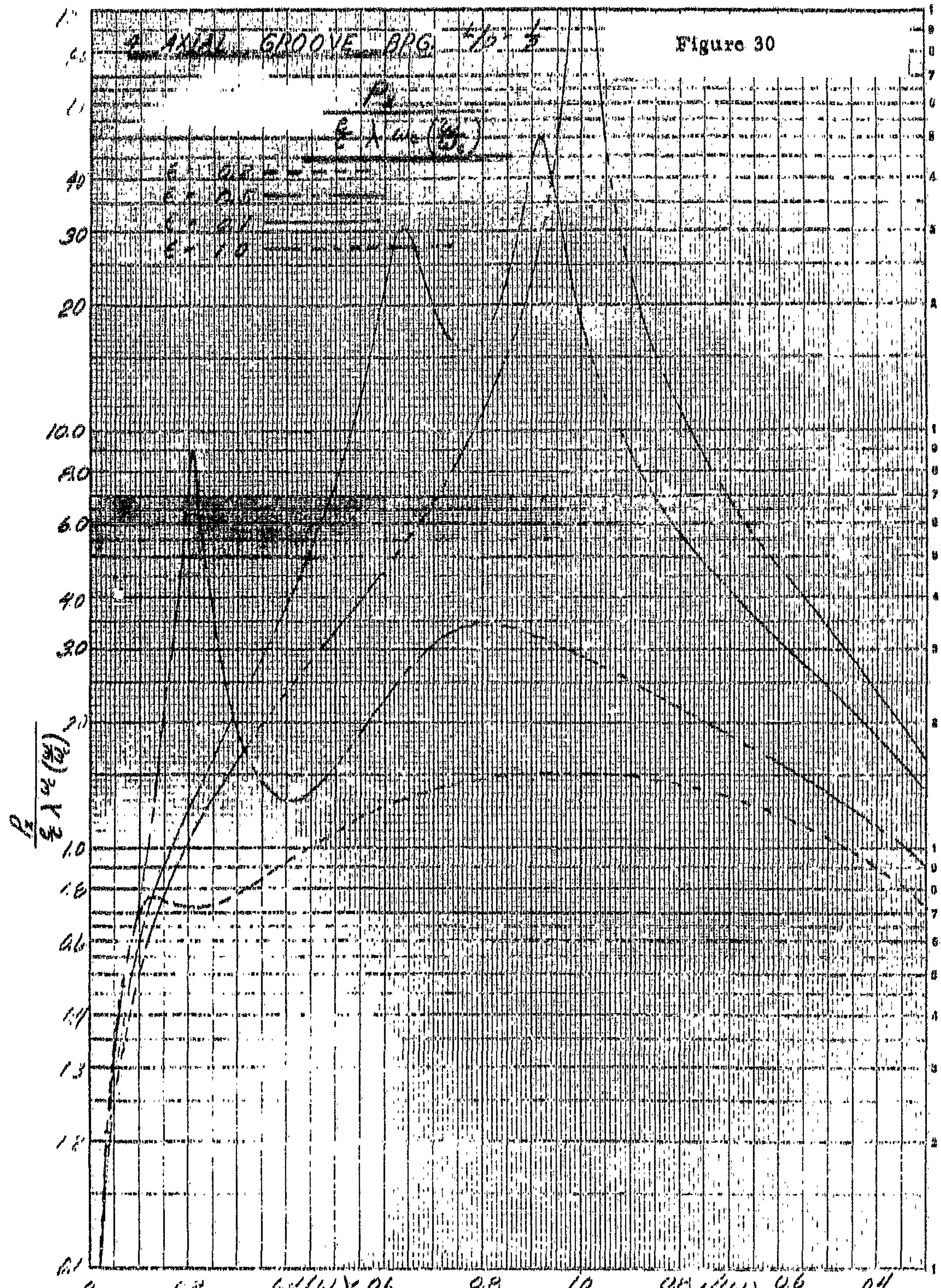

Figure 30

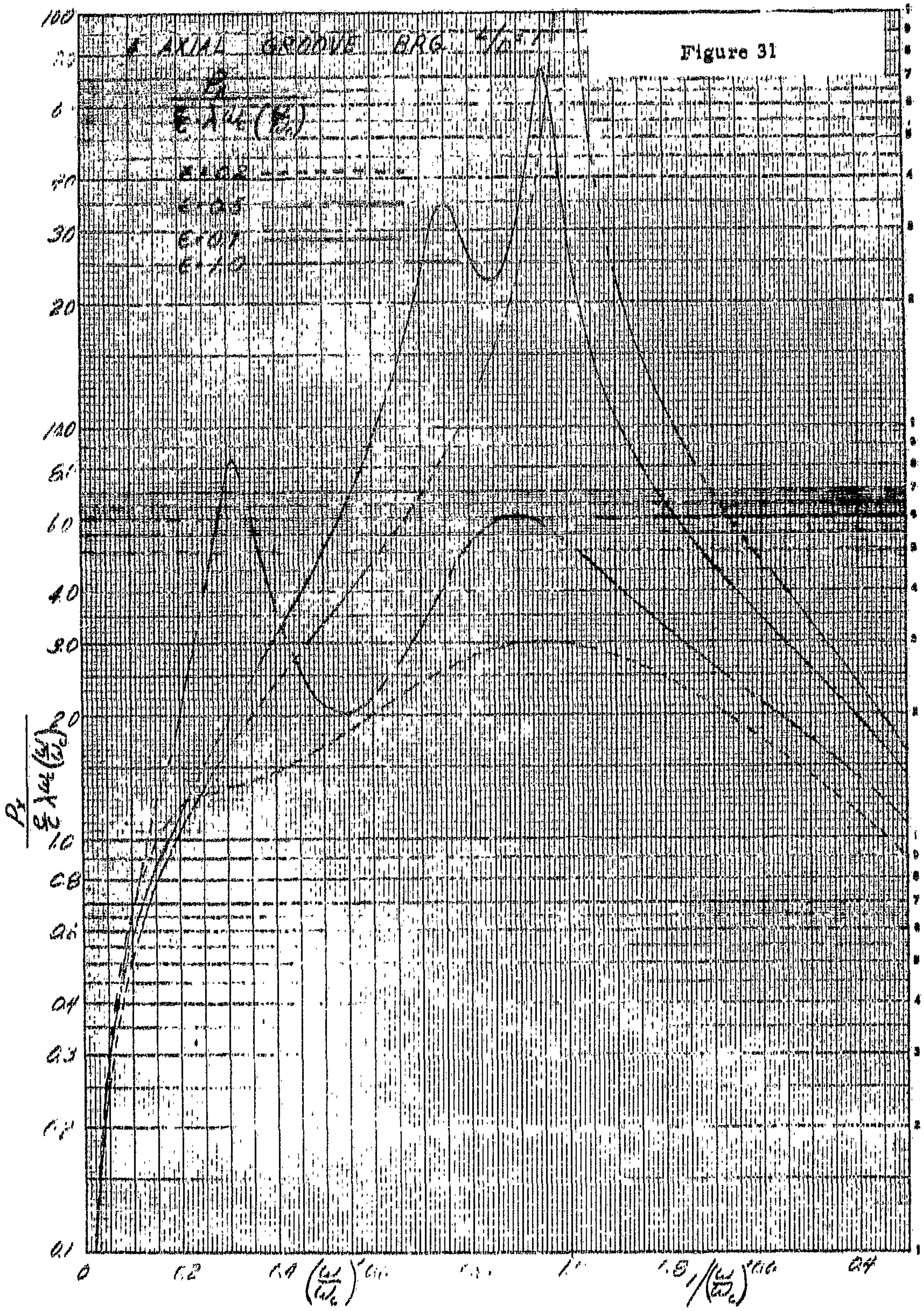

Figure 31

Figure 32

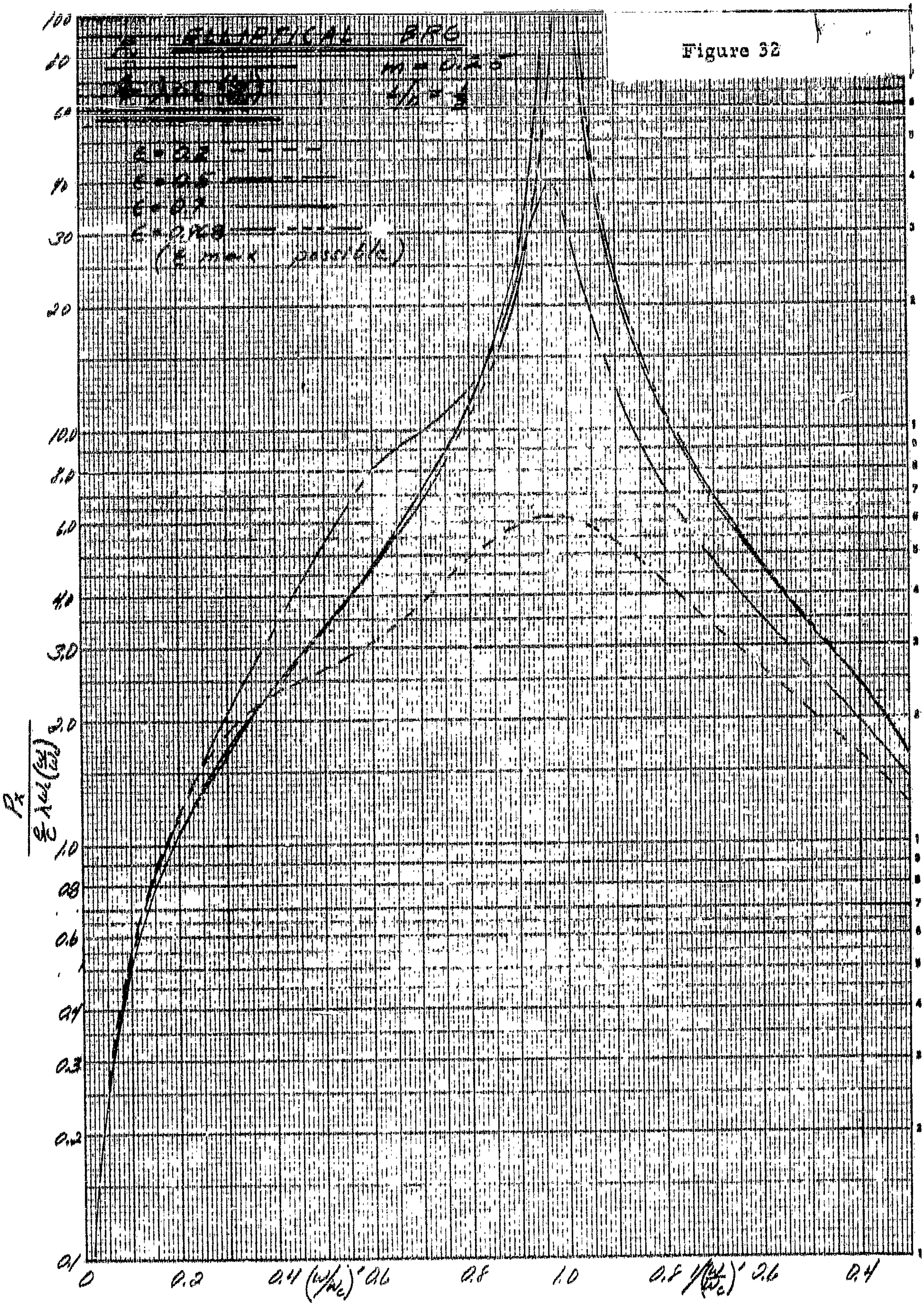
ELLIPTICAL BRG
m = 0.25
L/D = 1/2
ε = 0.2
ε = 0.6
ε = 0.7
ε = 0.748
(ε max possible)
100
80
60
40
30
20
10.0
8.0
6.0
4.0
3.0
2.0
1.0
0.8
0.6
0.4
0.3
0.2
0.1
0
0.2
0.4 (ω/ω_c)' 0.6
0.8
1.0
0.8 1/(ω/ω_c)' 0.6
0.4

Figure 33

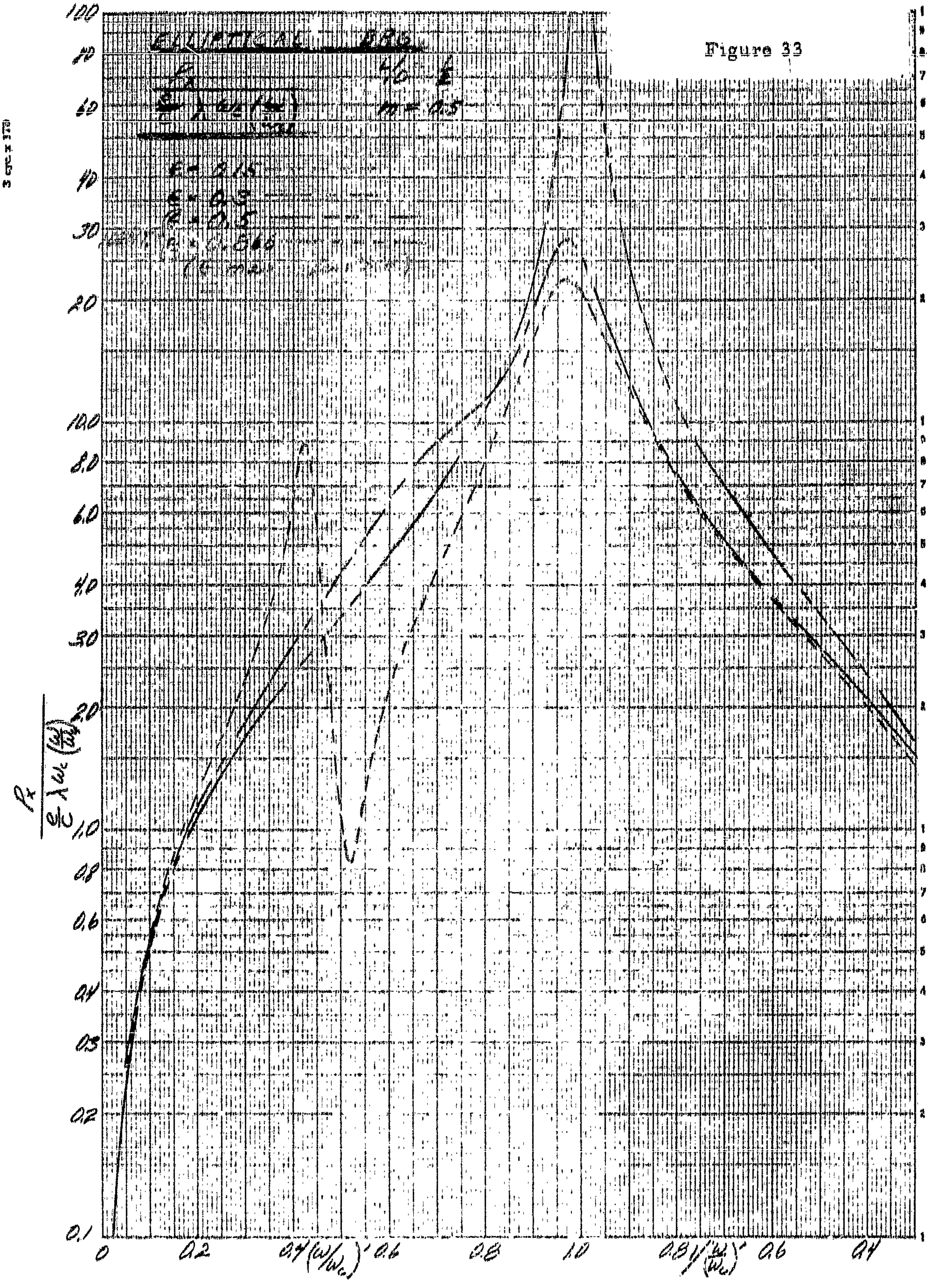
ELLIPTICAL ORB
m = 0.5
0.1
0.2
0.4
0.6
0.8
1.0
2.0
4.0
6.0
8.0
10.0
20
30
40
60
80
100
0
0.2
0.4 (ω/ωc)
0.6
0.8
1.0
0.8 1/(ω/ωc)
0.6
0.4

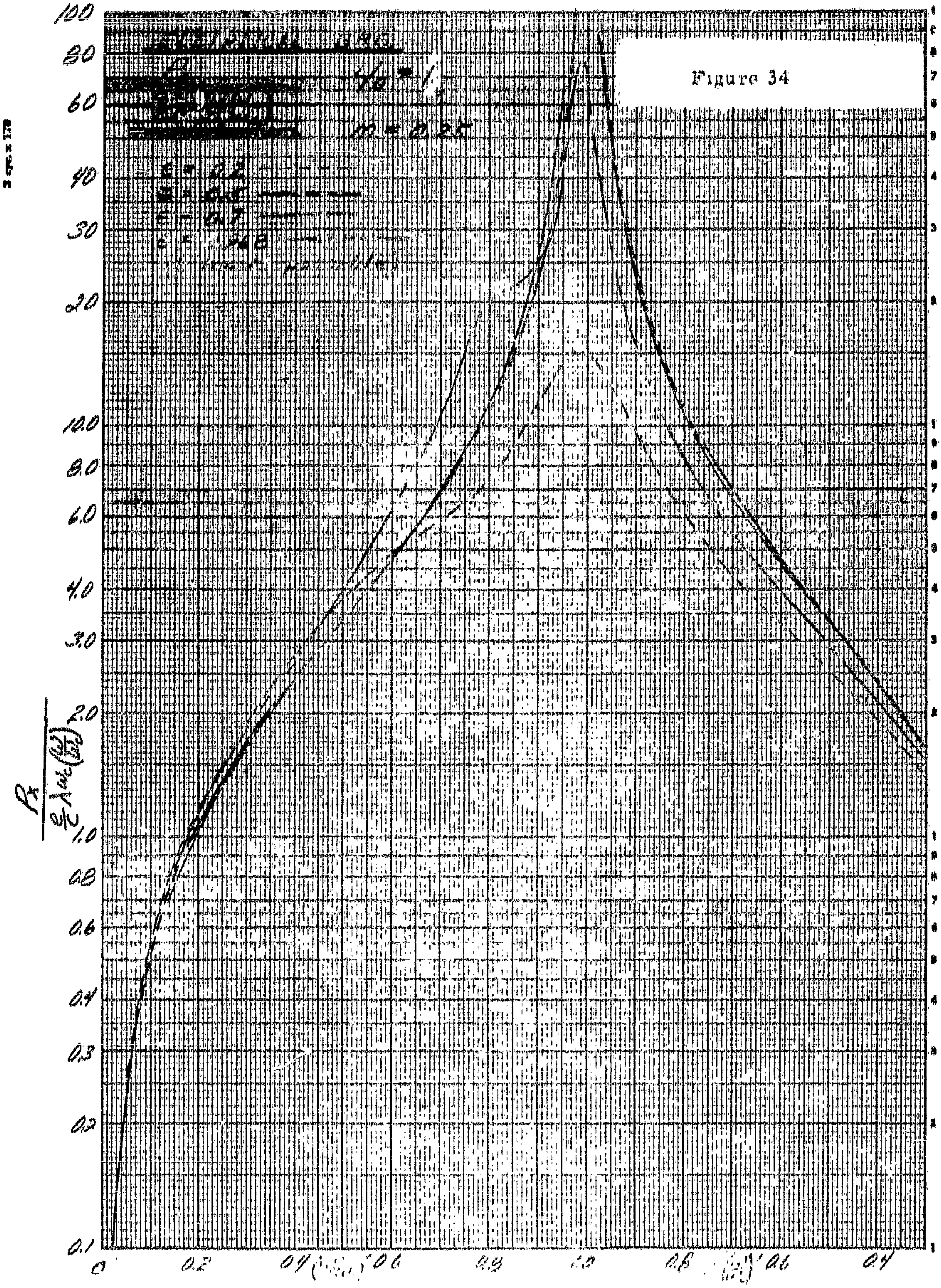

Figure 34
m = 0.25
100
80
60
40
30
20
10.0
8.0
6.0
4.0
3.0
2.0
1.0
0.8
0.6
0.4
0.3
0.2
0.1
0
0.2
0.4
0.6
0.8
1.0
0.8
0.6
0.4

Figure 35

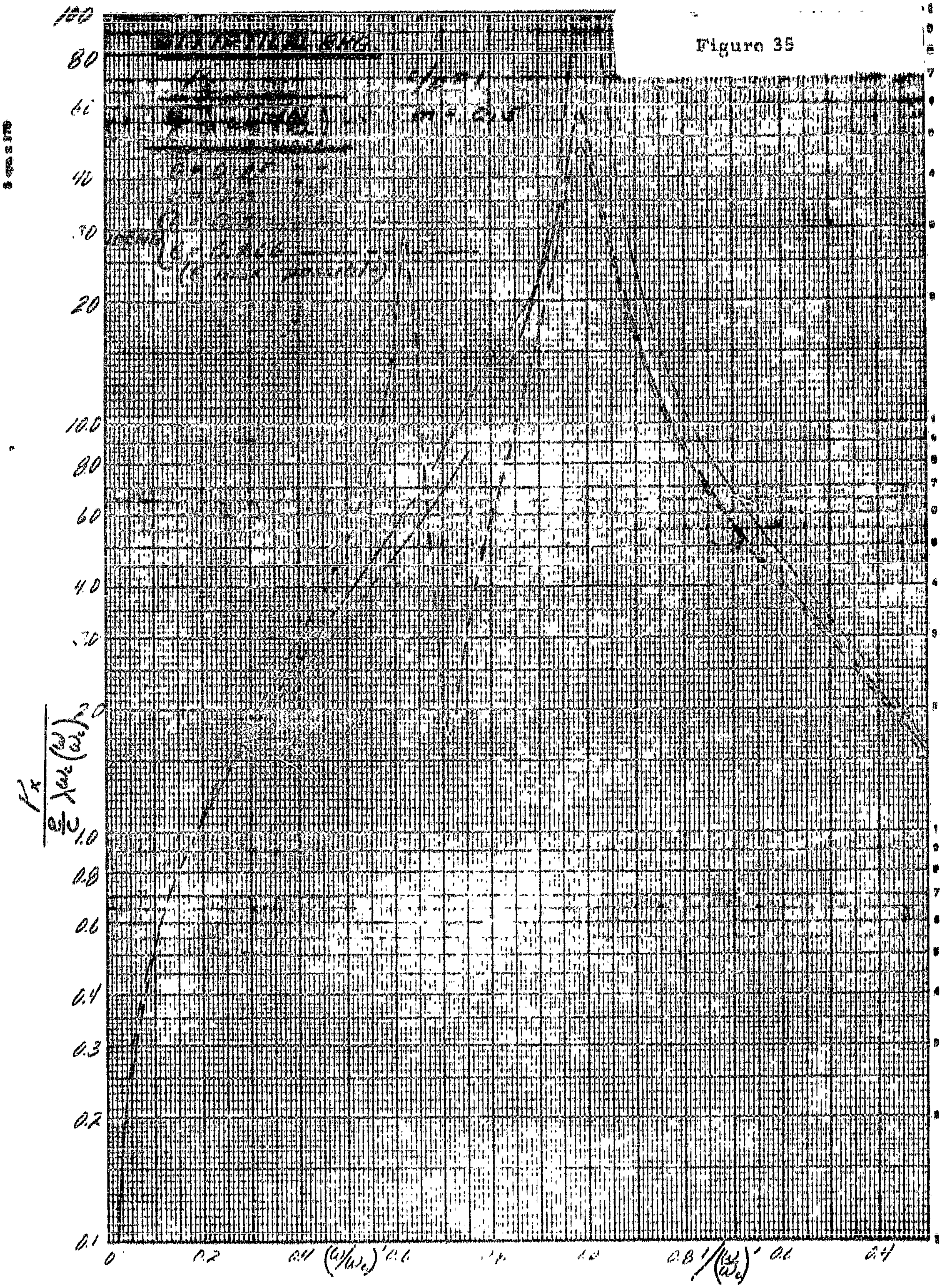

Figure 36

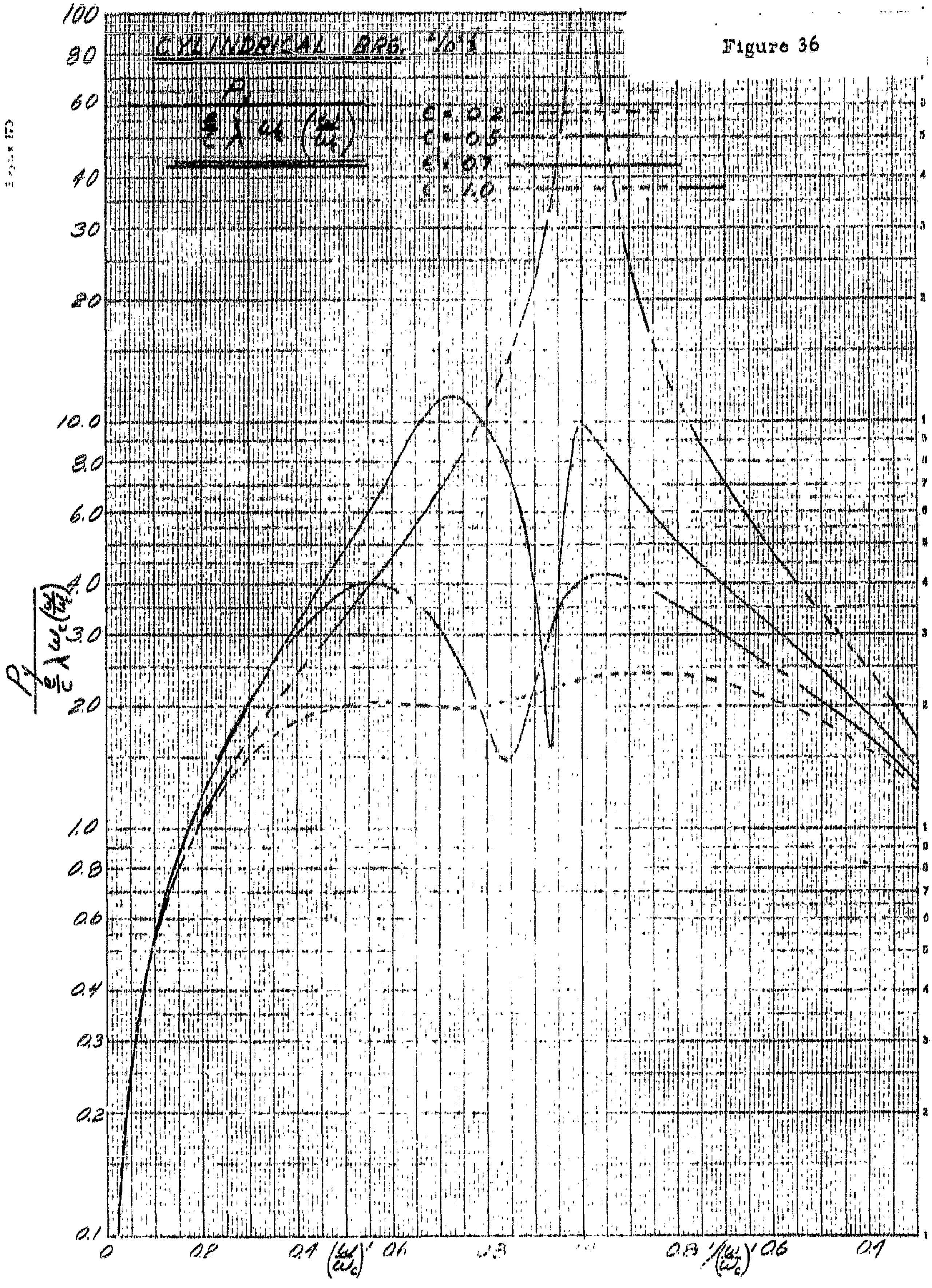
CYLINDRICAL BRG. L/D=1
ε = 0.2
ε = 0.5
ε = 0.7
ε = 1.0
100
80
60
40
30
20
10.0
8.0
6.0
4.0
3.0
2.0
1.0
0.8
0.6
0.4
0.3
0.2
0.1
0
0.2
0.4
0.6
0.8
0.8
0.6
0.4

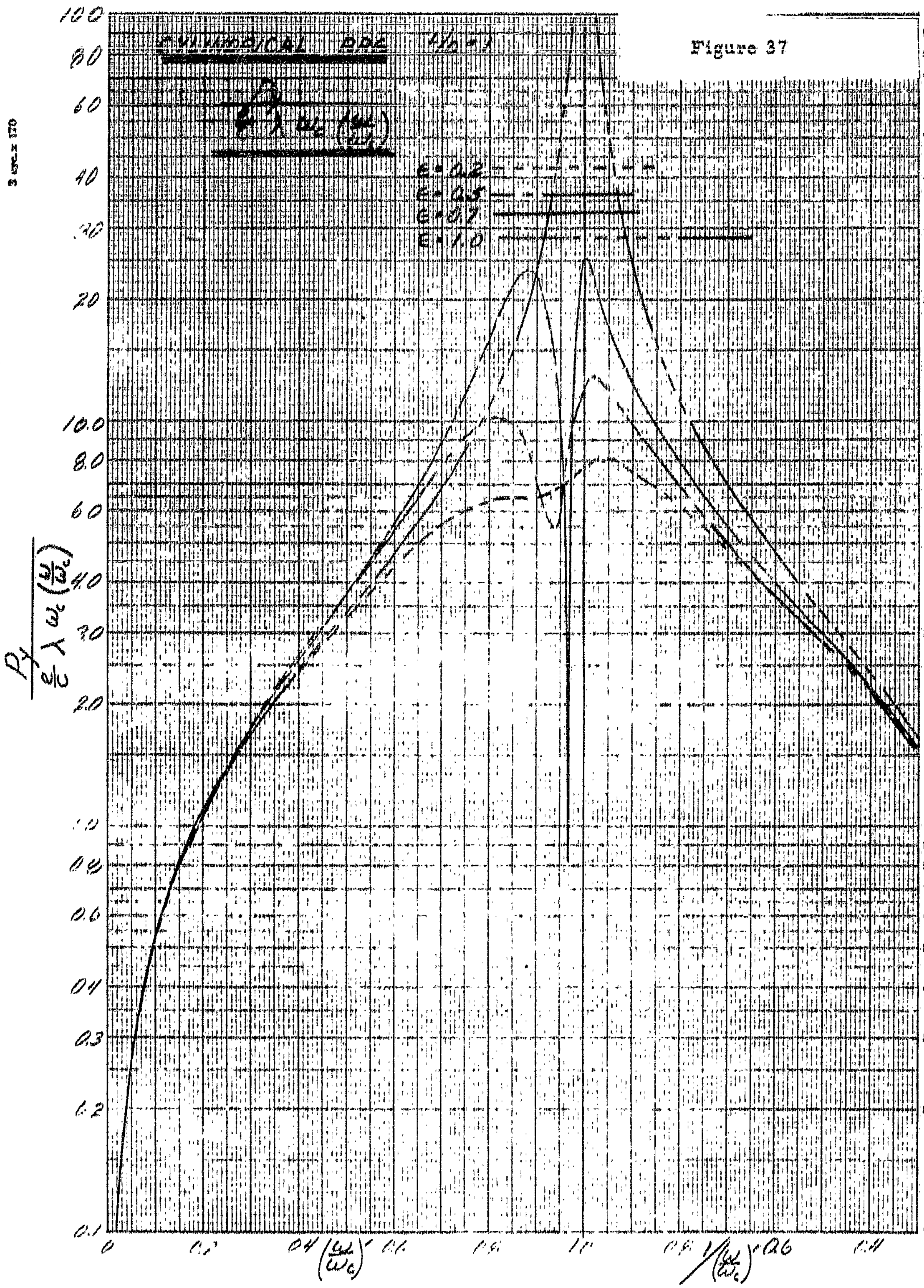
CYLINDRICAL ROD
ε = 0.2
ε = 0.5
ε = 0.7
ε = 1.0
100
80
60
40
30
20
10.0
8.0
6.0
4.0
3.0
2.0
0.8
0.6
0.4
0.3
0.1
0
0.4
1.0
0.6

Figure 37

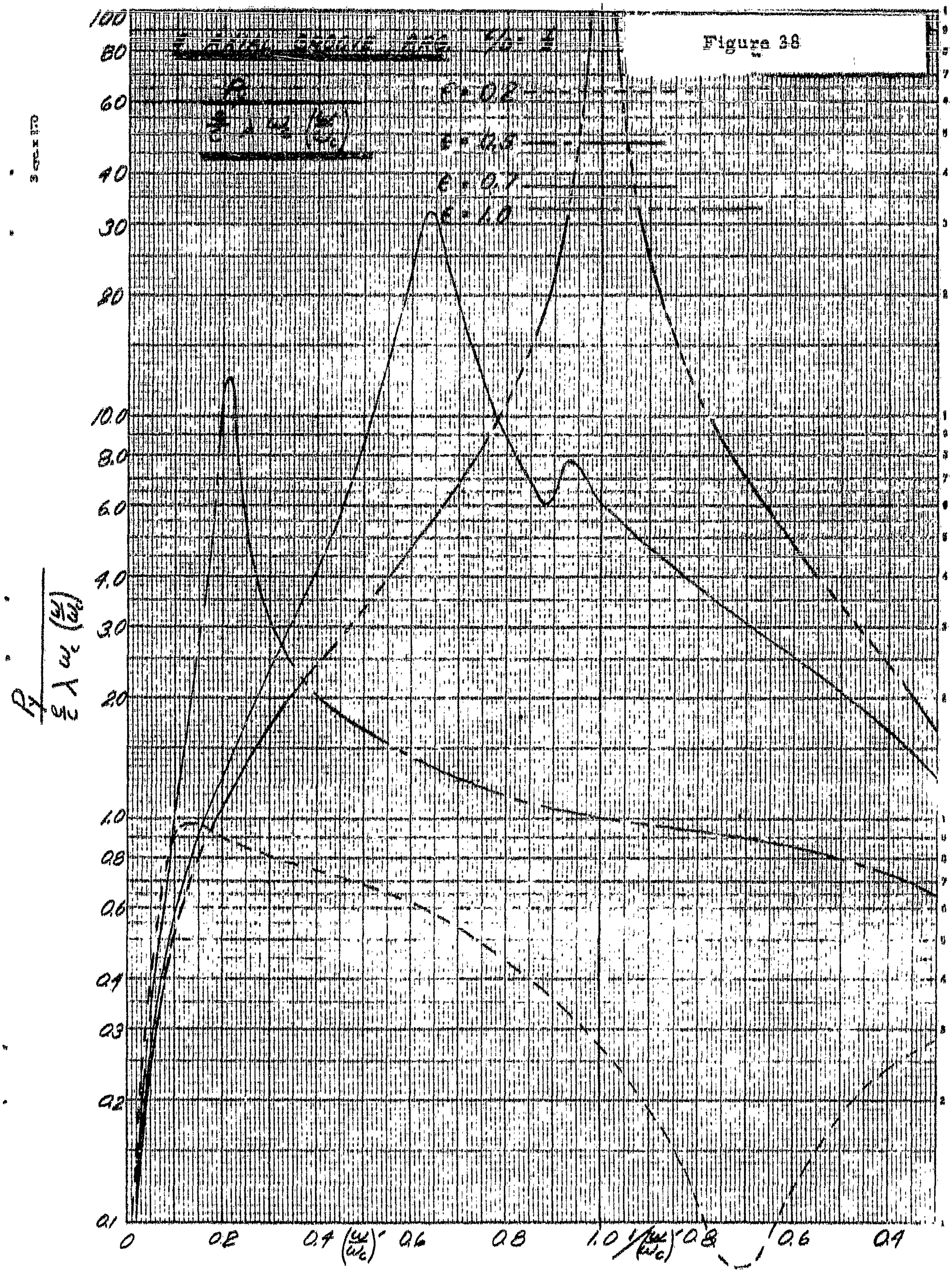

ε = 0.2
ε = 0.5
ε = 0.7
ε = 1.0
100
80
60
40
30
20
10.0
8.0
6.0
4.0
3.0
2.0
1.0
0.8
0.6
0.4
0.3
0.2
0.1
0
0.2
0.4 (ω/ω_c)
0.6
0.8
1.0 1/(ω/ω_c)
0.8
0.6
0.4

Figure 38

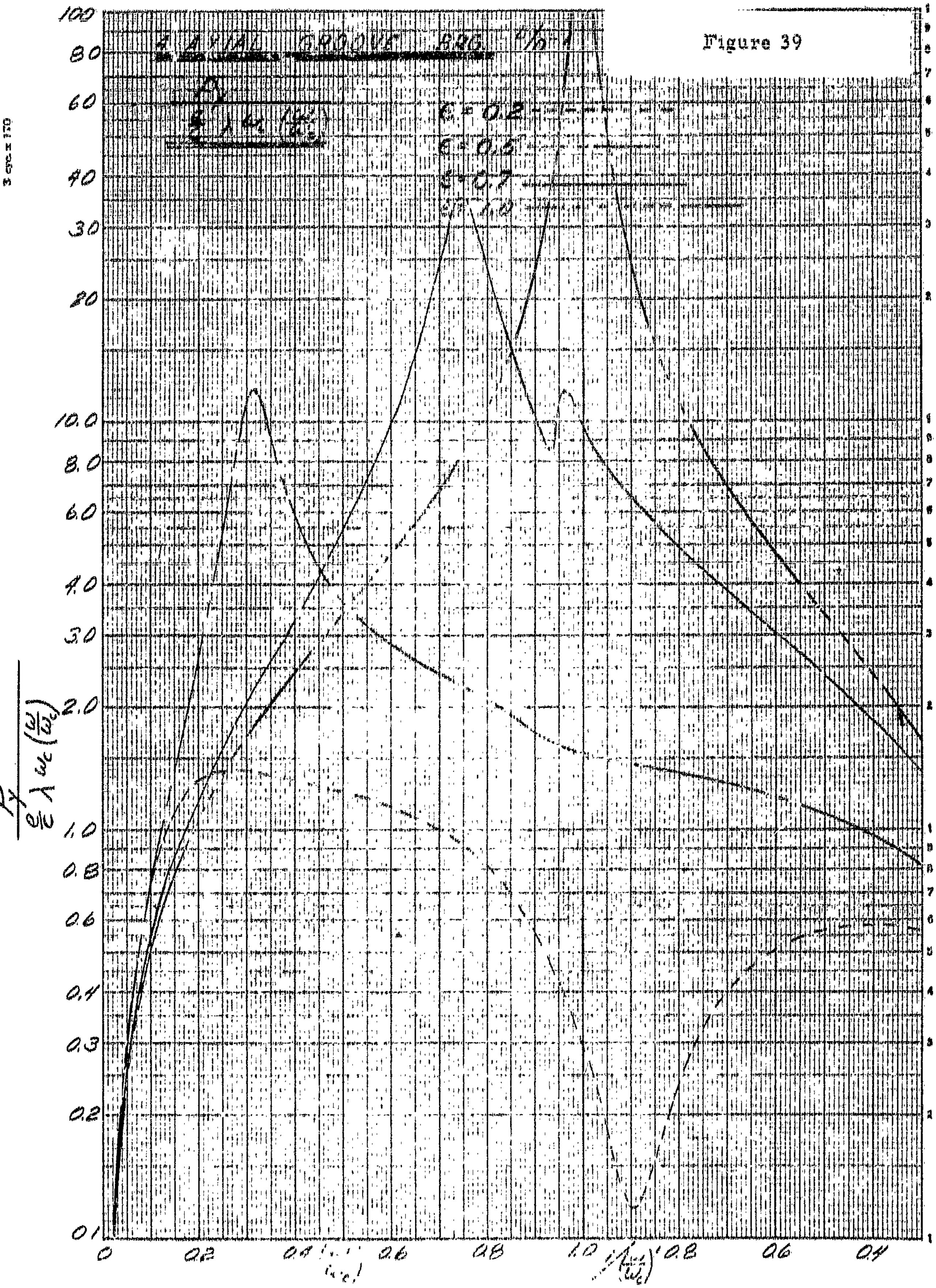
4 AXIAL GROOVE BRG.
ε=0.2
ε=0.5
ε=0.7
ε=1.0
100
80
60
40
30
20
10.0
8.0
6.0
4.0
3.0
2.0
1.0
0.8
0.6
0.4
0.3
0.2
0.1
0
0.2
0.4
0.6
0.8
1.0
0.8
0.6
0.4

Figure 39

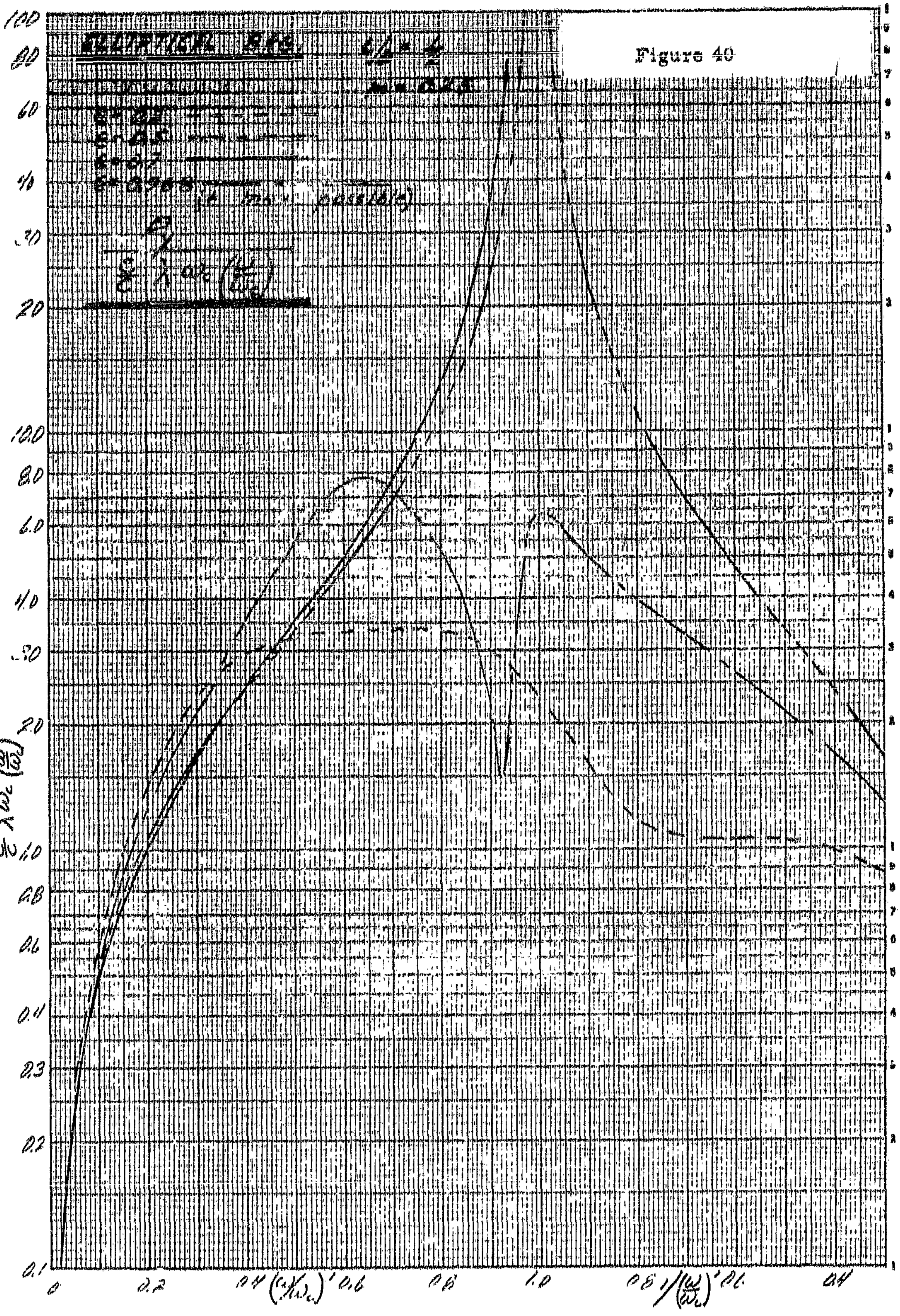
100
80
60
40
30
20
10.0
8.0
6.0
4.0
3.0
2.0
1.0
0.8
0.6
0.4
0.3
0.2
0.1
0
0.2
0.4
0.6
0.8
1.0

Figure 40

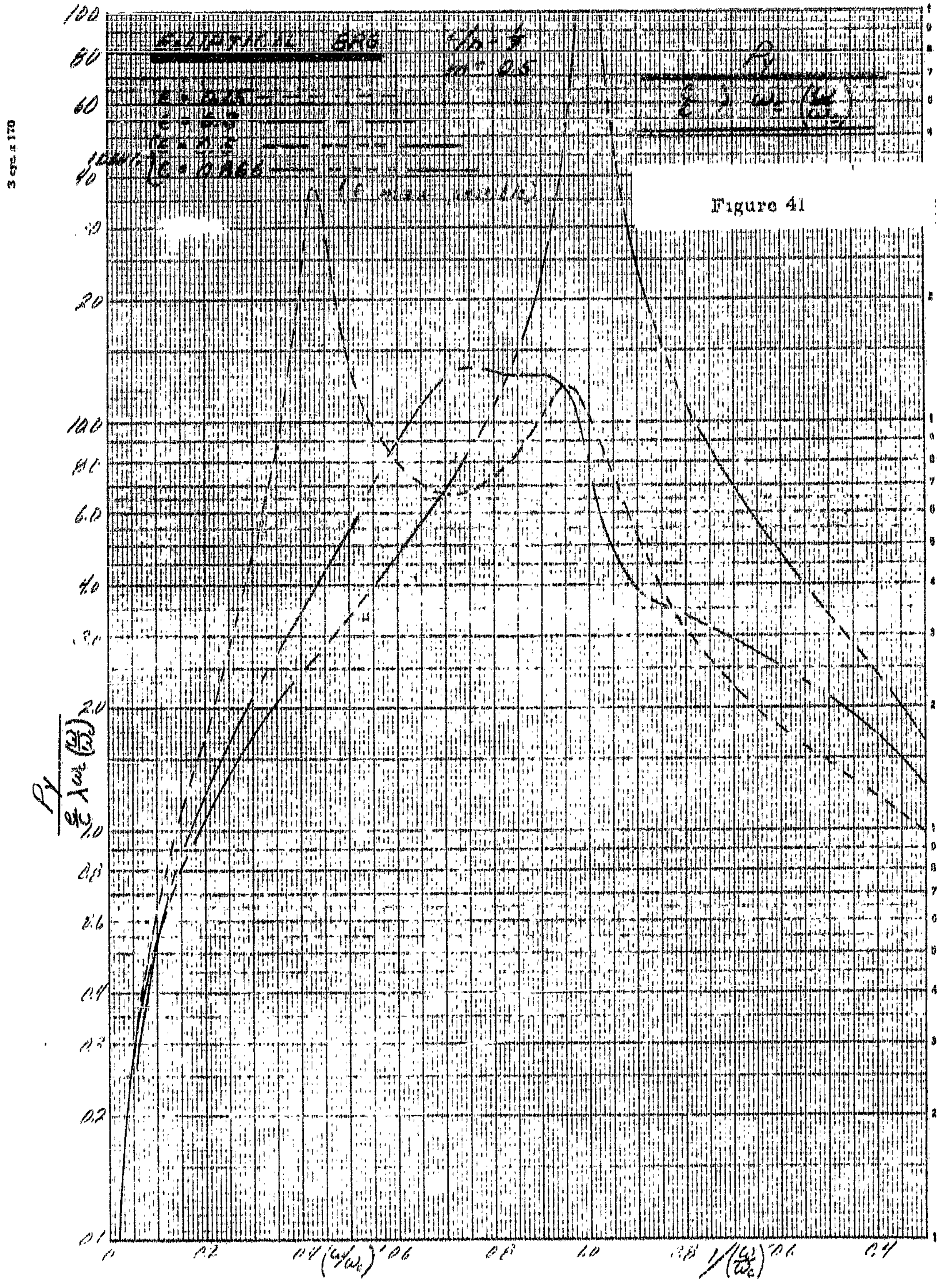

Figure 41

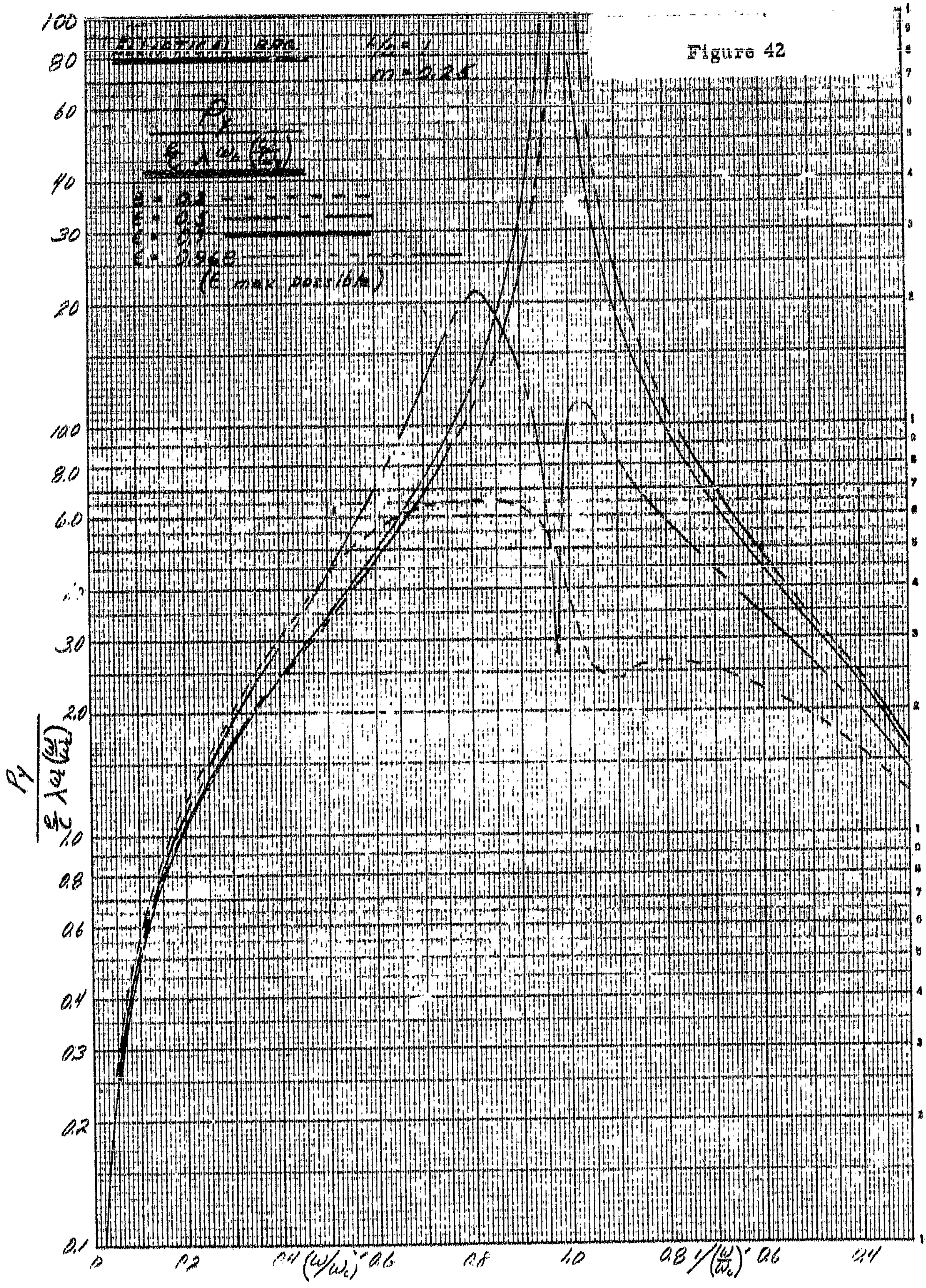
m = 0.25
(c max possible)
100
80
60
40
30
20
10.0
8.0
6.0
3.0
2.0
1.0
0.8
0.6
0.4
0.3
0.2
0.1
0
0.2
0.4 (ω/ω_c) 0.6
0.8
1.0
0.8 $1/(\omega/\omega_c)$ 0.6
0.4

Figure 42

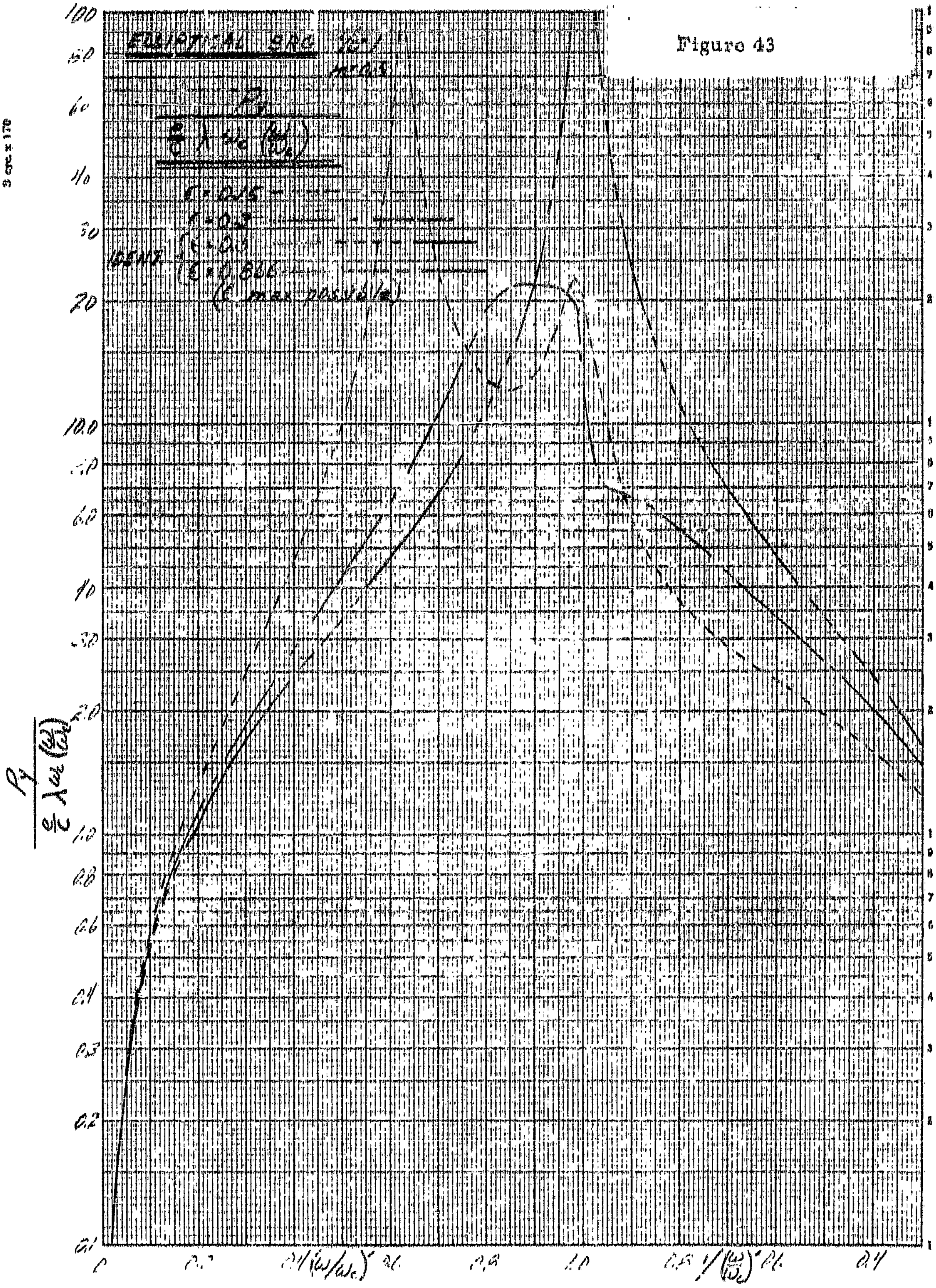

Figure 43

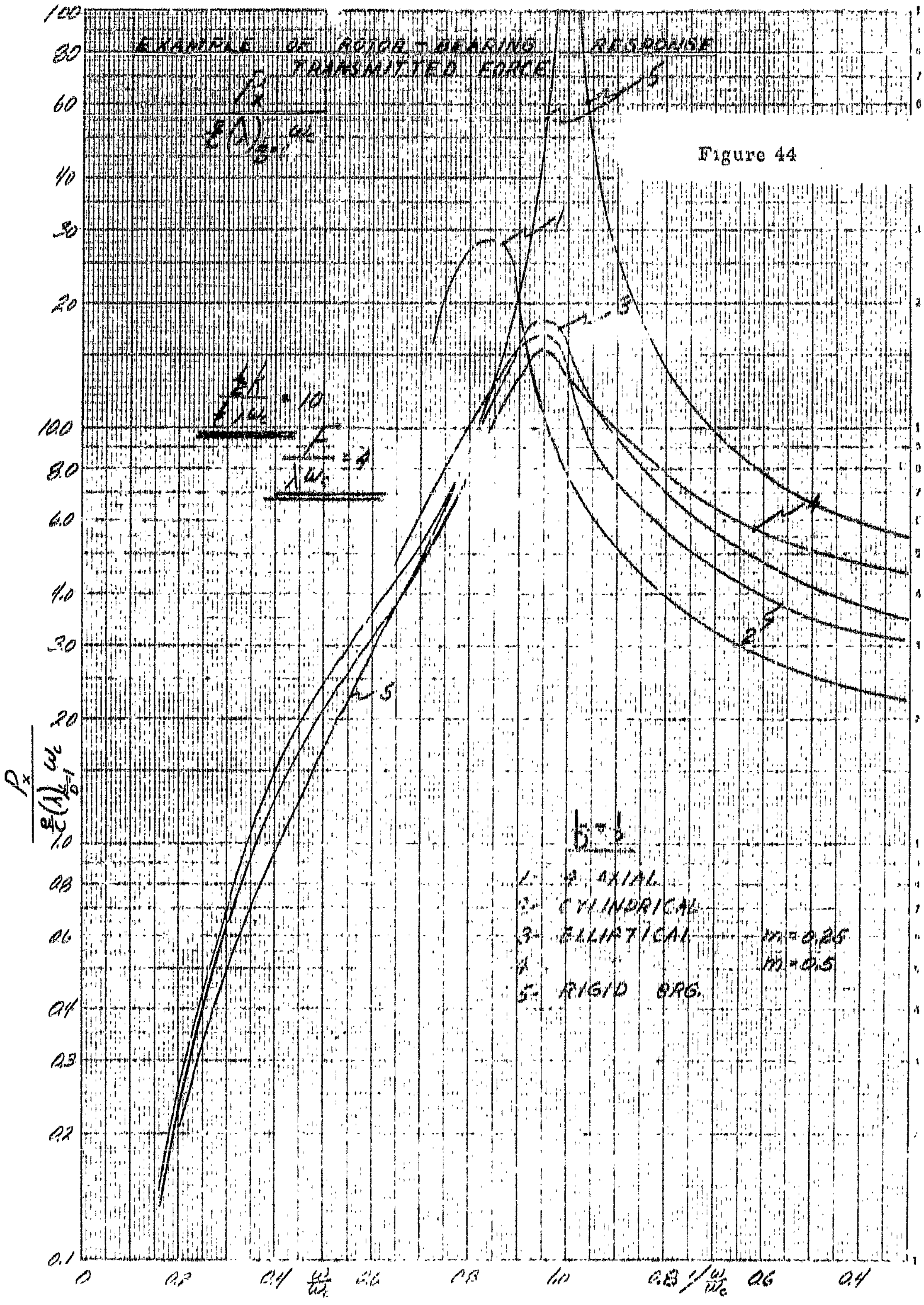
EXAMPLE OF ROTOR-BEARING RESPONSE
TRANSMITTED FORCE
b = 1
1- 3 AXIAL
2- CYLINDRICAL
3- ELLIPTICAL m=0.25
4 m=0.5
5- RIGID BRG.

Figure 44

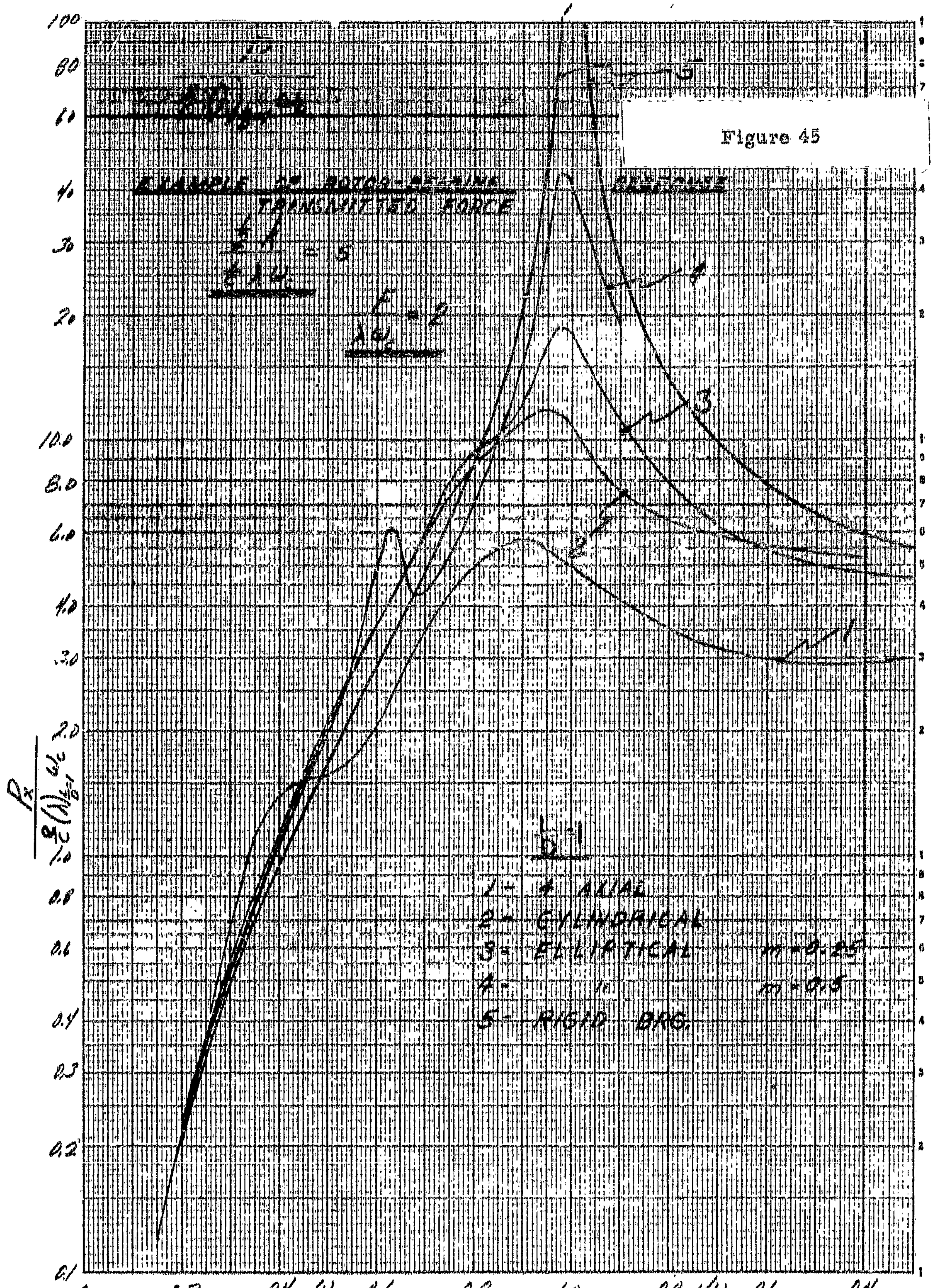
TRANSMITTED FORCE
1 - 4 AXIAL
2 - CYLINDRICAL
3 - ELLIPTICAL m = 0.25
4 - " m = 0.5
5 - RIGID BRG.
100
80
60
40
30
20
10.0
8.0
6.0
4.0
3.0
2.0
1.0
0.8
0.6
0.4
0.3
0.2
0.1
0
0.2
0.4
0.6
0.8
1.0
0.8
0.6
0.4

Figure 45

DESIGN CHART FOR CRITICAL SPEED CALCULATION

Cylindrical and 4-Axial Groove Bearing

Figure 46

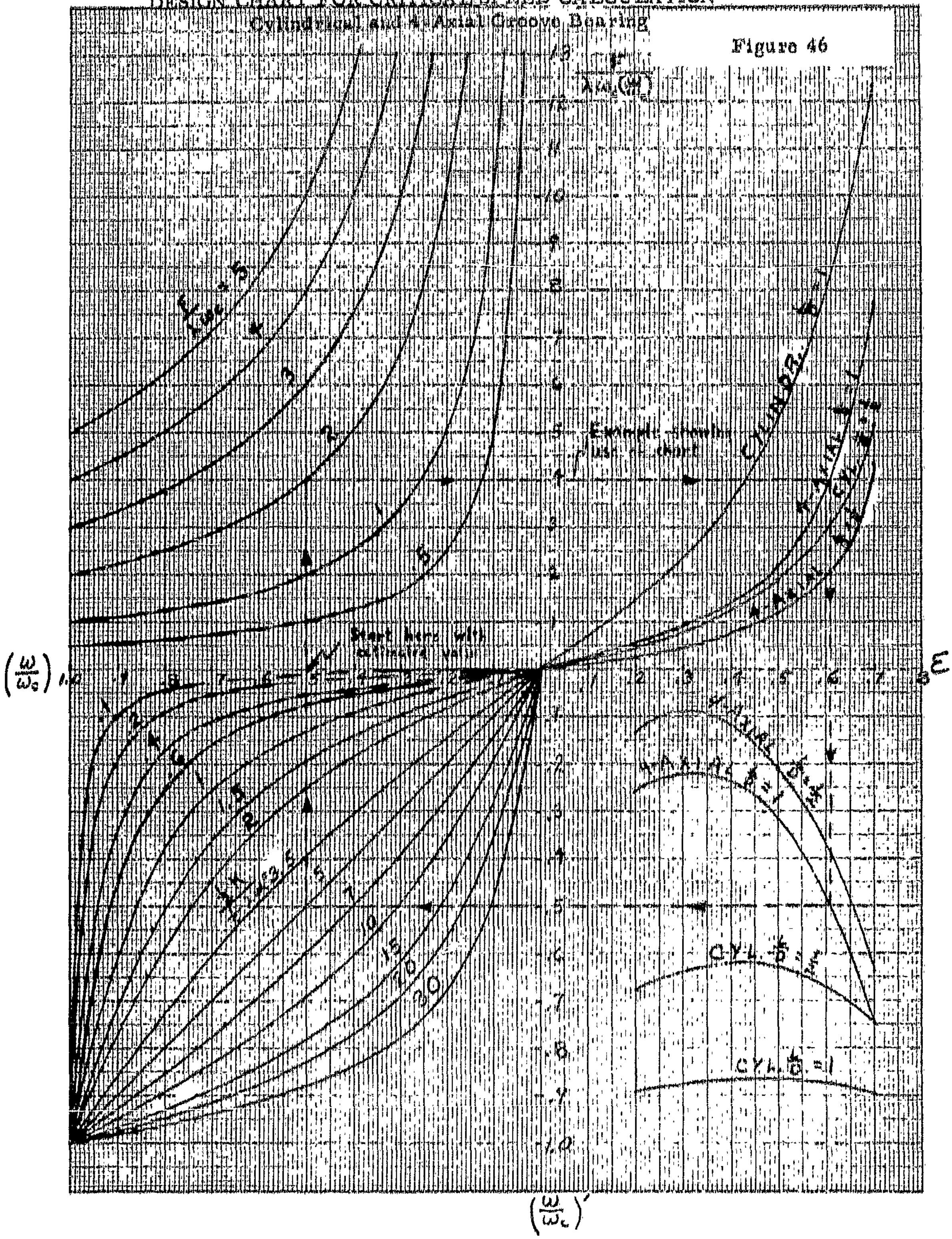

DESIGN CHART FOR CRITICAL SPEED CALCULATION
Elliptical Bearing

Figure 47

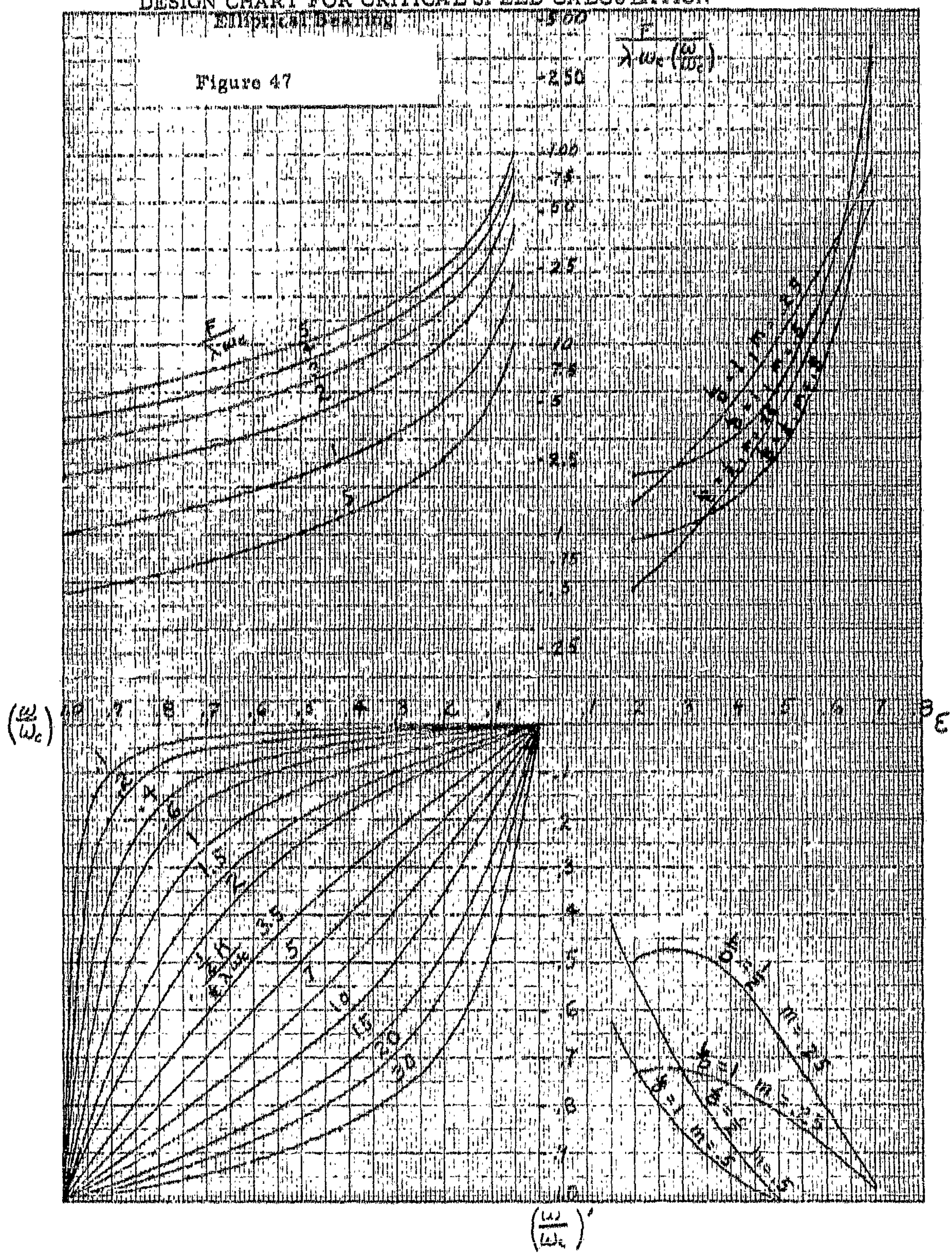

Elliptical Journal Path
Constant Eccentricity Ratio

Figure 48

Cylindrical Bearing $\frac{L}{D} = \frac{1}{2}$ $\varepsilon = .5$

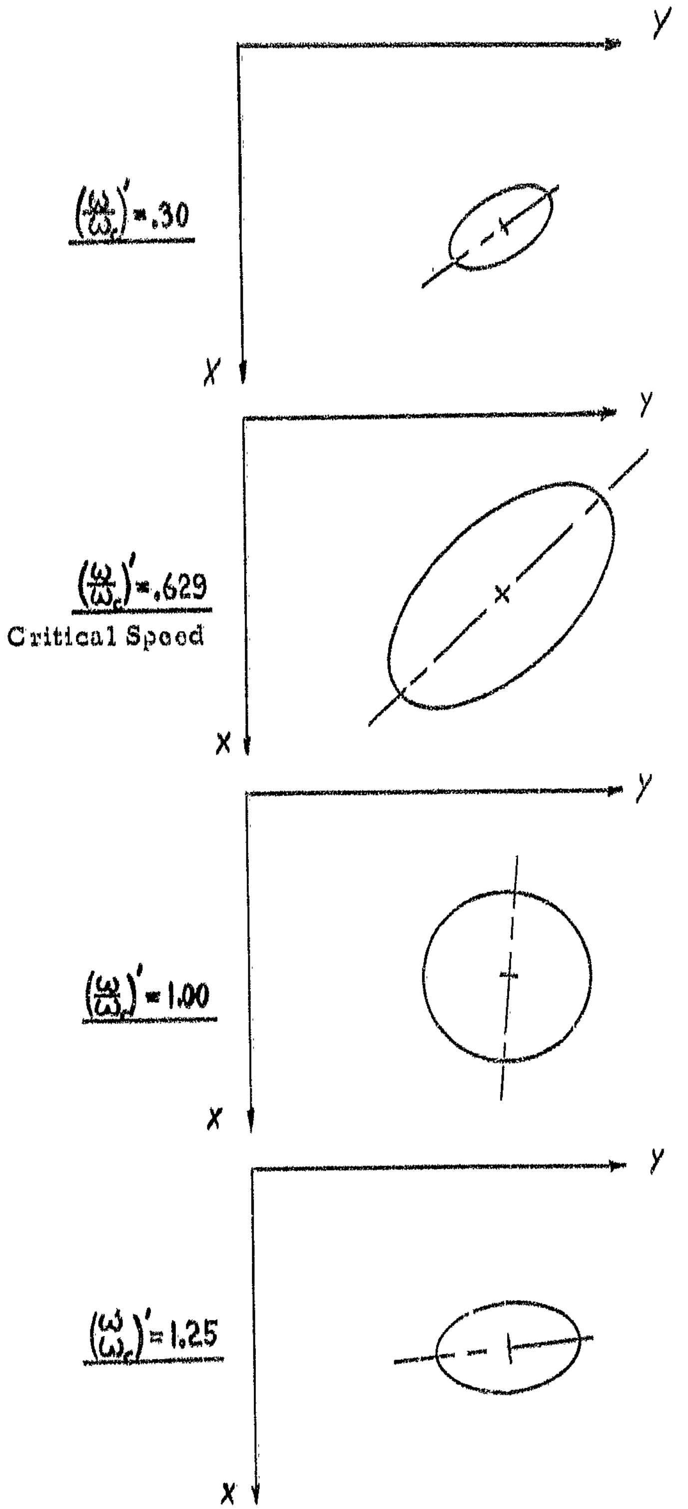

Scale factor

1 inch amplitude corresponds to .5 inch rotor eccentricity (Rotor eccentricity :

$$e = \frac{\text{Unbalance (lbs-in)}}{\text{Rotor Weight (lbs)}}$$)

Figure 49

Elliptical Journal Path

Cylindrical Bearing $\frac{L}{D} = \frac{1}{2}$ $\frac{F}{\lambda\omega_c} = 1.171$

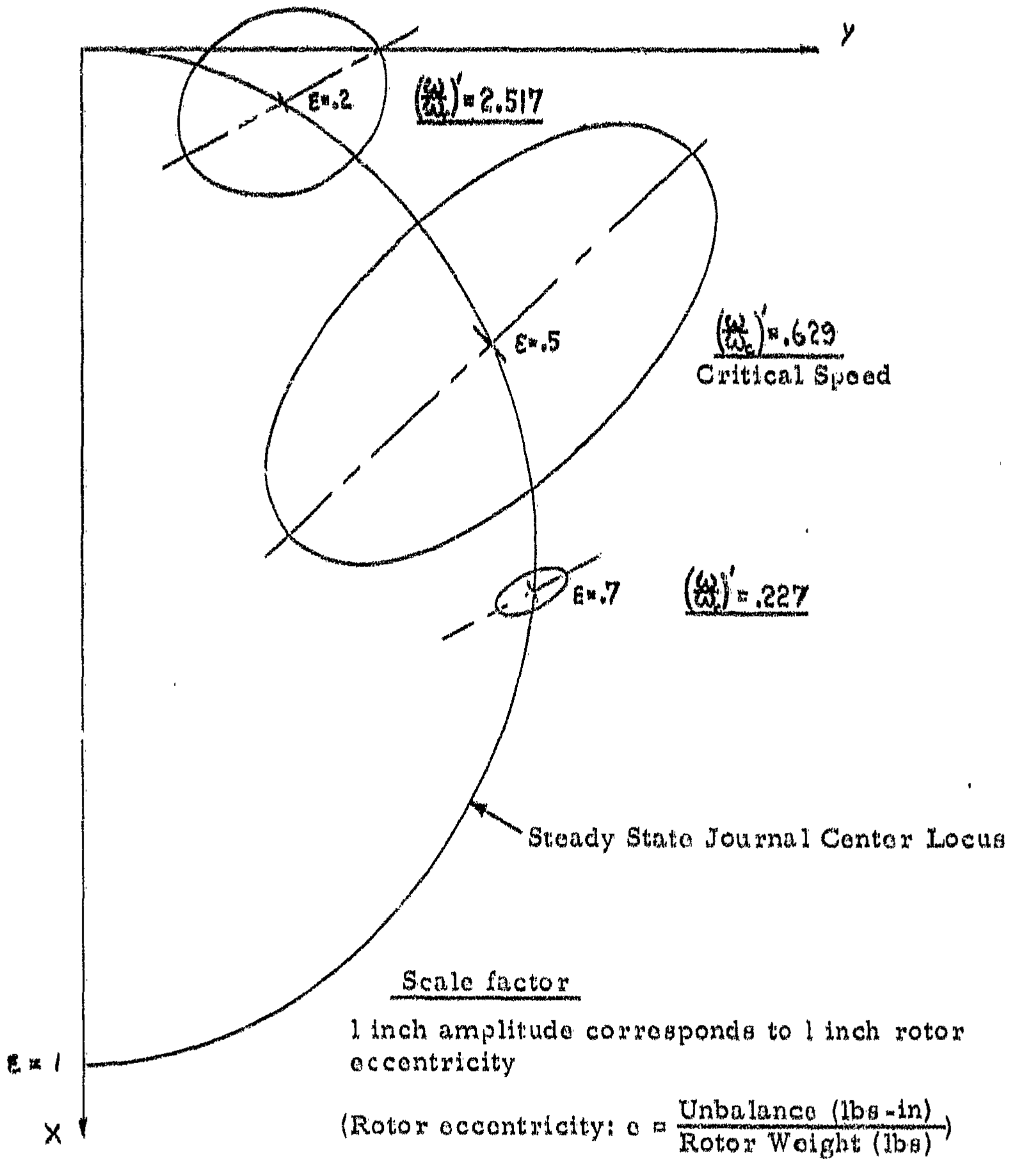

Scale factor

1 inch amplitude corresponds to 1 inch rotor eccentricity

(Rotor eccentricity: $e = \frac{\text{Unbalance (lbs-in)}}{\text{Rotor Weight (lbs)}}$)

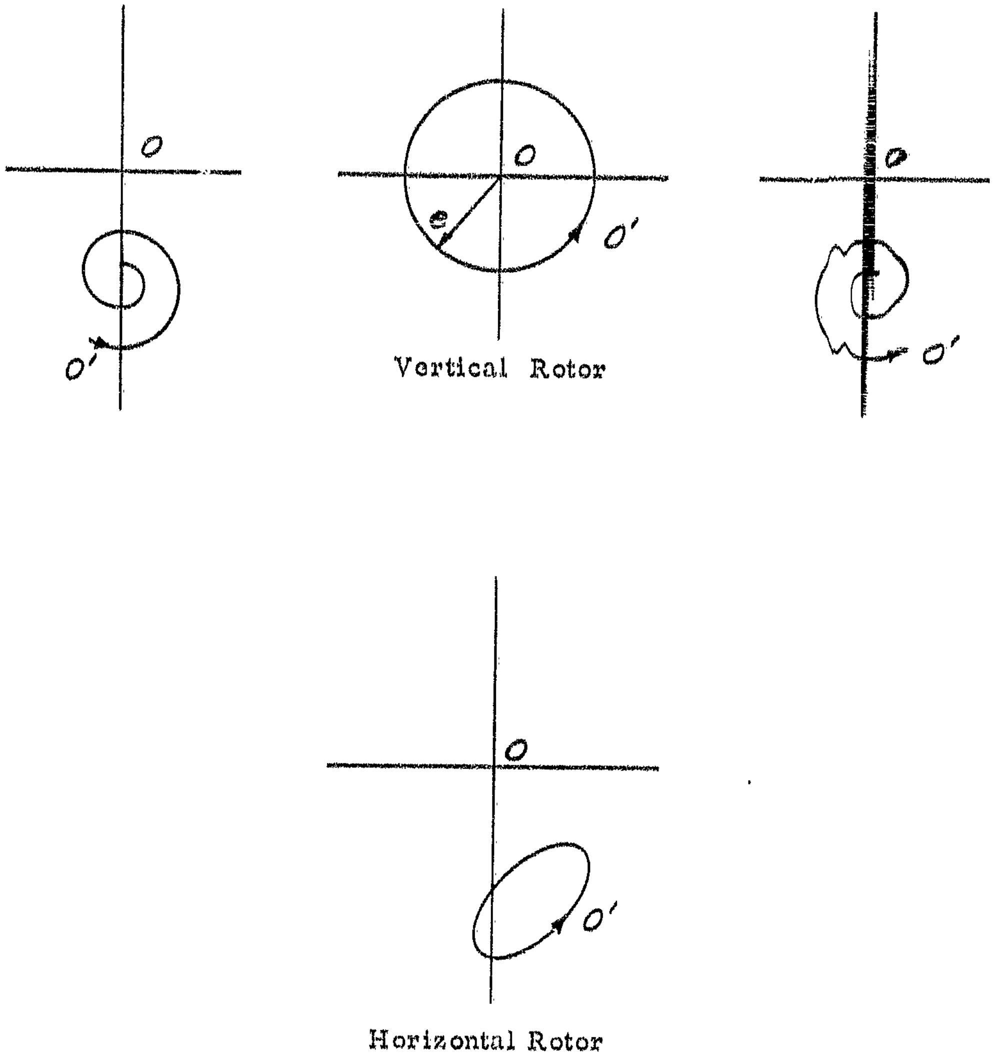

a) Stable Condition
e.g. acceleration

b) Stable Whirl
e.g. Synchronous whirl , Critical speed

c) Unstable Whirl
e.g. Resonant whip, Half frequency whirl

FIG. 50

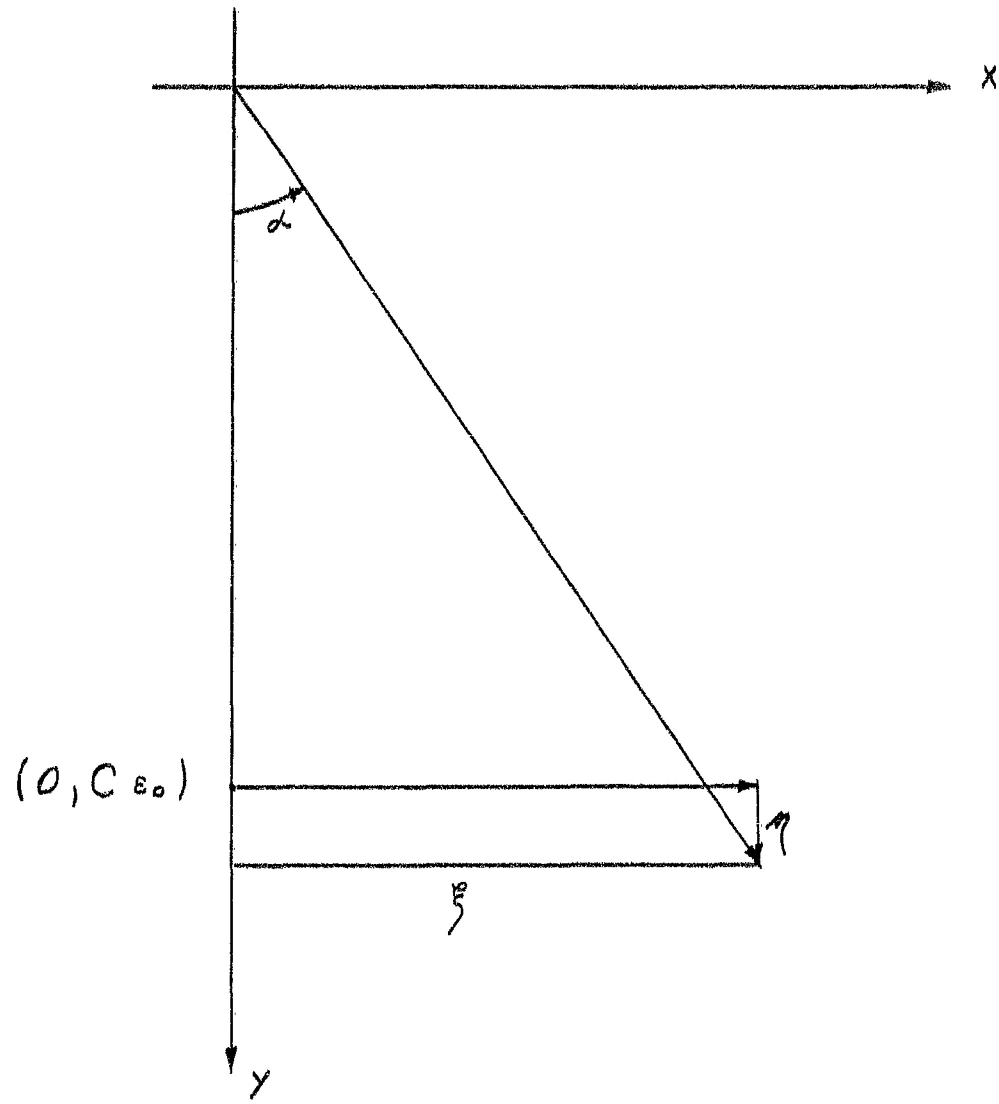

FIG. 51

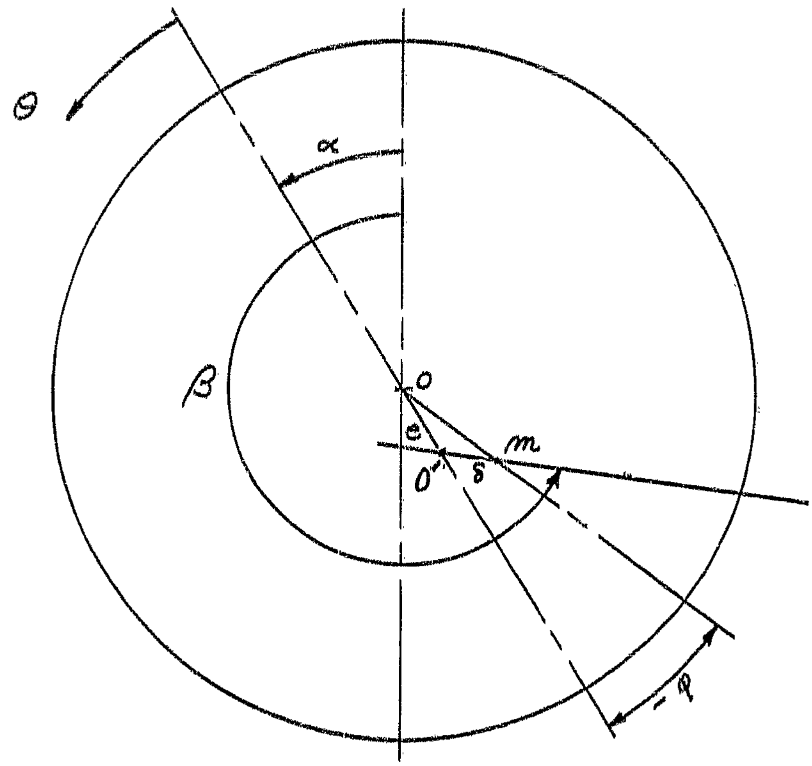

COORDINATE SYSTEM

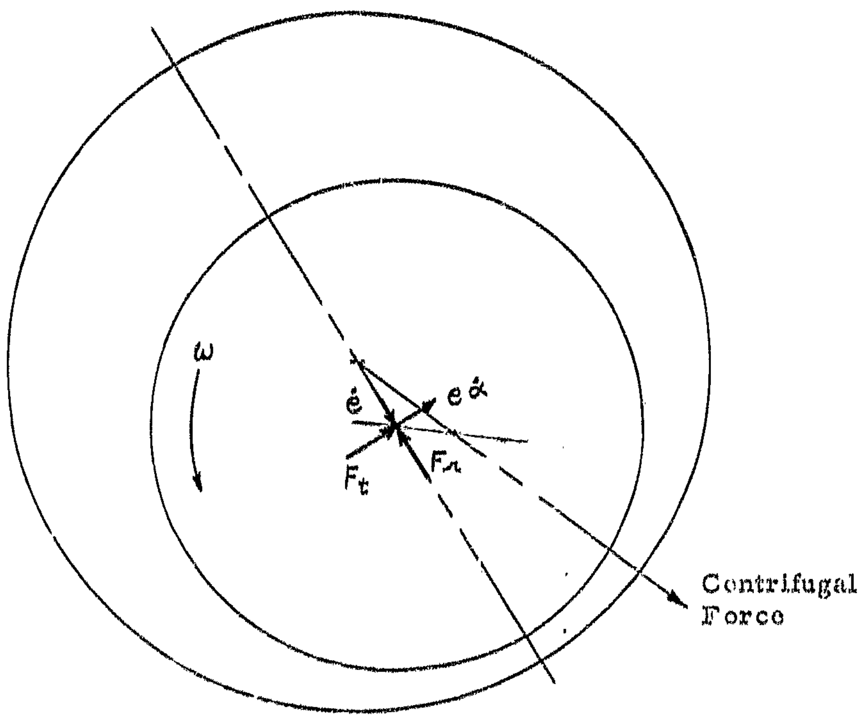

FORCES AND VELOCITIES

FIG. 52

NOMENCLATURE

A, B, E, F	Cosine and sine-components of rotor vibration amplitude, eq. (17), page 8	inch
a, b	Major and minor axis of elliptical journal center path, see fig. 7	inch
B_x, B_y	Effective bearing damping coefficient in vertical and horizontal direction	$\frac{lbs \cdot sec}{in}$
C	Radial bearing clearance	inch
C_{xx}	Damping coefficient in x-direction for velocity in x-direction	$\frac{lbs \cdot sec}{in}$
C_{xy}	Damping coefficient in x-direction for velocity in y-direction	$\frac{lbs \cdot sec}{in}$
C_{yx}	Damping coefficient in y-direction for velocity in x-direction	$\frac{lbs \cdot sec}{in}$
C_{yy}	Damping coefficient in y-direction for velocity in y-direction	$\frac{lbs \cdot sec}{in}$
D	Bearing diameter	inch
e	Bearing eccentricity = $C\varepsilon$, see fig. 1-5	inch
ϵ	Distance between center of gravity of rotor and shaft center at midspan	inch
F	Bearing reaction	lbs
F_α	Bearing force component α degrees from vertical	lbs
f_α	Dimensionless bearing force in α-direction = [illegible]	
F_r, F_t	Bearing force in radial and tangential direction	lbs
f_r, f_t	Dimensionless bearing force in radial and tangential direction = $\frac{F}{\lambda W}$	
F_v, F_h	Bearing force in vertical and horizontal direction	lbs
f_v, f_h	Dimensionless bearing force in vertical and horizontal direction = $\frac{F}{\lambda W}$	
f_{v1}, f_{h1}	Dimensionless vertical and horizontal force for lower lobe of elliptical bearing	
f_{v2}, f_{h2}	Dimensionless vertical and horizontal force for upper lobe of elliptical bearing	
F_x, F_y	Bearing force in x and y-direction	lbs
$\bar{h}$	Oil film thickness	inch
h	Dimensionless oil film thickness	
K_{xx}	Spring coefficient in x-direction for displacement in x-direction	$\frac{lbs}{in}$
K_{xy}	Spring coefficient in x-direction for displacement in y-direction	$\frac{lbs}{in}$
K_{yx}	Spring coefficient in y-direction for displacement in x-direction	$\frac{lbs}{in}$
K_{yy}	Spring coefficient in y-direction for displacement in y-direction	$\frac{lbs}{in}$
K_x, K_y	Effective spring coefficient in vertical and horizontal direction	$\frac{lbs}{in}$
k	Rotor stiffness	$\frac{lbs}{in}$
L	Effective bearing length	inch
M	Vibratory rotor mass	$\frac{lbs \cdot sec^2}{in}$
m	Bearing ellipticity, see figure 5	
N	Rotor speed	RPS
$\bar{p}$	Oil film pressure	psi
P_x, P_y	Force transmitted by bearing in vertical and horizontal direction	lbs
P_o	Force transmitted for rigid rotor supports	lbs
R	Bearing radius	inches
$\bar{x}, \bar{z}$	Circumferential and axial coordinates for oil film	inches
x, z	Dimensionless coordinates for oil film	
x, y	Vertical and horizontal coordinates for journal center motion, see fig. 1-5	inches
x_a, y_a	Vertical and horizontal coordinates for journal center, see fig. 6	inches
x_b, y_b	Vertical and horizontal coordinates for shaft center at midspan, see fig. 6	inches
ϕ	Bearing attitude angle, see fig. 1-5	
α	Angle between x axis and major axis of elliptical journal center path, see fig. 7	
ϕ_1, ϕ_2	Attitude angle for lower and upper lobe of elliptical bearing, see fig. 5	
γ_x, γ_y	Phase angle between transmitted force and amplitude, see eq. (25), page 12	
δ, η	Given by eq. (23), page 11	
ε	Bearing eccentricity ratio	
$\varepsilon_1, \varepsilon_2$	Eccentricity ratio for lower and upper lobe of elliptical bearing, see fig. 5	
θ	Polar coordinate for oil film	
$\varkappa$	Rotor parameter, given by eq. (20), page 14	
λ	Bearing parameter, given by eq. (4), page 3	lbs-sec
μ	Oil viscosity	$\frac{lbs \cdot sec}{in^2}$
φ_x, φ_y	Phase angle between amplitude and unbalance	
ψ_x, ψ_y	Given by eq. (23), page 11	
ω	Rotor speed	rad/sec
ω_o	Critical speed of rotor in rigid supports	rad/sec
$(\frac{\omega}{\omega_o})'$	Equivalent speed ratio, see eq. (19), page 14 and fig. 11	